LOST YET FOUND

CORTICAL HAND REPRESENTATION AFTER AMPUTATION

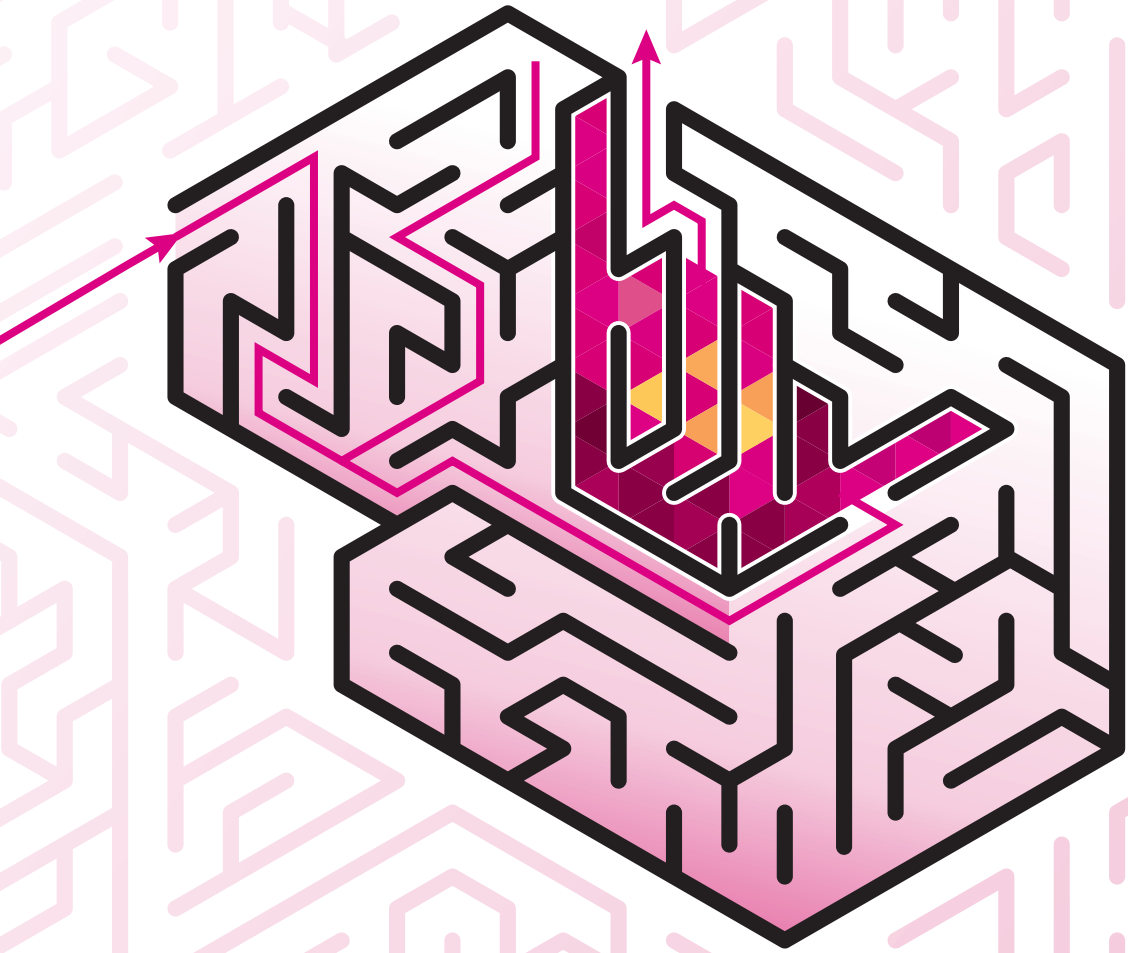

UMC Utrecht Brain Center

L.C.M. BRUURMIJN

Lost Yet Found

Cortical Hand Representation After Amputation

Mark Bruurmijn

Colofon

ISBN: 978-90-393-7665-2

Provided by thesis specialist Ridderprint, ridderprint.nl
Printing: Ridderprint
Cover design: Mark Bruurmijn
Layout:Anna Bleeker, persoonlijkproefschrift.nl

LOST YET FOUND

CORTICAL HAND REPRESENTATION AFTER AMPUTATION

CORTICALE REPRESENTATIE VAN DE HAND NA AMPUTATIE

(MET EEN SAMENVATTING IN HET NEDERLANDS)

Proefschrift

ter verkrijging van de graad van doctor aan de
Universiteit Utrecht
op gezag van de
rector magnificus, prof. dr. H.R.B.M. Kummeling,
ingevolge het besluit van het college voor promoties
in het openbaar te verdedigen op

donderdag 11 april 2024 des middags te 12.15 uur

door

Laurentius Cornelis Maria Bruurmijn

geboren op 14 december 1985
te Waalwijk

Promotor:
Prof. dr. N.F. Ramsey

Copromotoren:
Dr. M.A.H.L.L. Raemaekers
Dr. M.J. van Steensel

Beoordelingscommissie:
Prof. dr. R.M. Dijkhuizen (voorzitter)
Prof. dr. H.C. Dijkerman
Prof. dr. W.P. Medendorp
Prof. dr. R. Goebel
Dr. M. Tangermann

Table of contents

INTRODUCTION

Introduction

Locked-in Syndrome (LIS) is a condition in which a person is unable to make (voluntary) muscle movements (American Congress of Rehabilitation Medicine, 1995). A common cause for LIS is brain stem stroke, in which a lesion in the brain stem prevents the motor commands sent by the motor areas in the brain from passing down to the muscles. Another common cause for LIS can be found in motor neuron diseases, such as amyotrophic lateral sclerosis (ALS), a disease in which motor neurons in the brain and brainstem are affected (Smith & Delargy, 2005). The loss of motor abilities due to LIS can render communication impossible. This is a frustrating experience and can cause social isolation. Questionnaires show that communication is a determining factor for quality of life for people with LIS (Rousseau et al., 2015). Restoring communication is therefore crucial for their well-being.

To re-enable the means communication for people with LIS, assistive technologies have been developed. These communication devices can be controlled with residual voluntary movements. Eye movements or blinking are often the only voluntary movements that remain (American Congress of Rehabilitation Medicine, 1995). Eye trackers have been successfully deployed to allow individuals with LIS to control a mouse cursor on the screen, typing a text editor, or control dedicated software developed for communication. In the severe case of 'complete LIS', one has been deprived of all voluntary movements, including that of the eyes. However, even for indiviuals without complete LIS controlling an assistive device can be challenging: a Japanese survey among people with ALS found that 85.1% of assistive device users experienced troubles in using the device (Kageyama et al., 2020).

Brain-computer interfaces

If no motor output is left, signals directly from the brain can be used as a communication channel via a brain-computer interface (BCI). The term BCI refers to a variety of techniques involving the recording of brain signals and translating those signals in some useful control signal for a (communication) device (Wolpaw, 2007). This recording of brain signals can be done from outside the scalp or by implanting sensors, requiring surgery.

Non-invasive BCIs

Electro-encephalography (EEG) is a widespread, easy and relatively cheap non-invasive technique, measuring the electrical fields resulting from brain activity using electrodes on the scalp. There are several ways to turn the measured brain activity into a signal for controlling a communication device (Machado et al., 2010).

The first method is based on *event related potentials* (ERPs), the brain's response to a given stimulus, often a visual or auditory cue (Farwell & Donchin, 1988; Rezeika et al., 2018; Sellers & Donchin, 2006). A practical application is the control of a 'graphical keyboard', presented on a computer screen. The user is required to pay attention to the letter that he or she intends to type. All letters are successively highlighted. Once the letter of choice is highlighted, an ERP occurs and is detected using the scalp electrodes (Farwell & Donchin, 1988). This way, the letter is typed, and the user can focus on a new letter.

The second method is using brain signals directly reflecting the intentions of the user. Using the graphical keyboard as described above, the user can type a letter by activating the targeted brain area when the desired letter is highlighted on the screen (Rezeika et al., 2018). Examples of such target areas are the motor area, which becomes active when executing or attempting movements, or prefrontal brain areas involved in higher-level functions such as working memory, which can be voluntarily activated by performing a demanding task, such as making mental calculations.

Other non-invasive neural signal recording techniques include magneto-encephalography (based on the magnetic fields generated by brain activity) (Mellinger et al., 2007), functional near-infrared spectroscopy (based on the oxygenation level of blood, related to brain activity) (Naseer & Hong, 2015), and functional magnetic resonance imaging (functional MRI) (Andersson et al., 2011; Sorger & Goebel, 2020). These latter techniques can not be practically implemented for daily life activities, due to the size and technical requirements of the equipment. However, they can be useful for research purposes.

All techniques have their benefits and downsides. For EEG, due to the influence of tissue (mostly the skull) on the electric fields, the spatial detail and specificity is low compared to functional MRI. However, EEG is superior in temporal resolution compared to functional MRI. All non-invasive recording methods share the problem that they need to be set up every time the user wishes to use it. A survey has shown that set-up time is an important factor in user satisfaction and their willingness to use the device (Huggins, Wren, & Gruis, 2011).

Invasive BCIs

Brain signals can also be recorded directly from the brain using surgically implanted electrodes. They come in a wide variety, ranging from electrodes for recording the activity of a single locus, to microelectrode arrays with many electodes, able to measure activity from a patch of cortical activity up to an area of several square millimeters (Jacobs & Kahana, 2010). In electro-corticography (ECoG), electrodes do not penetrate the cortex, but only measure potentials from the cortical surface. These electrodes are commonly arranged into a grid ($n \times m$) or a strip ($1 \times n$), with a space between the electrodes in the order of millimeters to a centimeter. Although these offer a lower spatial resolution than microelectrode arrays, they are able to cover a larger area of cortex.

The main advantage of ECoG electrodes is their direct placement on the brain, eliminating the effects of the skull on the electric fields. This makes the signal quality, spatial detail and specificity superior to that of EEG. Also, once implanted and successfully set up, a BCI based on implanted electrodes is always available to the user. This comes at the costs of having a brain surgery, although some implementations allow for minimally invasive surgery.

The Utrecht NeuroProsthesis

The Utrecht NeuroProsthesis (UNP) is an invasive BCI developed in the University Medical Center Utrecht (Vansteensel et al., 2016). People with LIS caused by progressive ALS or brainstem stroke were implanted with ECoG electrode strips covering the prefrontal and the motor cortex. Neural

signal changes from the motor cortex, resulting from the individual's attempted hand movements, allow for controlling spelling software on a tablet computer.

Although the UNP offers a reliable communication channel for people unable to communicate otherwise, the possibilities to control the computer (the degrees of freedom) are few: the recorded brain signal is used for selecting letters on a graphical keyboard through attempted movement of the hand, and therefore is used as a 'click' signal that is either on or off. Increasing the degrees of freedom allows for extracting more than a binary signal and therefore faster BCI-based communication, and is one of the aims of BCI research.

Functional MRI in BCI research

While for a practical BCI applications an implantable device is superior to non-invasive solutions, non-invasive techniques such as functional MRI are essential for reseach. In contrast to recording direct electrical neural activity, functional MRI is an imaging technique that measures brain activity indirectly through oxygenation levels of the supplying blood. Oxygenation levels are measured in small volume elements (voxels), going down to sub-millimeter resolution. As active brain cells require more oxygen, voxels in an active brain region show increased oxygenation levels. Functional MRI therefore mainly provides a spatial activation pattern; the temporal resolution is low compared to recordings of electrical activity.

It has been shown that the spatial activity patterns measured with functional MRI are in agreement with patterns obtained using electrophysiological recordings, such as from the gamma frequency band in ECoG (Siero et al., 2014). Therefore, functional MRI is an ideal tool for both surgical planning (that is, the planning of placements of implantable electrodes) as well as for research on finding new successful targets for increasing the degrees of freedom for a BCI.

The primary sensorimotor cortex

The primary sensorimotor cortex comprises the primary motor cortex (M1) and the primary sensory cortex (S1). M1 is the brain area that is mainly responsible for controlling voluntary movements. It is commonly identified as Brodmann area 4 or the precentral gyrus, located in the frontal lobe of both hemispheres. M1 lies at the origin of the corticospinal tract, and contains pyramidal cells, the axons of which (the pyramidal fibers) run from M1 through the brain stem to the spinal cord.

The primary motor cortex is organised in a somatotopic way: the pyramidal cells within M1 are layed-out grouped by the body part they control (Penfield & Boldrey, 1937). Neurons controlling foot movements are located at the dorsal end of the precentral gyrus, and neurons controlling muscles in the face area are located ventrally. The hand is represented halfway, in a region that is often easy to recognise based on its anatomical shape, and is sometimes referred to as the "hand knob" (Yousry et al., 1997).

A large part (90%) of the pyramidal fibers in the corticospinal tract decussate, meaning that they cross over to the other hemisphere (Kim et al., 1993). This implies that the left motor cortex is controlling the right body parts, and vice versa.

Although both the concepts of the somatotopic map and contralateral control have been practically useful, especially in the field of BCI development, recent studies found that in reality, the story on the organization of M1 is likely to be more nuanced. For example, the borders between different body parts cannot always be drawn unambiguously, and some movements are accompanied by brain activity in multiple loci. Also, since part (10%) of the pyramidal fibers do not decussate (Alawieh, Tomlinson, Adkins, Kautz, & Feng, 2017), the motor areas are also suspected to play a role in ipsilateral movement control, that is: the left hemisphere affects body movements on the left side of the body.

In addition to the primary motor cortex, the primary sensory cortex (S1) is increasingly thought to be involved in movement control. It is located on the posterior side of the central gyrus, largely on the postcentral sulcus (or Brodmann areas 1, 2 and 3). This is the area to which sensory receptors in the skin, as well as the proprioceptors in the muscles, project. Similar to M1, S1 has a somatotopic organization. For planning and executing movements, information of both sensory and motor cortices is integrated, which makes S1 an interesting target for a BCI as well.

Decoding movements from the sensorimotor cortex

The somatotopic organization of the sensorimotor cortex can be exploited when designing a BCI based on voluntary movements. After all, if activity is measured somewhere in the cortex, it should be possible to deduce which body part was moved (or intended to move).

Not only does the topographic lay-out of the sensorimotor cortex exist for the body as a whole, also within regions dedicated to a single limb an orderly organization can be found. For example, using both functional MRI and intracranial brain recordings, it has been shown that in the hand area, the areas controlling each finger can be identified (Dechent & Frahm, 2003). Using this feature, we should be able to read (*decode*) from the cortex which finger was flexed and which finger was extended, and the recorded signal should reveal the hand gesture that has been made. If the measurements were sensitive and accurate enough to distinguish between the activation patterns of all 26 gestures associated with the letters of the alphabet, this could be used as a BCI for communication. The user could then just hand-spell the words to type.

In previous work of our group, several hand gestures from the sign lanuage alphabet were successfully decoded from the motor cortex, based on ECoG (Bleichner, Jansma, Sellmeijer, Raemaekers, & Ramsey, 2013; Branco et al., 2017) as well as functional MRI recordings (Bleichner et al., 2016). Brain activity patterns were recorded while the participants were instructed to make several hand gestures, with multiple trials per gesture. A so-called *classifier* was then used to investigate whether brain activity patterns for different gesture types could be discriminated from one another.

A classifier is a machine-learning algorithm able to discriminate between brain activity patterns elicited by, for example, different hand gestures. A classifier is first 'trained' by feeding it with brain activity patterns and telling it to which gesture each pattern belongs. After training, when presented with a new and unknown brain activity pattern, the classifier will find the best matching class, thereby 'predicting' which gesture was associated with the new unknown pattern.

As functional MRI provides spatial activity patterns, a relatively simple classifier can be constructed using so-called 'template matching'. For each gesture, a 'template pattern' is generated by averaging the activity patterns of all trials for that gesture. Then, a new and unknown trial is classified as the gesture whose template shows the highest correlation to the activity pattern of the unknown trial.

In template matching, all voxels contribute equally in calculating the correlation. This has the effect that if many non-informative voxels are included, the classification performance will drop, as the correlation between the trial and the templates will generally be lower. Therefore, an important step in training a classifier is *feature selection*. In this step, only the voxels that are expected to be informative are used for classification. Feature selection should be done using a separate dataset, such as a localiser task, or using a separate part of the data set that is then left out of the rest of the classifier training step.

Besides template (pattern) matching, more sophisticated classifiers can be used which take into account different weights for different features. A support vector machine is a versatile classifier that considers each activation pattern as a single point in a higher dimensional space and tries to find borders between classes (gestures). Although this automatically takes care of voxels that carry less discriminative power, feature selection remains an important step.

The sensorimotor cortex after denervation

People with LIS can *attempt* to make a movement, which does not result in overt motor output. However, it does elicit brain activity in the motor and sensory cortices. This activity can be recorded and used to control a BCI. However, for increasing the degrees of freedom, or the speed of communication, it is essential to investigate what happens if the sensorimotor cortex is detached from the body parts, and whether these attempted movements elicit the same detailed and somatotopically organized activation in the sensorimotor cortex.

Cortical reorganisation

There is evidence that the sensorimotor cortex adapts its organization after denervation. Denervation can occur in LIS after in brain stem lesion, but could also be a consequence of amputation. In both cases, motor output is blocked, while the cortex remains intact. The effects of denervation have been found especially regarding the somatotopic organisation. In animal studies on animals with an amputated limbs, it has for example been observed that the regions representing other body parts 'invade' the area that was formerly representing the (now missing) limb. This has also been found in humans, were functional MRI studies demonstrated a shift of the lip, chin and shoulder

areas into the region controlling a missing hand (Elbert et al., 1994; Lotze, Flor, Grodd, Larbig, & Birbaumer, 2001; Ramachandran, 1993).

Although cortical reorganization has been observed in numerous studies, there is growing evidence that the representation of a missing limb is not completely lost. Research using functional MRI shows activity in the sensorimotor cortex when amputees attempted to move their missing hand (Lotze et al., 2001; Roux et al., 2003; Turner et al., 2001). Even a detailed topographical map of individual fingers has been found in S1 of amputees (Kikkert et al., 2016). However, it is unknown whether such a detailed represention also remains present in M1 after denervation.

Representation of movement activity in the sensorimotor cortex

The aim of the studies presented in this thesis is to investigate the effects of denervation on the representation of movements, or, in other words, whether it still possible to infer what hand gesture is made by a person who has become unable to execute hand motion.

To study the effect of denervation, we first developed a new method for representing spatial brain activation patterns in the human sensorimotor cortex: Cartesian geometric representation with isometric dimensions (Cgrid, Chapter 1). This method uses anatomical landmarks to apply a rectangular grid on a region of interest on the brain. Brain activity patterns from functional MRI can then be projected to this new grid accordingly. The sensorimotor cortex, with its clearly defined boundaries, was particularly suitable for this new visualisation. We have verified the validity of this new method by correlation within- and between-subject activation patterns. Cgrid allows for an easy to interpret visualisation and the possibility of quantitative comparisons of brain activation patterns, for example in longitudinal studies of activity change after denervation.

Decoding movements in amputees

Although BCIs are currently mainly targeted at the LIS population, the prevalence of people with LIS is low. In addition, they require intensive medical care. This makes doing research in this population challenging, especially when multiple subjects need to be included. Therefore, for the studies described in chapters 2-4 of this thesis, people with arm amputation were recruited. In amputees, the motor cortex is still intact, but motor output is absent.

As a measure of 'intactness' (integrity) of the hand representation, we designed a study in which amputees were taught six different hand gestures from the American Sign Language Alphabet. While in the MRI scanner, amputees were instructed to make the hand gestures corresponding to the character that was presented to them on the screen. Gestures were attempted with the phantom hand and (in a separate task) executed with the intact hand (Chapter 2). A control group (subjects without amputation) performed the tasks by executing movements with their left and right hand (in separate tasks). To study whether attempted movements can still be decoded from the denervated sensorimotor cortex in amputees, a classifier was trained on fMRI activation patterns in the contralateral sensorimotor area to discriminate between the different gestures.

Decoding movement from the ipsilateral hemisphere

The majority of fibers in the sensorimotor pathways cross the midline to the contralateral side of the body. That implies that for example the left hand is mostly controlled by motor areas in the right hemisphere. However, not all fibers cross the midline. This means that also the ipsilateral sensorimotor area plays a role in movement control. However, its function is not fully understood.

In Chapter 3, the task and classifier training, as described for Chapter 2, were applied to brain activation patterns of the *ipsilateral* cortex during executed movements of the non-amputated controls (Chapter 3). In addition to discriminating between gestures from the same hand, we have also trained the classifier on activations of both the ipsilateral and contralateral hand in one data set. Finally, the classification approach was applied on movements (or attempted movements) of the ipsilateral hand in subjects with arm amputation (Chapter 4). This provides an important step forward in studying the feasibility for a BCI to be implanted in one hemisphere and being able to decode both hands, even in people unable to perform movements.

References

Alawieh, A., Tomlinson, S., Adkins, D., Kautz, S., & Feng, W. (2017). Preclinical and Clinical Evidence on Ipsilateral Corticospinal Projections: Implication for Motor Recovery. *Translational Stroke Research*, *8*(6), 529–540. doi:10.1007/s12975-017-0551-5

American Congress of Rehabilitation Medicine. (1995). Recommendations for use of uniform nomenclature pertinent to patients with severe alterations in consciousness. *Archives of Physical Medicine and Rehabilitation*, *76*(2), 205–209. doi:10.1016/s0003-9993(95)80031-x

Andersson, P., Pluim, J. P. W., Siero, J. C. W., Klein, S., Viergever, M. A., & Ramsey, N. F. (2011). Real-Time Decoding of Brain Responses to Visuospatial Attention Using 7T fMRI. *PLoS ONE*, *6*(11), e27638. doi:10.1371/journal.pone.0027638

Bleichner, M. G., Freudenburg, Z. V., Jansma, J. M., Aarnoutse, E. J., Vansteensel, M. J., & Ramsey, N. F. (2016). Give me a sign: decoding four complex hand gestures based on high-density ECoG. *Brain Structure and Function*, *221*(1), 203. doi:10.1007/s00429-014-0902-x

Bleichner, M. G., Jansma, J. M., Sellmeijer, J., Raemaekers, M., & Ramsey, N. F. (2013). Give Me a Sign: Decoding Complex Coordinated Hand Movements Using High-Field fMRI. *Brain Topography*, *27*(2), 248. doi:10.1007/s10548-013-0322-x

Branco, M. P., Freudenburg, Z. V., Aarnoutse, E. J., Bleichner, M. G., Vansteensel, M. J., & Ramsey, N. F. (2017). Decoding hand gestures from primary somatosensory cortex using high-density ECoG. *NeuroImage*, *147*, 130. doi:10.1016/j.neuroimage.2016.12.004

Dechent, P., & Frahm, J. (2003). Functional somatotopy of finger representations in human primary motor cortex. *Human Brain Mapping*, *18*(4), 272. doi:10.1002/hbm.10084

Elbert, T., Flor, H., Birbaumer, N., Knecht, S., Hampson, S., Larbig, W., & Taub, E. (1994). Extensive reorganization of the somatosensory cortex in adult humans after nervous system injury. *NeuroReport*, *5*(18), 2593. doi:10.1097/00001756-199412000-00047

Farwell, L. A., & Donchin, E. (1988). Talking off the top of your head: toward a mental prosthesis utilizing event-related brain potentials. *Electroencephalography and Clinical Neurophysiology*, *70*(6), 510–523. doi:10.1016/0013-4694(88)90149-6

Huggins, J. E., Wren, P. A., & Gruis, K. L. (2011). What would brain-computer interface users want? Opinions and priorities of potential users with amyotrophic lateral sclerosis. *Amyotrophic Lateral Sclerosis*, *12*(5), 318–324. doi:10.3109/17482968.2011.572978

Jacobs, J., & Kahana, M. J. (2010). Direct brain recordings fuel advances in cognitive electrophysiology. *Trends in Cognitive Sciences*, *14*(4), 162–171. doi:10.1016/j.tics.2010.01.005

Kageyama, Y., He, X., Shimokawa, T., Sawada, J., Yanagisawa, T., Shayne, M., … Hirata, M. (2020). Nationwide survey of 780 Japanese patients with amyotrophic lateral sclerosis: their status and expectations from brain–machine interfaces. *Journal of Neurology*, *267*(10), 2932–2940. doi:10.1007/s00415-020-09903-3

Kikkert, S., Kolasinski, J., Jbabdi, S., Tracey, I., Beckmann, C. F., Johansen-Berg, H., & Makin, T. R. (2016). Revealing the neural fingerprints of a missing hand. *ELife*, *2016*(5), e15292. doi:10.7554/elife.15292.001

Kim, S., Ashe, J., Hendrich, K., Ellermann, J., Merkle, H., Ugurbil, K., & Georgopoulos, A. (1993). Functional magnetic resonance imaging of motor cortex: hemispheric asymmetry and handedness. *Science*, *261*(5121), 615–617. doi:10.1126/science.8342027

Lotze, M., Flor, H., Grodd, W., Larbig, W., & Birbaumer, N. (2001). Phantom movements and pain An fMRI study in upper limb amputees. *Brain*, *124*(11), 2268. doi:10.1093/brain/124.11.2268

Machado, S., Araújo, F., Paes, F., Velasques, B., Cunha, M., Budde, H., … Ribeiro, P. (2010). EEG-based Brain-Computer Interfaces: An Overview of Basic Concepts and Clinical Applications in Neurorehabilitation. *Reviews in the Neurosciences*, *21*(6), 451–468. doi:10.1515/revneuro.2010.21.6.451

Mellinger, J., Schalk, G., Braun, C., Preissl, H., Rosenstiel, W., Birbaumer, N., & Kübler, A. (2007). An MEG-based brain–computer interface (BCI). *NeuroImage*, *36*(3), 581–593. doi:10.1016/j.neuroimage.2007.03.019

Naseer, N., & Hong, K.-S. (2015). fNIRS-based brain-computer interfaces: a review. *Frontiers in Human Neuroscience*, *9*, 3. doi:10.3389/fnhum.2015.00003

Penfield, W., & Boldrey, E. (1937). Somatic motor and sensory representation in the cerebral cortex of man as studied by electrical stimulation. *Brain*, *60*(4), 389–443. doi:10.1093/brain/60.4.389

Ramachandran, V. S. (1993). Behavioral and magnetoencephalographic correlates of plasticity in the adult human brain. *Proceedings of the National Academy of Sciences*, *90*(22), 10413. doi:10.1073/pnas.90.22.10413

Rezeika, A., Benda, M., Stawicki, P., Gembler, F., Saboor, A., & Volosyak, I. (2018). Brain-Computer Interface Spellers: A Review. *Brain Sciences*, *8*(4), 57. doi:10.3390/brainsci8040057

Rousseau, M.-C., Baumstarck, K., Alessandrini, M., Blandin, V., Villemeur, T. B. de, & Auquier, P. (2015). Quality of life in patients with locked-in syndrome: Evolution over a 6-year period. *Orphanet Journal of Rare Diseases*, *10*(1), 88. doi:10.1186/s13023-015-0304-z

Roux, F.-E., Lotterie, J.-A., Cassol, E., Lazorthes, Y., Sol, J.-C., & Berry, I. (2003). Cortical Areas Involved in Virtual Movement of Phantom Limbs: Comparison with Normal Subjects. *Neurosurgery*, *53*(6), 1342–1353. doi:10.1227/01.neu.0000093424.71086.8f

Sellers, E. W., & Donchin, E. (2006). A P300-based brain–computer interface: Initial tests by ALS patients. *Clinical Neurophysiology*, *117*(3), 538–548. doi:10.1016/j.clinph.2005.06.027

Siero, J. C. W., Hermes, D., Hoogduin, H., Luijten, P. R., Ramsey, N. F., & Petridou, N. (2014). BOLD matches neuronal activity at the mm scale: A combined 7T fMRI and ECoG study in human sensorimotor cortex. *NeuroImage*, *101*, 177. doi:10.1016/j.neuroimage.2014.07.002

Smith, E., & Delargy, M. (2005). Locked-in syndrome. *BMJ*, *330*(7488), 406–409. doi:10.1136/bmj.330.7488.406

Sorger, B., & Goebel, R. (2020). Brain-Computer Interfaces. *Handbook of Clinical Neurology*, *168*, 289–302. doi:10.1016/b978-0-444-63934-9.00021-4

Turner, J. A., Lee, J. S., Martinez, O., Medlin, A. L., Schandler, S. L., & Cohen, M. J. (2001). Somatotopy of the motor cortex after long-term spinal cord injury or amputation. *IEEE Transactions on Neural Systems and Rehabilitation Engineering*, *9*(2), 154. doi:10.1109/7333.928575

Vansteensel, M. J., Pels, E. G. M., Bleichner, M. G., Branco, M. P., Denison, T., Freudenburg, Z. V., ... Ramsey, N. F. (2016). Fully Implanted Brain–Computer Interface in a Locked-In Patient with ALS. *New England Journal of Medicine*, *375*(21), 2060. doi:10.1056/nejmoa1608085

Wolpaw, J. R. (2007). Brain-computer interfaces as new brain output pathways. *The Journal of Physiology*, *579*(3), 613–619. doi:10.1113/jphysiol.2006.125948

Yousry, T. A., Schmid, U. D., Alkadhi, H., Schmidt, D., Peraud, A., Buettner, A., & Winkler, P. (1997). Localization of the motor hand area to a knob on the precentral gyrus. A new landmark. *Brain*, *120*(1), 141–157. doi:10.1093/brain/120.1.141

CHAPTER 1

A novel 2d standard Cartesian Representation for the human sensorimotor cortex

—

Bruurmijn MLCM, Schellekens W, Raemaekers MAH, Ramsey NF. A Novel 2D Standard Cartesian Representation for the Human Sensorimotor Cortex. Neuroinformatics. 2020 Apr;18(2):283-293. doi: 10.1007/s12021-019-09441-y. PMID: 31797264; PMCID: PMC7083812.

Abstract

For some experimental approaches in brain imaging, the existing normalization techniques are not always sufficient. This may be the case if the anatomical shape of the region of interest varies substantially across subjects, or if one needs to compare the left and right hemisphere in the same subject.

Here we propose a new standard representation, building upon existing normalization methods: Cgrid (Cartesian geometric representation with isometric dimensions). Cgrid is based on imposing a Cartesian grid over a cortical region of interest that is bounded by anatomical (atlas-based) landmarks. We applied this new representation to the sensorimotor cortex and we evaluated its performance by studying the similarity of activation patterns for hand, foot and tongue movements between subjects, and similarity between hemispheres within subjects. The Cgrid similarities were benchmarked against the similarities of activation patterns when transformed into standard MNI space using SPM, and to similarities from FreeSurfer's surface-based normalization.

For both between-subject and between-hemisphere comparisons, similarity scores in Cgrid were high, similar to those from FreeSurfer normalization and higher than similarity scores from SPM's MNI normalization. This indicates that Cgrid allows for a straightforward way of representing and comparing sensorimotor activity patterns across subjects and between hemispheres of the same subjects.

Acknowledgements

This work was made possible by the ERC Advanced Grant FP7-IDEAS-ERC 320708 (iCONNECT) granted to NFR.

There are no conflicts of interest.

Introduction

In functional brain imaging (functional MRI; fMRI), spatial normalization is often applied, where scans are transformed into a common space, so that the same coordinates in different subjects correspond to the homologous anatomical location in the brain. This makes statistics at a group level possible, allowing for the comparison of brain activity patterns between groups of subjects, for example patients and healthy controls. The quality of the normalization is a central determinant of the quality of the group-level statistics (Pizzagalli, Auzias, Delon-Martin, & Dojat, 2013), making accurate normalization a crucial part of the processing pipeline.

To join multiple brain images together for comparison of brain activation between groups (for example patients versus controls) or determining common areas of activation (mapping), several options are available and widely used. One is 3D normalization either using a single image (for example Talairach template), an average of co-registered images from multiple individuals unrelated to the study (for example MNI templates), or an average of study participants themselves (for example DARTEL (Ashburner, 2007)). Alternatively, activity can be mapped on an inflated brain, where sulci are projected to a spherical surface or a flattened cortex map (Fischl, Sereno, & Dale, 1999), both of which allow for subsequent normalization (Qiu & Miller, 2007; Van Essen e.a., 2001).

For certain research questions, the existing techniques for representing brain activity patterns do not suffice, due to the fact that borders between regions (defined by gyral and sulcal patterns) reflect the natural 3D folding patterns of the brain (Pizzagalli e.a., 2013). Some applications, for example a quantitative comparison of topographical mapping of sensory and motor functions, would benefit from a representation in the form of a 2D rectangular mesh. This constitutes an easy to interpret and uniform space, and would allow for easy comparison of activation patterns and distances between foci, while accounting for individual differences in the shape and size of sensorimotor cortex. Moreover, such a representation could make cross-hemispheric comparisons more direct and accurate, something which is not possible using existing normalization methods, as they typically do not conduct a registration of the two hemispheres. It also would accommodate a more direct comparison or combination of data from different studies.

A two-dimensional, grid-shaped representation has been described for the central sulcus, which was obtained by extraction of a 3D mesh of the central sulcus, which was subsequently reparametrized with the y axis along the direction of the central sulcus, and the x axis along the direction of the sulcal depth (Coulon e.a., 2011). Although Coulon's method elegantly maps the sulcus onto a grid, the sensorimotor cortex in fact extends also into the adjacent gyri, which is not included in their approach. Therefore, it is worthwhile transforming the whole pre- and postcentral gyrus into a Cartesian grid.

Here, we propose a novel extension to existing methods for standardization of regions in the human brain allowing for quantitative comparisons, which maps the whole gyri to a Cartesian grid: Cgrid (Cartesian geometric representation with isometric dimensions). Cgrid builds upon methods for inflating the cortex, and constitutes imposing a Cartesian grid on the region of interest

using anatomical (atlas-based) landmarks. One brain region that seems particularly suitable for transforming into a rectangular mesh are the primary sensory and motor areas (S1 and M1), because of their more or less rectangular shapes with clear top, bottom and side boundaries. Cgrid is therefore first applied and validated on the precentral and postcentral gyrus. This special case is called 'Cgrid-SMX', where SMX stands for 'sensorimotor cortex'.

Cgrid is meant to extend upon standard data preprocessing, and adding the possibility to easily compare patterns between subjects and between hemispheres. The presented implementation requires segmentation and atlas-based parcellation in FreeSurfer (Fischl, 2012) and flat mapping with Caret (Van Essen e.a., 2001), but accommodates any similar method.

The Cgrid-SMX mapping was evaluated using data from 20 healthy volunteers who each performed four motor tasks (moving left hand, right hand, feet, and tongue). As activation patterns for these basic motor tasks are expected to be similar across subjects, and within subjects across hemispheres, the similarities of the patterns of activity were calculated as a measure of validity of the transformation. The results were compared to the similarities obtained by SPM's normalization to MNI space (a commonly used normal space) as well as to the similarity of activation patterns after FreeSurfer normalization. This was to provide a benchmark for the performance of our new method.

Methods

Subjects

Twenty healthy volunteers participated in this study (age 26.7±8.8 years, 9 females, all right handed). Subjects had no history of neurological or psychiatric disorders. Data acquisition was approved by the medical-ethical committee of the University Medical Center Utrecht and all subjects gave their written informed consent in agreement with the declaration of Helsinki (2013).

MRI data acquisition and analysis

MRI data were recorded using a Philips 3T Ingenia system. A structural T1-weighted MRI image was acquired (TR/TE = 8.4/3.8 ms, voxel size: 1.00 × 1.00 × 1.00 mm^3), followed by functional EPI images (TR/TE = 2500/39 ms, flip angle = 75°, axial orientation, FOV (AP, FH, LR) = 235 × 120 × 200 mm^3, interleaved slice ordering, acquisition matrix 80 × 40 × 80, voxel size: 2.94 × 3.00 × 2.94 mm^3). For data preprocessing, we used the software packages FreeSurfer (Fischl, 2012), Caret (Van Essen e.a., 2001) and SPM (Friston, Ashburner, Kiebel, Nichols, & Penny, 2007). Custom scripts for the Cgrid-SMX normalization were written in Matlab (The MathWorks Inc., Natick, MA) and IDL (Exelis Visual Information Solutions, Boulder, Colorado).

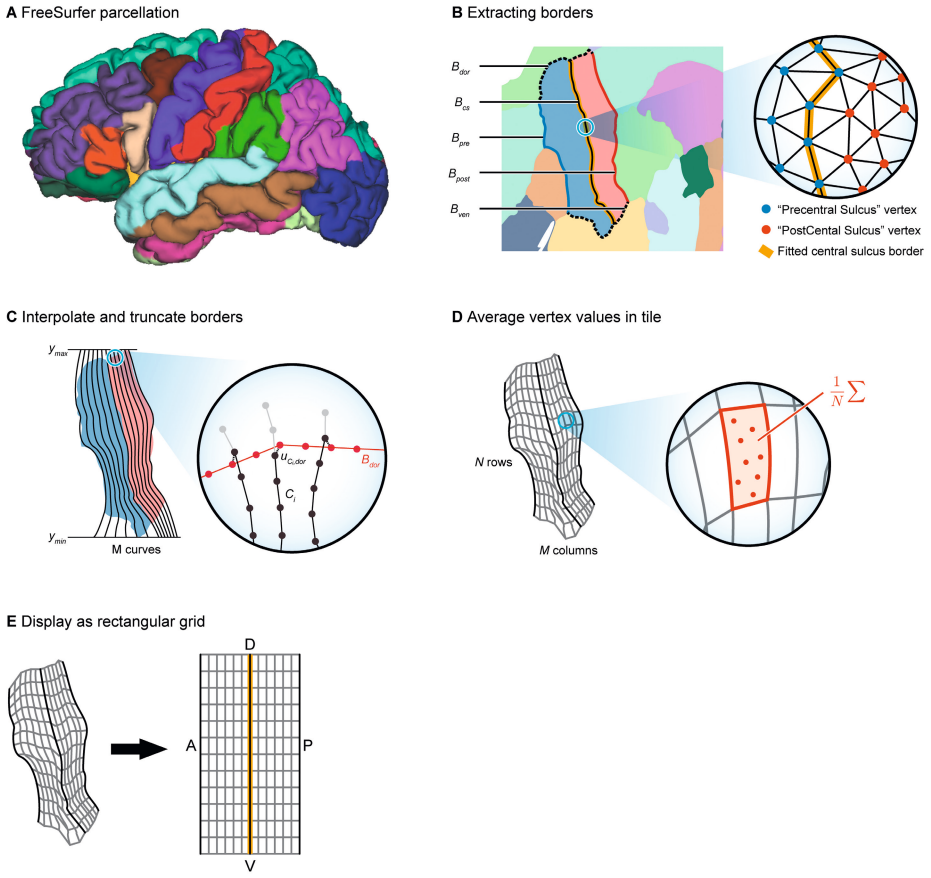

Figure 1: *Applying Cgrid to the sensorimotor cortex. A: Brain parcellation from FreeSurfer. B: Flatmap representation, with the five borders that were extracted using labels from FreeSurfer's cortical parcellation according to Eq. 2-6 (solid lines: "vertical borders" and dashed lines: "horizontal borders"). A vertex was considered to be part of a border if it had a neighboring vertex with another FreeSurfer label. C: 10th-order polynomials were fitted through the three vertical borders, and in-between vertical curves were created by interpolation between y_min and y_max. Each curve C_i was then truncated using the horizontal dorsal and ventral borders (drawn in red in the inset) by selecting the node points closest to any node on these horizontal borders. D: Truncated vertical curves were divided into vertical segments, resulting in N×M "tiles". To map beta values from statistical maps to Cgrid, a beta value for each tile is calculated by averaging the beta values of vertices inside that tile. E: A Cgrid can be visualized as a rectangular grid, where the central sulcus is the middle, the anterior aspect (A) on the left side, posterior (P) on the right side, ventral (V) at the bottom and dorsal (D) at the top.*

Structural MRI preprocessing

For each subject, the cortical surface was reconstructed from the T1-weighted image using FreeSurfer, and automatically parcellated into ROIs using the Desikan-Killiany atlas (Desikan e.a., 2006) (Figure 1A). Each individual's surface was then flattened using Caret, making sure that the central sulcus was oriented vertically (that is, dorsal aspect at the top, ventral aspect at the bottom, which is necessary for the Cgrid procedure).

Definition of the Cgrid standard space

The flattened cortex was represented as a face-vertex mesh in 2D. Each vertex v has an x- and y-coordinate, v_x and v_y. Notably, because a flat map is a deformation of a spherical surface, distances on the flat map will not exactly correspond to distances on the brain. Therefore we will consider distances on the flat map to be measured in arbitrary units (a.u.), although 1 a.u. will approximate 1 mm. Each vertex was tagged with the ROI label indicating the underlying Desikan-Killiany atlas region, and $L(v)$ denotes the ROI label of vertex v. The topology describes which vertices are connected to form the faces of the mesh. Let the set of neighboring vertices of vertex be denoted by Ω_v.

The first step in defining the Cgrid standard space was the extraction of five anatomical borders. A border B between two ROIs was defined as the set of vertices having ROI label L_1, while having one or more neighboring vertices with another ROI label L_2 :

$$B(L_1, L_2) = \{v | L(v) = L_1, \exists w \in \Omega_v : L(w) = L_2\} \quad \text{(Eq. 1)}$$

Three 'vertical borders' (the central sulcus border B_{cs}, the precentral sulcus border B_{pre} and the postcentral sulcus border B_{post}, Figure 1B) were defined using Eq. 1, where curly brackets indicate that L_2 can be one of the given labels:

$$B_{cs} = B(\text{"Precentral gyrus"}, \text{"Postcentral gyrus"}) \quad \text{(Eq. 2)}$$

$$B_{pre} = B(\text{"Precentral gyrus"}, \{\text{"Pars opercularis"}, \text{"Caudal middle frontal"}, \text{"Superior frontal"}\}) \quad \text{(Eq. 3)}$$

$$B_{post} = B(\text{"Postcentral gyrus"}, \{\text{"SupraMarginal"}, \text{"SuperiorParietal"}\}) \quad \text{(Eq. 4)}$$

Two 'horizontal borders' were defined, constraining the sensorimotor cortex at the dorsal (B_{dor}) and ventral (B_{ven}) side:

$$B_{dor} = B(\{\text{"PrecentralGyrus"}, \text{"PostcentralGyrus"}\}, \text{"ParacentralLobule"}) \quad \text{(Eq. 5)}$$

$$B_{ven} = B(\{\text{"PrecentralGyrus"}, \text{"PostcentralGyrus"}\}, \text{"Insula"}) \quad \text{(Eq. 6)}$$

The next step consisted of fitting a 10th order polynomial through each of the three vertical borders. The order 10 was chosen empirically and was found to result in a good balance between capturing the shape of the borders and still allowing for extrapolation, which is needed in a next step. For generating these fits, the vertical coordinate of the vertices (v_y, the coordinate on the dorsal-ventral axis) was treated as the independent variable, and the horizontal coordinate (v_x, the coordinate on the anterior-posterior axis) as the dependent variable. The vertical curves were resampled and extrapolated such that they ran from y_{min} to y_{max} in unit steps (arbitrary units), thereby making sure that they covered the whole sensorimotor cortex, where y_{min} and y_{max} were defined by:

$$y_{min} = \min\{v_y | v \in B_{ven}\} \quad \text{(Eq. 7)}$$

$$y_{max} = \max\{v_y | v \in B_{dor}\} \quad \text{(Eq. 8)}$$

In-between vertical polynomial curves were then created by linear interpolation of each of the 11 polynomial coefficients regularly at $M + 1$ points, thereby effectively dividing the sensorimotor cortex into M "columns" (Figure 1C).

As each in-between curve C_i ran from y_{min} and y_{max}, some of them extended too far outside the sensorimotor cortex. Therefore, they needed to be truncated at the dorsal and ventral borders. Let the X_i nodes on the ith interpolated vertical curve $C_i = \{u_j | j = 1..X_i\}, u = (u_x, u_y)$. Ventral and dorsal cuts for curve C_i were defined as the nodes $u_{C_i,med}$ and $u_{C_i,dor}$ on the interpolated curves closest to any point on B_{ven} and B_{dor}, where $d(u, v)$ denotes the Euclidean distance between vertices (v) and nodes on the curve (u):

$$u_{C_i,ven} = \underset{u \in C_i}{\operatorname{argmin}}\, d(u, v) \qquad \forall v \in B_{ven} \quad \text{(Eq. 9)}$$

$$u_{C_i,dor} = \underset{u \in C_i}{\operatorname{argmin}}\, d(u, v) \qquad \forall v \in B_{dor} \quad \text{(Eq. 10)}$$

Each curve C_i was then divided into N_{rows} segments by resampling C_i from $u_{C_i,med}$ to $u_{C_i,dor}$ in 0.1 arbitrary unit steps. For this step, the length of each curve was first estimated by:

$$l_i = \sum_{j=1}^{X_i - 1} d(u_j, u_{j+1}) \quad \text{(Eq. 11)}$$

Each of the vertical curves was then resampled again, where the distances between the nodes equaled l_i/N. This resulted in a grid imposed on the sensorimotor cortex, consisting of N rows and M columns, denoted as $N \times M$ "tiles".

The final step consisted of mapping all vertices from the cortical surface into the newly defined standard space, by treating each tile as a polygon and determining which vertices are enclosed by that polygon. As a result, each vertex was associated with one tile in Cgrid. This association allows for mapping any kind of MRI data to Cgrid space, for example anatomical data, such as cortical thickness, or functional data. This mapping consists of two steps: first, the MRI data needs to be projected onto the cortical surface reconstruction vertices (using tools from the FreeSurfer package). Second, per tile a value (thickness, functional beta, etc.) can be calculated by taking the mean of all vertices for that tile (Figure 1D). In the Evaluation section, the mapping to Cgrid-SMX space is demonstrated with task-based functional data.

By convention, Cgrid visualizations in this paper are displayed (and processed) such that the precentral sulcus border is always on the left, and the postcentral border is always on the right. This means that the left half of the Cgrid images represents the precentral gyrus (M1), and the right part represents the postcentral gyrus (S1), regardless of the hemisphere (Figure 1E).

Evaluation

Task-based fMRI activation maps for the 20 subjects were mapped to Cgrid-SMX. Activation patterns were generated for four movement tasks (see 'Task design', below). Cgrid-SMX space was evaluated by calculating the within-subject (left-right) and between-subject similarities of activation patterns in Cgrid space. For this, a Pearson correlation between Cgrid-SMX activation patterns was used. To benchmark the results, Cgrid-SMX pattern similarities were then compared to within- and between-subject pattern similarities in MNI space from SPM. We focused on four regions of interest (ROIs): left M1, left S1, right M1, and right S1.

Task design

Subjects executed four separate movement tasks: following a visual cue, subjects were instructed to move their right hand ("Hand-Right task", opening and closing), their left hand ("Hand-Left task", opening and closing), their tongue ("Tongue task", moving from left to right), or both feet ("Feet task", rotating both feet about the ankle simultaneously). Each task was set up as a block design, with pseudorandom block durations ranging from 15 to 45 seconds followed by rest blocks ranging from 15 to 45 seconds.

Cgrid activation maps

Task data was slice-time corrected, realigned and coregistered to the subject's anatomical scan to correct for movements using SPM12 (http://www.fil.ion.ucl.ac.uk/spm/). A GLM analysis with one regressor for movement was applied to the task data using the contrast 'movement versus baseline', resulting in one statistical map (beta map) per task. These beta maps were then projected onto the cortical surface reconstruction vertices using FreeSurfer (with projection fraction 0.5 and a smoothing of 6 mm FWHM). A beta value was then computed per tile by taking the mean of the beta values for all vertices within that tile. This resulted in beta maps in Cgrid-SMX space for each of the four ROIs.

MNI activation maps

To benchmark the performance of Cgrid space, functional scans were also normalized to MNI for all subjects using SPM12, and likewise smoothed with 6 mm FWHM Gaussian kernel. After normalization and smoothing, a GLM with one regressor for movement was fit to the task data and statistical maps were created using the contrast 'movement versus baseline'.

Four ROI masks in MNI space (left M1, left S1, right M1, and right S1) were initially taken from the Brainnetome Atlas (Fan e.a., 2016). Since the method of calculating similarities between hemispheres requires left and right ROIs to be symmetrical, the right M1 was flipped to the left hemisphere, and combined with left M1 (voxel-wise union). The resulting ROI was then flipped back to the right hemisphere. The same was done for S1. The resulting ROIs were used to mask the beta map and obtain activity patterns for the four tasks in each of the four ROIs.

Within-subject pattern similarity (left-right)

As the Cgrid-SMX space is expected to minimize anatomical differences between the left and right motor cortex, left and right activation patterns should demonstrate high similarity within subjects. For the Feet task and Tongue task, the similarity between left and right Cgrid patterns was calculated using Pearson correlation. For the hand tasks, the correlation between contralateral activation patterns was calculated, that is: the similarity between the left pattern from the Hand-Right task and the right pattern from the Hand-Left task. All Pearson correlations were transformed to 'similarity (z-)scores' using the Fisher z-transform (which is equal to the hyperbolic function arctanh), to allow averaging and statistical testing across subjects. The 6 similarity scores for each subject (Tongue, Hand and Feet for M1 and S1) were then averaged per subject over ROIs and tasks to obtain a single within-subject (left-right) similarity per subject for Cgrid. Similarity scores can be transformed back to (group-averaged) correlations using the inverse Fisher z-transform (the hyperbolic function tanh).

Similarity scores for MNI space were calculated similarly, and differences in similarity scores between Cgrid-SMX and MNI space were assessed using a paired-samples t-test.

Between-subject pattern similarity

To assess between-subject pattern similarity, a per-subject similarity score was calculated using a leave-one-out approach, where a pattern of the subject under investigation was correlated with the mean patterns of the other subjects. This resulted in similarity scores per task and ROI for every subject, which were then averaged to obtain a mean similarity score per subject. The same approach was applied to the patterns in MNI space, and a paired-samples t-test was conducted to compare the between-subject similarity scores for Cgrid and MNI space.

Since MNI is a 3D space and Cgrid is a 2D space, the differences in the dimensionality of the approaches might bias the performance. FreeSurfer includes surface based normalization through spherical registration, using the FS-average as template. All subjects were normalized using this approach. Then, activation patterns in FS-average space were extracted by selecting the beta valvues in the nodes of the pre- and postcentral gyrus. A between-subject similarity was calculated per subject following the same scheme as for the Cgrid and MNI, using a leave-one-out approach.

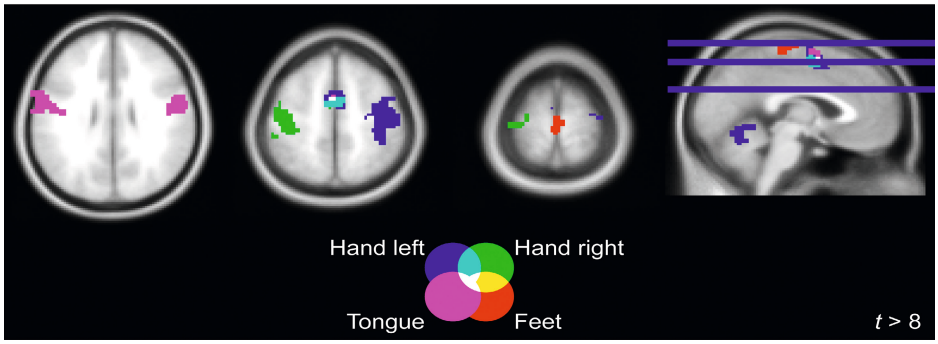

Figure 2: *Group activation map of the movement tasks (contrasts used: Feet > baseline, Tongue > baseline, Left hand > baseline, and Right hand > baseline). Contrasts are displayed on a standard MNI brain with threshold t > 8.*

Effect of smoothing on between-subject correlations

For the within- and between-subject similarities, a Gaussian smoothing kernel of 6 mm FWHM was used. However, since the impact of a smoothing kernel can be different between Cgrid (2D space) and MNI space (3D), we tested the effect of the smoothing kernel on the similarities. This was done by repeating the between-subject analysis described above, using different smoothing kernels both in MNI space and on the cortical surface in the Cgrid pipeline (see above). Kernel sizes of 4, 6, 8, 10, 12, 18, 25 and 35 mm FWHM were used. A two-way repeated measures ANOVA was conducted to compare the effects of method and smoothing kernel size on the between-subject similarity score.

Results

Defining Cgrid space

Surfaces reconstructions of all 20 subjects were generated using FreeSurfer. The five borders (central sulcus, precentral sulcus, postcentral sulcus, ventral border, and dorsal border) were extracted and visual inspection of the fitted curves confirmed that a 10th order polynomial fit was sufficient to capture the shape of the borders accurately in all subjects.

A Cgrid standard space was defined and resulted in a 28×84 tiled mesh per hemisphere in all subjects. A tile covered 2.62±0.71 mm^2 (mean±sd) and contained 6±1 vertices. On average, 21±10 tiles (1.8% of all tiles) did not contain any vertices that were labelled as being part of the sensorimotor cortex; these tiles were mostly located at the edges of the Cgrid and were excluded from the correlation analyses.

Mapping beta maps to Cgrid space

Volumetric statistical group maps of the tasks showed sensorimotor activation in distinctive foot, hand, and tongue areas (see Figure 2). The feet and tongue tasks activated both the left and right sensorimotor cortex. There was no excessive motion (mean absolute translation over all subjects and tasks: 0.17 ± 0.10 mm; mean rotation: $2.8\times10^{-3} \pm 2.3\times10^{-3}$ degrees).

Visual inspection of the resulting Cgrid group-mean activation maps, averaged over subjects, confirmed that Cgrid was capable of capturing the different activation hotspot patterns associated with movement of the respective body parts (Figure 3). Feet activation was located at the dorsal side of the sensorimotor cortex, tongue activation was located towards the ventral side, and hand activation was located mostly contralaterally at approximately 1/3 of the dorsal-ventral axis.

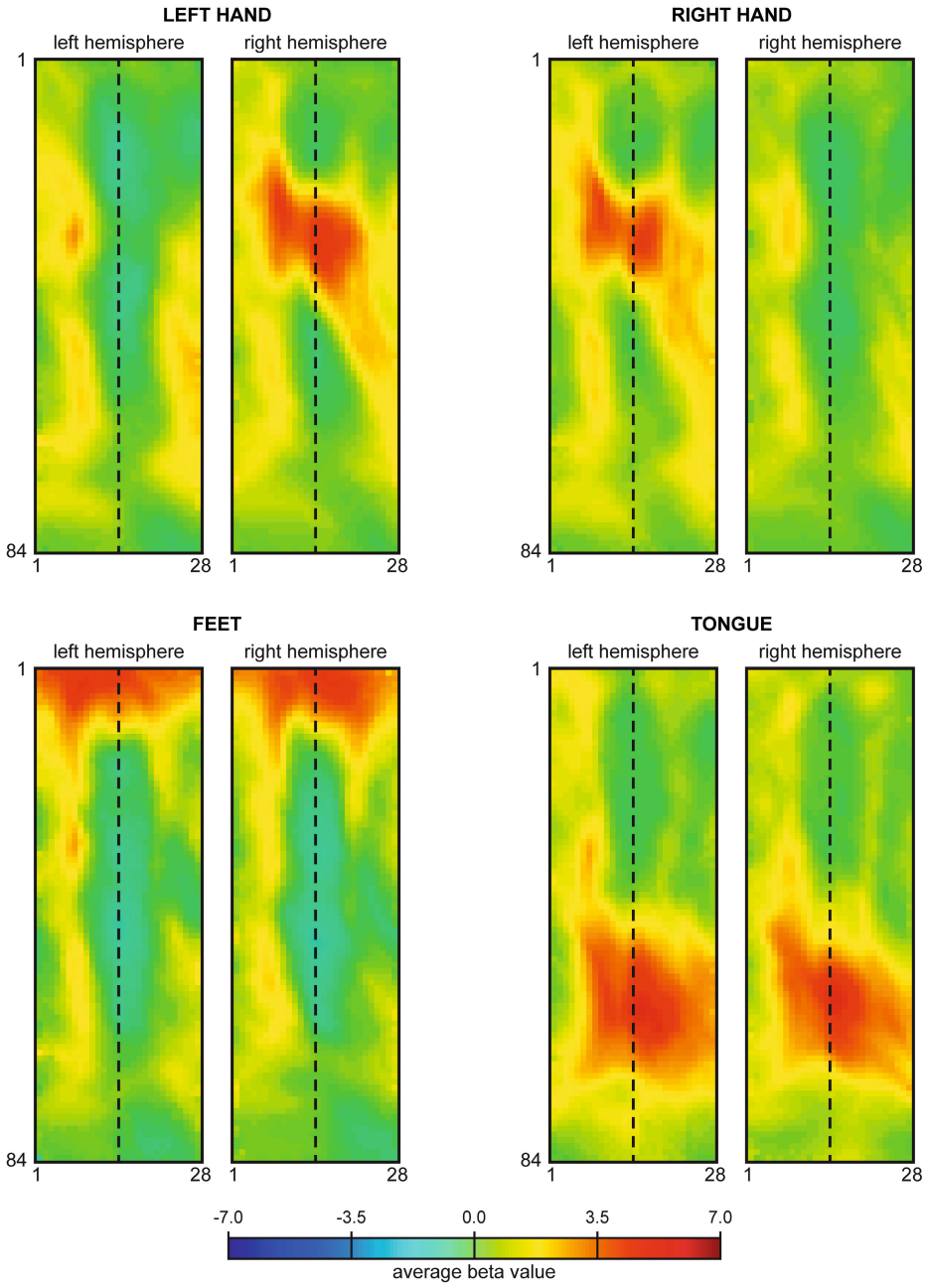

Figure 3: *Beta maps in Cgrid, averaged over 20 subjects, for every task in both hemispheres. The dashed line indicates the central sulcus. The left border lies in the precentral sulcus, the right border on the postcentral sulcus (see fig 1B). Note that for all Cgrid-SMXs the left side is anterior in the brain.*

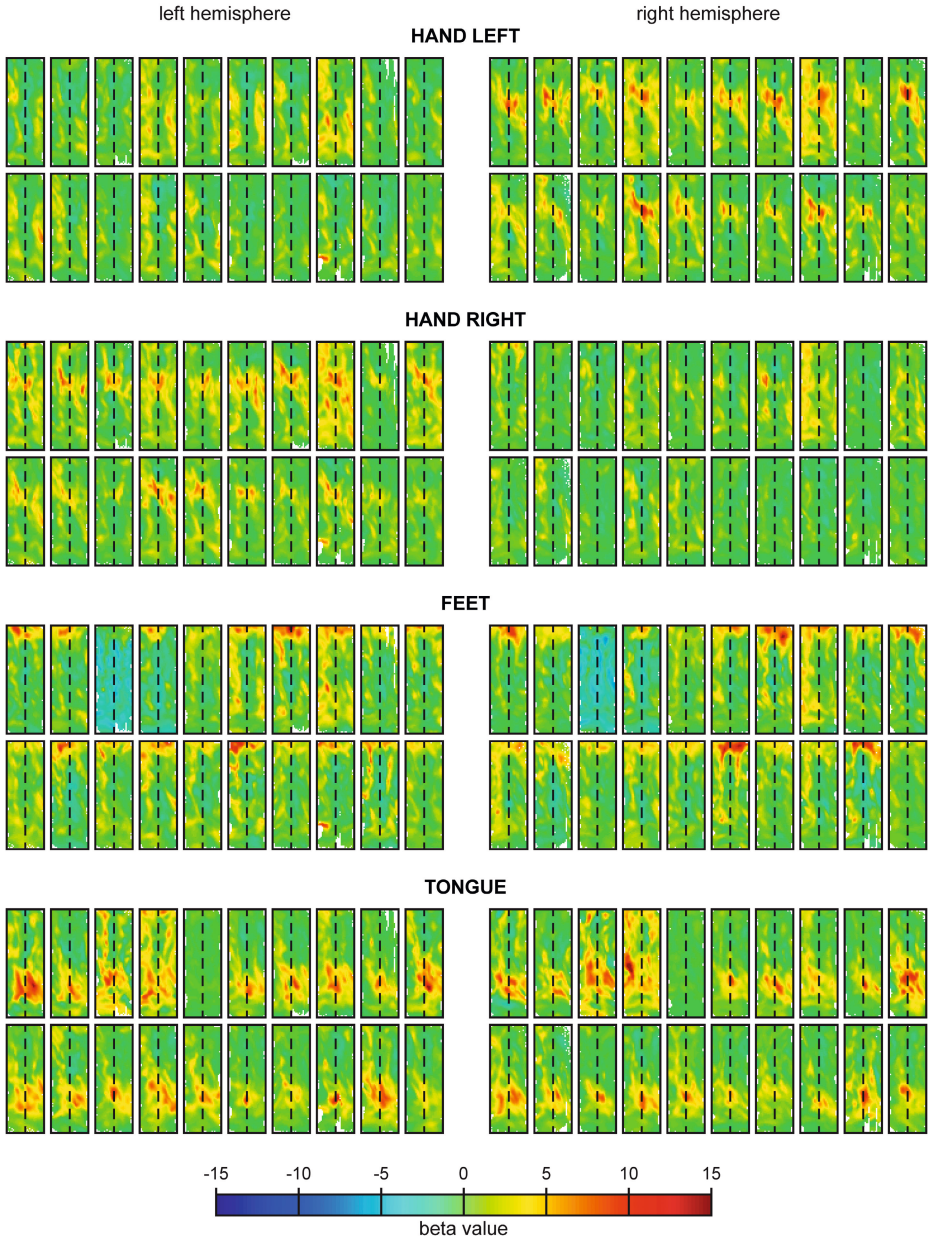

Figure 4: *Beta maps in Cgrid for every subject (N=20) and every task in both hemispheres.*

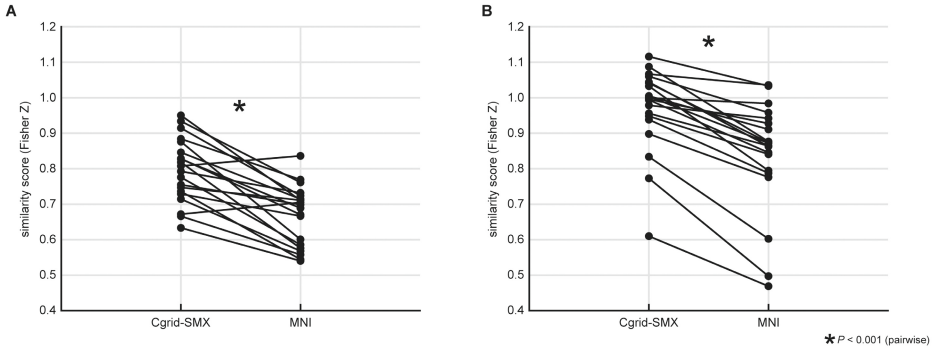

Figure 5: *A: Within-subject similarities (averaged over tasks and hemispheres) per subject, for Cgrid (red dots) and MNI space (blue dots). Similarities in Cgrid space were significantly higher than in MNI space. B: Between-subject similarities (averaged over tasks and hemispheres) per subject, for Cgrid (red dots) and MNI space (blue dots). Similarities in Cgrid space were significantly higher than in MNI space.*

Average activation hotspots for all tasks were mostly located within the central sulcus. Whereas the group average of Cgrid patterns demonstrated strong hotspot-like activation, task activation patterns per individual did not necessarily consist of only a single hotspot, but were sometimes complex patterns, varying somewhat across subjects (Figure 4).

Within-subject pattern similarity (left-right)

The similarities between left and right hemispheric patterns within subjects from feet, hand, and tongue tasks were computed using Fisher z-transformed Pearson correlations for both Cgrid and MNI space. A second-level paired t-test demonstrated a significantly higher similarity in Cgrid (Fisher Z = 0.80 ± 0.09, mean ± standard deviation) than in MNI space (Fisher Z=0.67 ± 0.08); $t(19) = 6.70$, $p < 0.001$ (Figure 5A).

Between-subject pattern similarity

The similarity of patterns between subjects was calculated per task and per ROI using Pearson correlations using a leave-one-out approach. A paired t-test demonstrated a significantly higher correlation in Cgrid (Fisher Z = 0.92 ± 0.09) than in MNI space (Fisher Z = 0.84 ± 0.16); $t(19) = 8.25$, $p < 0.001$ (Figure 5B).

Similarity scores were also calculated directly using FreeSurfer surfaces in averaged space (FS-average). There was no significant difference between similarity scores Cgrid and FS-average (Fisher Z = 0.93 ± 0.10); $t(19) = -1.84$, $p = 0.082$ (Figure 6).

Effect of smoothing on between-subject correlations

Calculating between-subject similarities with different smoothing kernels resulted in higher similarity scores with larger smoothing kernels for both Cgrid-SMX and MNI space (Figure 7). A two-way repeated measures ANOVA showed a significant effect of method on the between-subject similarity score, indicating that Cgrid similarities are higher than similarities in MNI space for all smoothing kernel sizes.

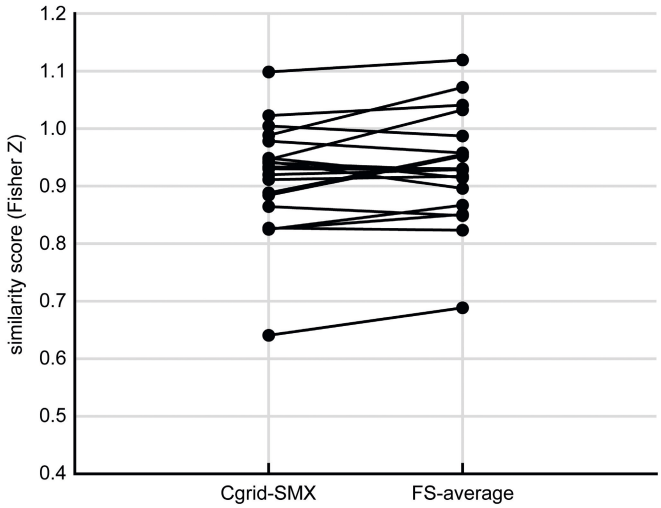

Figure 6: *Between-subject similarities in Cgrid-SMX and in the FreeSurfer normalized space (FS-average). There was no significant difference in similarity scores between the two methods.*

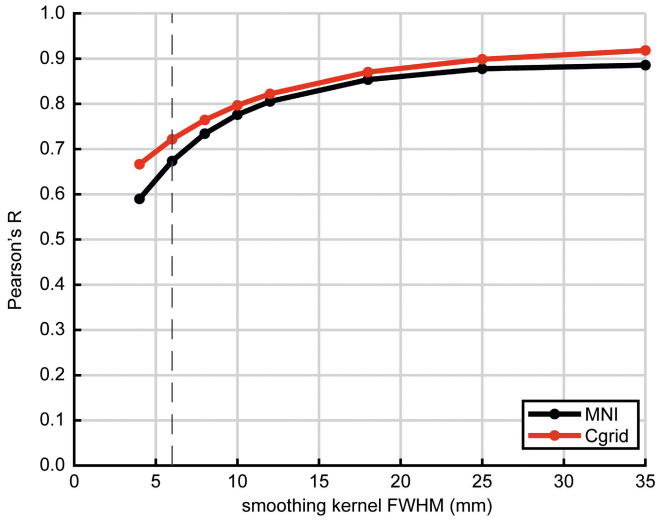

Figure 7: *Between-subject correlations (averaged over tasks and ROIs) as a function of smoothing kernel size. The dashed line indicated the kernel size used for smoothing in both the Cgrid-SMX and MNI space analyses throughout the text (6 mm FWHM).*

Discussion

We introduce Cgrid-SMX as a Cartesian representation of the sensorimotor cortex, based on anatomical atlas-based landmarks and building upon existing data processing methods. Cgrid imposes a grid on the sensorimotor areas, thereby effectively transforming them into a rectangular, tiled mesh. Cgrid was successfully applied to 20 healthy subjects on both the left and right hemisphere. Results of comparing sensorimotor activity patterns between individuals and between hemispheres yielded high similarity scores, exceeding those obtained with analysis of the same data in MNI space, but equal to similarity scores calculated in FreeSurfer space. Nevertheless, these findings indicate that Cgrid yields a representation that allows for a straightforward way of comparing activity patterns in sensorimotor cortex, which performs at least as good as representations from the more standard FreeSurfer and MNI approaches in terms of pattern similarities.

Transforming regions of the brain into a grid-like representation has also been reported in literature. It has been applied to the visual cortex, based on statistical modelling of the borders using visual stimuli (Corouge, Dojat, & Barillot, 2004). Also the central sulcus has been transformed into a 2D grid mesh (Coulon e.a., 2011), and even the whole cortex has been parametrized using the alignment of sulci (Auzias e.a., 2013). However, there are some key differences between these approaches and Cgrid. First, the method described by Coulon only covers the cortex inside the central sulcus, vwhereas our method maps the surface of the whole gyrus. Second, the Cgrid method is described in such a way that it can be applied on any brain region, as long as clear borders can be defined. It does not statistically model the borders, but rather extracts them from existing atlases. This makes Cgrid a versatile tool, since it is easy to select a different set of borders if desired. Third, the simple geometry of the Cgrids allows for an easy to interpret visualization, which was one of the goals for the development of Cgrid.

The validity of using Cgrid was confirmed by multiple findings. First, analysis of Cgrid-transformed group-averaged activity patterns associated with movement (feet, left hand, right hand, and tongue) resulted in focal activation hotspots. The location of these hotspots allowed for a clear differentiation between the studied motor functions and preserved the topographical distinction between body parts, according to what is known from literature: feet activity was located near the medial wall, tongue activity was bilaterally located in the ventral sensorimotor area, and hand activation was located about halfway the dorsal-ventral axis, mainly on the contralateral hemisphere. Second, as Cgrid is designed as a representation accounting for anatomical differences, we expected a high similarity between the left and right Cgrid activation patterns within a subject, and also a high similarity between Cgrid activation patterns across subjects. Indeed, averaged over tasks and ROIs, similarity scores were high both for within- (Fisher $Z = 0.8$, corresponding to a Pearson correlation of $R = 0.66$) and between-subject (Fisher $Z = 0.97$, $R = 0.75$) comparisons. This indicates that there is a good correspondence of the functional localization in Cgrid both between left and right cortex within subjects, and between subjects, supporting the utility of the common space transformation. Finally, we compared the within-subject similarities and between-subject

similarities of Cgrid activation patterns to those in MNI space, as this is the most widely used standard space for normalization.

When benchmarking Cgrid activity patterns against those from MNI, both within- and between-subject similarities were higher for Cgrid than for MNI space. It should be noted, however, that the comparison of these two methods should be taken with some caution. First, different spaces (2D flat map and 3D MNI volume) required the use of different atlases. The Desikan-Killiany atlas is provided with FreeSurfer and is the atlas from which borders for Cgrid are detected, but this atlas has been developed for surface-based analysis and can therefore not be used in 3D volumes. While a volumetric version of the Desikan-Killiany atlas exists, it only labels the grey matter voxels of the FreeSurfer average, rendering it unsuitable as an atlas for SPM volumetric normalization. Although the use of different atlases is not optimal, the labels used by these two different atlases (precentral and postcentral) indicate highly similar brain areas. Any difference in results that originates from differences in labels would be small. Second, although smoothing kernels with the same sizes were used in both Cgrid and MNI, the effect of smoothing may differ, as in Cgrid smoothing was done in 2D on the surface, and in MNI in 3D on the whole volume. Smoothing in 3D can possibly also include signals from for example white matter, or even from areas that are relatively remote when measures across the surface of the cortex, but proximate in 3D space. Comparison of the two normalization methods over a wide range of smoothing kernels, however, revealed that correlations were generally higher in Cgrid than in MNI space, even with larger kernels. Third, calculating a similarity between patterns from both hemispheres in MNI space was only possible when mirroring the masks for the somatosensory cortex across the longitudinal fissure. This is because for the correlation, left and right ROIs need to be symmetrical (with the same number of voxels and same spatial configuration), which is not necessarily the case in an atlas. Therefore, we mirrored the ROIs, although this does not yield an ROI that is perfectly anatomically aligned and possibly affects the correlation between left and right. Note that the limitation in this approach reflects one of the advantages of Cgrid, where coordinates within the left and the right hemisphere are automatically matched. Forth and finally, the comparison between MNI and Cgrid was performed only using the default settings for normalization in SPM12, and therefore indicate that Cgrid yields higher pattern similarities than normalization to MNI space in a commonly used implementation. Results of the comparison might differ when alternative settings are used. However, the aim was not to optimize the MNI normalization, but to provide a benchmark that reflects a well-known and commonly used normalization method.

In testing validity of the Cgrid approach it is assumed that the topographical organization of the sensorimotor cortex is in proportion to its shape. This means that even if the absolute location of an activity hotspot differs from one subject to another, the hotspot's relative location—that is, the location relative to the dimensions of the sensorimotor cortex—is assumed to be the same across subjects. Likewise, this assumption applies also to the left versus the right hemisphere. Cgrid exploits this postulated relative organization of the sensorimotor cortex, and effectively places the sensorimotor cortex of each individual in a proportional space. As a result, the anatomical differences between subjects are discounted for, as well as differences between the left and right

sensorimotor cortex. Subjects displayed some variations in not only the magnitude and location of activity, but also in the extent of activation along the sensorimotor cortex (compare for example the tongue activity on the right hemisphere in subjects 4 and 6). These differences may reflect variations in cortical representation, but may also well reflect differences in how tasks (even simple tasks) are performed. The calculated similarity scores are derived from Pearson correlations of the complete Cgrid pattern, and thus include areas that should not activate during the task. This makes this measure sensitive to engagement of additional body parts in a given task.

Cgrid employs several cumulative preprocessing steps that may increase the chances of biasing results for individual subjects. It is however difficult to evaluate on theoretical grounds the impact of each individual processing step and its interaction with the other steps. Similarities from Cgrid representations were compared to other methods for brain normalization, where biases should have similar effects. If individual results would be excessively biased, such bias would negatively impact the similarity across subjects, and our method would perform worse than the others, which was not the case.

Given a flattened surface reconstruction, the Cgrid method is automatic. We used Caret to generate these, which requires some manual steps, but this could be automated as well. Although the current implementation of the mapping is fully automatic, manual adjustments on the procedure may be needed in cases where the integrity of gyri and sulci is compromised, for example in patients suffering from brain atrophy or lesions. An algorithm monitoring the deviation of precentral and postcentral borders with respect to the central sulcus could be devised to notify the user if a manual adjustment is needed.

Cgrid is particularly suitable for studying activity patterns on the left and right sensorimotor cortex within subjects, and for the comparison of groups of subjects (for example healthy and diseased), as well as for longitudinal studies on for example normal development or disease-related processes, where it can be used to quantify and visualize changes in activation hotspots over time. It might be less beneficial in cases where very detailed patterns in individual subjects are studied, as transformation of these patterns could be disruptive. Advantages of Cgrid are that it provides a clear, easy to interpret and consistent representation of the sensorimotor cortex. It allows for a straightforward comparison of activation patterns between groups of subjects, but also for quantification of possible alterations (for example shifts and focality) in activation patterns in longitudinal studies, for example in the areas of development, progressive disease or plasticity (Bruurmijn, Pereboom, Vansteensel, Raemaekers, & Ramsey, 2017). As the sensorimotor cortex for each individual is mapped onto the same space, Cgrid allows for comparing whole activity patterns at once, even if they consist of multiple distributed hotspots. In principle, the Cgrid approach can be extended to other primary anatomical regions, and perhaps even to associative cortex where topography is less consistent. Moreover, Cgrid allows for mapping of any cortical parameter, and can accommodate weighing of tile values by the number of included vertices to better represent their quantity where relevant.

In conclusion, we present a Cartesian representation of the anatomical sensorimotor cortex in humans, with the aim to facilitate quantitative comparisons of brain activity within and between

subjects and visualize results. Results of data from 20 subjects show that the Cgrid performs equal or better than comparisons in MNI space, while carrying the benefit of enabling spatial quantitative comparisons of activity patterns.

Information sharing statement

The Cgrid method has been put into a toolbox and can be downloaded from https://github.com/mathijsraemaekers/Cgrid-toolbox.

The ethics protocol limits data publication from a public repository, but does allow data sharing upon request. Please contact the corresponding author.

References

Ashburner, J. (2007). A fast diffeomorphic image registration algorithm. NeuroImage, 38(1), 95. http://doi.org/10.1016/j.neuroimage.2007.07.007

Auzias, G., Lefevre, J., Le Troter, A., Fischer, C., Perrot, M., Regis, J., & Coulon, O. (2013). Model-Driven Harmonic Parameterization of the Cortical Surface: HIP-HOP. IEEE Transactions on Medical Imaging, 32(5), 873. http://doi.org/10.1109/tmi.2013.2241651

Bruurmijn, M. L. C. M., Pereboom, I. P. L., Vansteensel, M. J., Raemaekers, M. A. H., & Ramsey, N. F. (2017). Preservation of hand movement representation in the sensorimotor areas of amputees. Brain, 140(12), 3166. http://doi.org/10.1093/brain/awx274

Corouge, I., Dojat, M., & Barillot, C. (2004). Statistical shape modeling of low level visual area borders. Medical Image Analysis, 3(8), 353–360. http://doi.org/10.1016/j.media.2004.06.023

Coulon, O., Pizzagalli, F., Operto, G., Auzias, G., Delon-Martin, C., & Dojat, M. (2011). Two new stable anatomical landmarks on the Central Sulcus: Definition, automatic detection, and their relationship with primary motor functions of the hand. 2011 Annual International Conference of the IEEE Engineering in Medicine and Biology Society. http://doi.org/10.1109/iembs.2011.6091921

Desikan, R. S., Ségonne, F., Fischl, B., Quinn, B. T., Dickerson, B. C., Blacker, D., e.a. (2006). An automated labeling system for subdividing the human cerebral cortex on MRI scans into gyral based regions of interest. NeuroImage, 31(3), 968. http://doi.org/10.1016/j.neuroimage.2006.01.021

Fan, L., Li, H., Zhuo, J., Zhang, Y., Wang, J., Chen, L., e.a. (2016). The Human Brainnetome Atlas: A New Brain Atlas Based on Connectional Architecture. Cerebral Cortex, 26(8), 3508. http://doi.org/10.1093/cercor/bhw157

Fischl, B. (2012). FreeSurfer. NeuroImage, 62(2), 774. http://doi.org/10.1016/j.neuroimage.2012.01.021

Fischl, B., Sereno, M. I., & Dale, A. M. (1999). Cortical Surface-Based Analysis. NeuroImage, 9(2), 179. http://doi.org/10.1006/nimg.1998.0395

Friston, K. J., Ashburner, J., Kiebel, S. J., Nichols, T. E., & Penny, W. D. (2007). Statistical Parametric Mapping: The Analysis of Functional Brain Images. Academic Press.

Pizzagalli, F., Auzias, G., Delon-Martin, C., & Dojat, M. (2013). Local landmark alignment for high-resolution fMRI group studies: Toward a fine cortical investigation of hand movements in human. Journal of Neuroscience Methods, 218(1), 83. http://doi.org/10.1016/j.jneumeth.2013.05.005

Qiu, A., & Miller, M. I. (2007). Cortical Hemisphere Registration Via Large Deformation Diffeomorphic Metric Curve Mapping. Med Image Comput Comput Assist Interv, 10(1), 186–193. http://doi.org/10.1007/978-3-540-75757-3_23

Van Essen, D. C., Drury, H. A., Dickson, J., Harwell, J., Hanlon, D., & Anderson, C. H. (2001). An Integrated Software Suite for Surface-based Analyses of Cerebral Cortex. Journal of the American Medical Informatics Association, 8(5), 443. http://doi.org/10.1136/jamia.2001.0080443

CHAPTER 2

Preservation of hand movement representation in the sensorimotor areas of amputees

Bruurmijn MLCM, Pereboom IPL, Vansteensel MJ, Raemaekers MAH, Ramsey NF. Preservation of hand movement representation in the sensorimotor areas of amputees. Brain. 2017 Dec 1;140(12):3166-3178. doi: 10.1093/brain/awx274. PMID: 29088322; PMCID: PMC6411136.

CHAPTER 2

Abstract

Denervation due to amputation is known to induce cortical reorganization in the sensorimotor cortex. Although there is evidence that reorganization does not lead to a complete loss of the representation of the phantom limb, it is unclear to what extent detailed, finger-specific activation patterns are preserved in motor cortex, an issue which is also relevant for development of brain-computer interface solutions for paralyzed people. We applied machine learning to obtain a quantitative measure for the functional organisation within the motor and adjacent cortices in amputees, using high-resolution functional MRI and attempted hand gestures.

Subjects with above-elbow arm amputation ($n = 8$) and non-amputated controls ($n = 9$) made several gestures with either their right or left hand. Amputees attempted to make gestures with their amputated hand. Images were acquired using 7 tesla functional MRI. The sensorimotor cortex was divided into four regions, and activity patterns were classified in individual subjects using a support vector machine.

Classification scores were significantly above chance for all subjects and all hands, and were highly similar between amputees and controls in most regions. Decodability of phantom movements from primary motor cortex reached the levels of right hand movements in controls. Attempted movements were successfully decoded from primary sensory cortex in amputees, albeit lower than in controls but well above chance level despite absence of somatosensory feedback. There was no significant correlation between decodability and years since amputation, or age.

The ability to decode attempted gestures demonstrates that the detailed hand representation is preserved in motor cortex and adjacent regions after denervation. This encourages targeting sensorimotor activity patterns for development of brain-computer interfaces.

Introduction

The sensorimotor areas of the human brain are somatotopically organized, with regions of the primary motor cortex (M1) and primary sensory cortex (S1) being associated with movement and sensory representations of various body parts. It has become clear that this somatotopic organization is quite detailed and that representations of individual fingers (Dechent and Frahm, 2003; Siero *et al.*, 2014) and even separate muscles (Hadoush *et al.*, 2011) can be identified.

Denervation due to amputation or nerve damage disrupts normal sensorimotor function. Subsequent cortical reorganization in the sensorimotor area has been reported in numerous animal studies, where intact body parts 'invade' areas associated with the missing limb (Donoghue and Sanes, 1987; Merzenich *et al.*, 1984; Wu and Kaas, 1999). Sensorimotor reorganization occurs also in humans, as evidenced by transcranial magnetic stimulation studies in amputees describing increased excitability of motor areas contralateral to the amputated limb, where stump muscles demonstrate higher response amplitudes which can be induced from a larger scalp area than responses in the intact arm (Cohen *et al.*, 1991; Röricht *et al.*, 1999). Also, magnetoencephalography and fMRI studies with upper limb amputees have reported a shift of lip (Lotze *et al.*, 2001), chin (Elbert *et al.*, 1994), and shoulder (Dettmers *et al.*, 2001) representation into the deafferented cortical hand area has been demonstrated.

Increasing evidence demonstrates that denervation does not result in a complete loss of representation of the affected limb, as the sensorimotor cortex still appears to be engaged in so-called 'attempted movements'. When amputees attempt moving their phantom limb, the corresponding sensorimotor areas show fMRI activation similar to executed movements in able-bodied subjects (Lotze *et al.*, 2001; Roux *et al.*, 2003; Turner *et al.*, 2001). Moreover, for postcentral and parietal regions, it has been shown that this persistent representation is relatively detailed. For example, in a tetraplegic patient using intracranial recordings, movement goals and trajectories have been successfully decoded from posterior parietal cortex (Aflalo *et al.*, 2015). Using microstimulation, a persistent hand representation in S1 was also found in a long-term spinal cord injury patient (Flesher *et al.*, 2016). In amputees, an individual finger topography of the phantom hand has been reported in the somatosensory cortex (Kikkert *et al.*, 2016).

Although abovementioned studies provide evidence that a persistent hand representation still exists after denervation, they primarily focus on somatosensory areas, using simple (one-finger or coarse hand) movements. It is unknown whether the intact representation also applies to for example the primary motor cortex (M1), and to what extent it allows for the decoding of composite (multiple-finger) movements after denervation. This is not only relevant for understanding plasticity, but also for development of clinical brain-computer interface (BCI) solutions for severe paralysis, the feasibility of which was recently reported (Vansteensel *et al.*, 2016).

We have previously shown that the sensorimotor organization in able-bodied subjects allows for a quantitative discrimination of four gestures from the American Manual Alphabet, based on

electrocorticography and on 7T fMRI activation patterns (Bleichner *et al.*, 2013; 2016). Gestures are especially suitable for testing persistent hand representations, because their differentiation constitutes a comprehensive evaluation of discrimination between spatial activity patterns. In the current 7T fMRI study, we investigated the discriminability of cortical representations of attempted gestures in arm amputees, to study and quantify the detailed integrity of the denervated sensorimotor cortex. Similar to our previous studies with able-bodied subjects (Bleichner *et al.*, 2013; 2016), we used a machine learning method for 'decoding', which refers to identifying movements based on their cortical activation pattern. Such decoding is highly sensitive to the discriminability, hence spatial integrity, of cortical hand representations and can be used not only to reveal effects of denervation, but also to quantitatively compare discriminability to control subjects. Since all fingers are represented in the relatively small hand knob on M1 (Siero *et al.*, 2014), any change in representation is likely to cause an increase in correlations between individual finger foci, resulting in reduced discriminability of different gestures and thus in a decline in decoding performance. Another advantage of a decoding approach is that it does not require an a priori model of the cortical organisation, which is known to be challenging especially in M1 (Graziano and Aflalo, 2007; Hluštík *et al.*, 2001). We specifically investigated four regions of the sensorimotor system: the primary motor cortex, the primary sensory cortex, the anterior precentral gyrus, and the posterior postcentral gyrus.

Materials and Methods

Subjects

Eight subjects with arm amputation were recruited (age 52 ± 12 years, 1 female). All subjects had transhumeral arm amputation (7 right arm, 1 left arm amputation), acquired 16.4 ± 11.5 years ago (range: 1.7–31.1 years ago). Nine control subjects were also recruited (no arm amputation, age 44 ± 21 years, 4 females). All subjects were right-handed or were right-handed before amputation according to the Edinburgh Handedness Inventory (Oldfield, 1971). An overview of all subjects is given in Table 1.

The study was approved by the medical-ethical committee of the University Medical Center Utrecht and all subjects gave their written informed consent in agreement with the declaration of Helsinki (2013).

Table 1. Subject details.

	Code	Sex	Age	Amputation side	Years since amputation [yrs]	Phantom pain[a]	Reason for amputation
Controls	C1	m	50				
	C2	f	23				
	C3	m	28				
	C4	m	21				
	C5	f	20				
	C6	f	63				
	C7	m	60				
	C8	f	75				
	C9	m	53				
Amputees	A1	m	52	Right	1.7	2	traffic accident
	A2	f	67	Right	6.2	4	cancer
	A3	m	62	Right	37.1	1	traffic accident
	A4	m	60	Right	6.3	6	cancer
	A5	m	49	Right	21.8	8	machine accident
	A6	m	30	Right	23.1	0	accident
	A7	m	52	Right	17.1	2	post-traumatic dystrophy
	A8	m	40	Left	17.7	4	machine accident

[a] *On the day of scanning, subjects rated their momentary phantom pain on a scale from 0 (no pains) to 10 (heavy pains).*

Experimental design

Data acquisition

MRI data were recorded using a Philips Achieva 7T MRI system with a 32-channel head coil. Anatomical T1- and PD-weighted images were acquired first (TR/TE = 6/1.4 ms, FA = 8°, voxel size = 1 × 1 × 1 mm^3). A functional Localizer task was performed to ensure the hand area was within the imaging field of view, followed by the Gesture task. Prism glasses allowed subjects to look at the screen located at the end of the scanner bore, on which the tasks were presented. Finger positions of both hands in control subjects and of the intact hand in amputees were recorded using MRI-compatible data gloves (5DT Inc., Irvine, USA).

Localizer task and analysis

Subjects were instructed to repeatedly open and close their hands during presentation of a green cue ('move block'), and rest during a red cue ('rest block'). Control subjects were asked to open and close both hands, while amputated subjects only used their intact hand. The task consisted of 3 rest blocks and 2 move blocks (30 seconds each).

EPI images were acquired (TR/TE = 2000/27 ms, FA = 70°, acquisition matrix size = 104 × 129, 33 slices, voxel size = 1.6 × 1.6 × 1.6 mm) during this task. The results were analyzed in real time

using Philips IVIEWBOLD analysis software, and were used to optimally position the fMRI field of view for the Gesture task. For two subjects (C1 and C2), the Localizer task was not yet part of the protocol. For these two subjects, the positioning of the Gesture task EPI scans was based on the anatomical location of the hand knob in transversal and sagittal planes.

Gesture task

Six gestures, shown in Figure 1, were selected from the American Manual Alphabet. These gestures were chosen for maximum differences in flexion-extension combinations.

One of the six characters was presented every 15.6 seconds for subjects C1 and C2, and 16 seconds for all others. The character was presented for 6 seconds, followed by a fixation cross. Subjects were instructed to make the corresponding gesture as soon as a character appeared and hold it until the character disappeared. Subjects performed 4 runs (each with 60 trials; 10 per character): two with their right hand (runs 'R1' and 'R2') and two with their left hand (runs 'L1' and 'L2'). Control subjects (C1-9) used executed movements, whereas amputated subjects (A1-8) used attempted movement with their phantom hand, and executed movements with their intact hand. All subjects were naive to sign language and practiced at home daily for 15 minutes during one week.

An EPI sequence was used (TR/TE = 1300/27 ms for subjects C1 and C2, TR/TE = 1600/27 ms for all other subjects, FA = 70°, acquisition matrix size = 104 × 129, 26 slices, no gap, voxel size = 1.6 × 1.6 × 1.6 mm^3). All EPI scans were acquired in transversal orientation, such that both the left and right hand region were in the field of view.

Data analysis

FMRI preprocessing and Statistical maps

Preprocessing and first level analysis were performed with SPM12 (http://www.fil.ion.ucl.ac.uk/spm/) for each combined pair of runs (L1 with L2, and R1 with R2). Functional images were slice-time corrected, realigned to the mean functional image, and coregistered with the T1-weighted anatomical scan. For a group visualization, the data was smoothed using an 8 mm kernel and normalized to MNI using SPM12. For the decoding analysis, no normalization and no smoothing was applied, to preserve the detail required for classification. A design matrix was fitted using a general linear model (GLM), entering the two runs as separate sessions. Twelve regressors were used (one for each of the six gestures for each run), from which six *t*-maps for the six gestures were derived.

Regions of interest

Gestures were classified from four parallel regions of interest (ROIs) per hemisphere. The main focus was on the primary motor (M1) and primary sensory (S1) cortices, which were defined as the walls of the pre- and postcentral gyrus inside the central sulcus, as we know from our previous work that most informative voxels for classification are located in the central sulcus (Bleichner *et al.*, 2013). To prevent the risk of missing information located futher from the central sulcus (Martuzzi *et al.*,

2012), two additional ROIs were defined: the anterior part of the precentral gyrus (pre-M1), and the posterior part of the postcentral gyrus (post-S1, roughly corresponding with Brodmann area 2).

The ROIs were obtained from volumetric parcellation using FreeSurfer (http://surfer.nmr.mgh.harvard.edu/), by combining the Desikan-Killiany atlas (Desikan *et al.*, 2006), with regions '$PrecentralGyrus_{DKA}$' and '$PostcentralGyrus_{DKA}$', and the Destrieux atlas (Destrieux *et al.*, 2010), with regions '$PrecentralSulcus_{DA}$', '$PrecentralGyrus_{DA}$', '$CentralSulcus_{DA}$', '$PostcentralGyrus_{DA}$', and '$PostcentralSulcus_{DA}$'. For the definition of ROIs in this paper, see Table 2. A combined mask 'GRAND' was defined as the union of M1, S1, pre-M1, and post-S1. In individuals, the exact boundary between M1 and S1 may not always be located exactly in the fundus of the central sulcus. Therefore, to verify that classification scores from M1 are not due to S1 activity, we also calculated the classification scores for a conservative definition of M1, $M1_{no\text{-}fundus}$, where a substantial part of the central sulcus was left out.

Classification procedure and statistics

Patterns of BOLD activation were classified using a multi-voxel pattern analysis approach with a support vector machine (SVM) classifier (Haxby *et al.*, 2001). Classification was performed for each of the four ROIs and 'GRAND' contralateral to the hand that the subject was instructed to move. For classification the number of voxels was constrained to avoid inclusion of voxels not involved in the task (Bleichner *et al.*, 2013). Therefore, for each ROI separately, as well as for 'GRAND', we only kept the 250 voxels with the highest *t*-values across the *t*-maps for the different gestures (Mitchell *et al.*, 2004). The BOLD signal in each included voxel was subsequently detrended and transformed into *z*-scores. The amplitude of the BOLD response for each trial was calculated for each of the 250 voxels by taking the mean signal over scans 5, 6, and 7 for subjects C1 and C2, and scans 4, 5, and 6 for all other subjects. These windows were chosen because previous decoding studies have shown maximum decodability around 6 to 8 seconds after stimulation onset (Andersson *et al.*, 2011; Bleichner *et al.*, 2013).

Because an SVM is a binary classifier, six SVMs were combined in a 'one versus all others' approach: the SVMs were trained to distinguish each gesture from the combined set of all other gestures. In this approach, when testing an unknown sample, the class for which the distance from the data point to the decision boundary is largest wins. All SVM classifiers used a linear kernel with regularization parameter ('soft margin') $C = 1$.

Table 2. ROI definitions based on the Desikan-Killiany atlas (subscript DKA) and Destrieux atlas (subscript DA), where ∪ denotes the voxel-wise union, and ∩ the intersect of ROIs.

ROI name	Definition
M1	$PrecentralGyrus_{DA} \cup (CentralSulcus_{DA} \cap PrecentralGyrus_{DKA})$
S1	$PostcentralGyrus_{DA} \cup (CentralSulcus_{DA} \cap PostcentralGyrus_{DKA})$
pre-M1	$PrecentralSulcus_{DA}$
post-S1	$PostcentralSulcus_{DA}$
'GRAND'	M1 ∪ S1 ∪ pre-M1 ∪ post-S1
$\mathbf{M1}_{no\text{-}fundus}$	$PrecentralGyrus_{DA}$

The classifier was trained and validated using a leave-6-out cross validation scheme (20 folds), in which for each fold, one trial for each gesture was left out (validation set), while the classifier was trained on the remaining trials (the training set). Classification results are reported as mean and standard deviation. To evaluate the effects for ROI, hand, and group, we applied a three-way repeated-measures GLM, with two within-subject factors (ROI: 4 levels, and Hand: 2 levels) and two groups (amputees and controls) at significance level 0.05. To investigate whether there was an effect of amputation in any ROI of the denervated hemisphere in amputees, only significant interactions were followed with a post-hoc two-way GLM and individual two-sample t-tests for comparing between ROIs.

Spatial extent of features inside ROIs

To assess the spatial layout of the selected features, the ROIs (M1 and S1 only) were first mapped to a normalised space as follows. The borders of the sensorimotor cortex were extracted from a flat map parcellation, and three polynomials were fitted: through the central sulcus, through the anterior border of the precentral gyrus, and through the posterior border of the postcentral gyrus. Interpolating between these polynomials resulted in a 28×84 tiled mesh of the sensorimotor area. The volumetric M1 and S1 ROIs, used for classification, were remapped onto the normalized tiles. Spatial extent of activity was quantified for M1 and S1 by calculating the median distance of each selected voxel to its ROI's center of mass. The spatial extent of features was compared between hemispheres and groups, using a repeated measures GLM with two measures (S1 and M1), with hemisphere as within-subject factor (two levels: left and right) and group as between-subject factor.

BOLD response analysis

We assessed the effect of denervation on the BOLD response amplitude. Per voxel and per trial, each time point in the detrended BOLD signal was converted into percent signal change with respect to the BOLD signal of the first scan of each trial. Per subject, BOLD responses were then averaged over trials for each of the ROIs.

The BOLD responses were then averaged between 4 and 8 seconds (comparable to the window used for classification) and were statistically compared using a three-way repeated-measures GLM and post-hoc tests analogous to the analysis of the classification scores.

Correlation with phantom pain, age, and years since amputation

Amputees rated their ability to make the gestures with their phantom hand on a score from 0 ("very difficult") to 10 ("very easy"). They rated their average everyday phantom pain on a score from 0 ("no pain") to 10 ("heavy pains"). To investigate any relationship between phantom movement ability, phantom pain, age, or years since amputation and the classification of the phantom hand, Pearson correlations were calculated using a significance level of 0.05 (Bonferroni corrected for five tests).

Gesture execution performance and data glove amplitude

Excessive movements of the hand that should be kept still during a task could possibly influence classification scores. Therefore, the amount of motion of the still hand was compared to the amount of motion of the moving hand. The amplitude of the finger flexion sensors of the data glove was chosen as measure for movement.

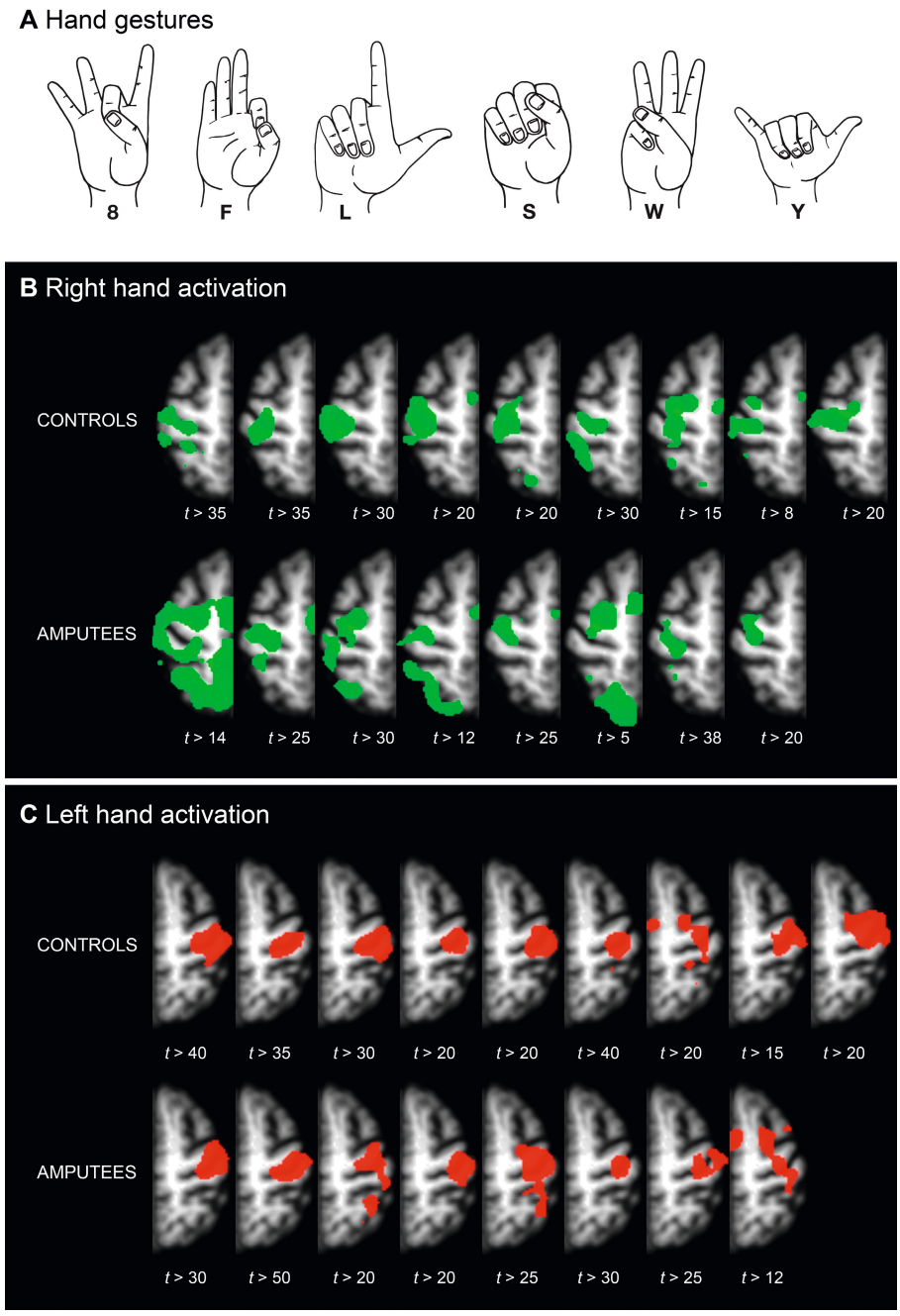

Figure 1. *Thresholded t-maps for hand activation. A: Hand gestures used for this study. These gestures were chosen for maximum mutual differences in flexion-extension combinations. B: Activation for right/phantom hand. C: Activation for left/intact hand. The contrast used for this image was '8'+'F'+'L'+'S'+'W'+'Y'>baseline. In all subjects, there is clear activation inside the contralateral central sulcus, which is associated with hand control. T-values are set per subject for visualization purposes. Images are in neurological orientation.*

Results

GLM analysis

Significant activity was found for all subjects for the contrast of all gestures versus baseline in M1 and S1 ($P < 0.05$, Bonferroni corrected for total numbers of voxels in the imaged volume). Figure 1B displays activity at individually tailored thresholds to indicate foci with strongest activity.

Support vector machine classification

Mean classification scores for the six gestures were significantly above chance level (binomial test, $P < 0.001$) for all contralateral ROIs, in controls and in amputees, for both hands (Figure 2). For left and right hands of controls, classification scores ranged from 23% to 91%, depending on ROI. Intact hand scores of amputees ranged between 35% and 96%, and phantom hand scores between 25% and 84%.

Three-way repeated-measures GLM

The three-way repeated measures GLM revealed a significant main effect of ROI [$F(3,13) = 29.7$, $P < 0.001$], a significant two-way interaction between ROI and Group [$F(3,13) = 4.29$, $P = 0.026$] and a significant three-way interaction between Hand, ROI, and Group [$F(3,13) = 20.64$, $P < 0.001$].

As post-hoc test, a two-way repeated-measures GLM was performed on each of the two hands separately. For the left/intact hand, there was a significant effect of ROI [$F(3,13) = 24.79$, $P < 0.001$], but no significant interaction between ROI and Group [$F(3,13) = 1.38$, n.s.]. For the right/phantom hand, there was a significant effect of ROI [$F(3,13) = 20.37$, $P < 0.001$], and a significant interaction between ROI and Group [$F(3,13) = 14.70$, $P < 0.001$].

Lastly, independent t-tests were used post-hoc to compare the decodability between controls and amputees for each ROI in the right/phantom hand. The ROIs that demonstrated a significant difference in decodability were S1 [$t(15) = 2.77$, $P = 0.014$] and pre-M1 [$t(15) = -2.18$, $P = 0.046$]. Other ROIs did not significantly differ between groups [M1: $t(15) = -0.49$, n.s.; post-S1: $t(15) = -1.30$, n.s.].

Classification on ROI 'GRAND'

Gestures were also decoded from the combined ROI 'GRAND'. In controls, decodability was 77% ± 13% for the right hand and 70% ± 15% for the left hand. In amputees, scores were 64% ± 14% for the phantom hand and 79% ± 11% for the intact hand. A two-way repeated-measures GLM indicated a significant interaction between Group and Hand [$F(1,15) = 12.95$, $P = 0.003$].

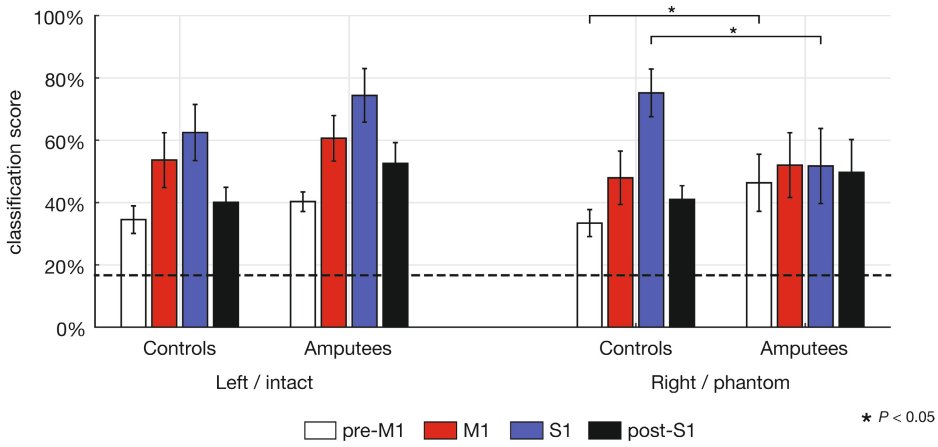

Figure 2. *Classification scores per ROI for both groups and both hands. Bars indicate mean classification scores and 95% confidence intervals. The dashed line at 16.7% indicates chance level. Significant post-hoc independent t-tests are indicated by a star (P < 0.05).*

Spatial extent of features inside ROIs

Figure 3 displays the spatial characteristics of cortical activity. The standardized location of the center of mass within M1 and S1 was highly comparable across hands and groups (Figure 3B-C). GLM analyses demonstrated no effect of group or hand on the extent of features in M1 and S1, indicating that there was no difference in extent of spatial distribution of the highest activated voxels between hemispheres, or between controls and amputees (Figure 3D).

BOLD response analysis

All subjects showed comparably shaped BOLD responses in all ROIs (Figure 4). BOLD response amplitudes were compared per ROI between and within groups.

The three-way repeated measures GLM revealed a significant main effect of ROI [$F(3,13) = 24.6$, $P < 0.001$], significant two-way interactions between ROI and Group [$F(3,13) = 5.39$, $P = 0.012$] and ROI and Hand [$F(3,13) = 5.58$, $P = 0.011$], and a significant three-way interaction between Hand, ROI, and Group [$F(3,13) = 6.36$, $P = 0.011$].

A two-way repeated-measures GLM was performed to follow up effects within each of the two hands separately. For the left/intact hand, there was a significant effect of ROI [$F(3,13) = 33.7$, $P < 0.001$], but no significant interaction between ROI and Group [$F(3,13) = 2.17$, n.s.]. For the right/phantom hand, there was a significant effect of ROI [$F(3,13) = 11.9$, $P = 0.001$], and a significant interaction between ROI and Group [$F(3,13) = 4.50$, $P = 0.022$].

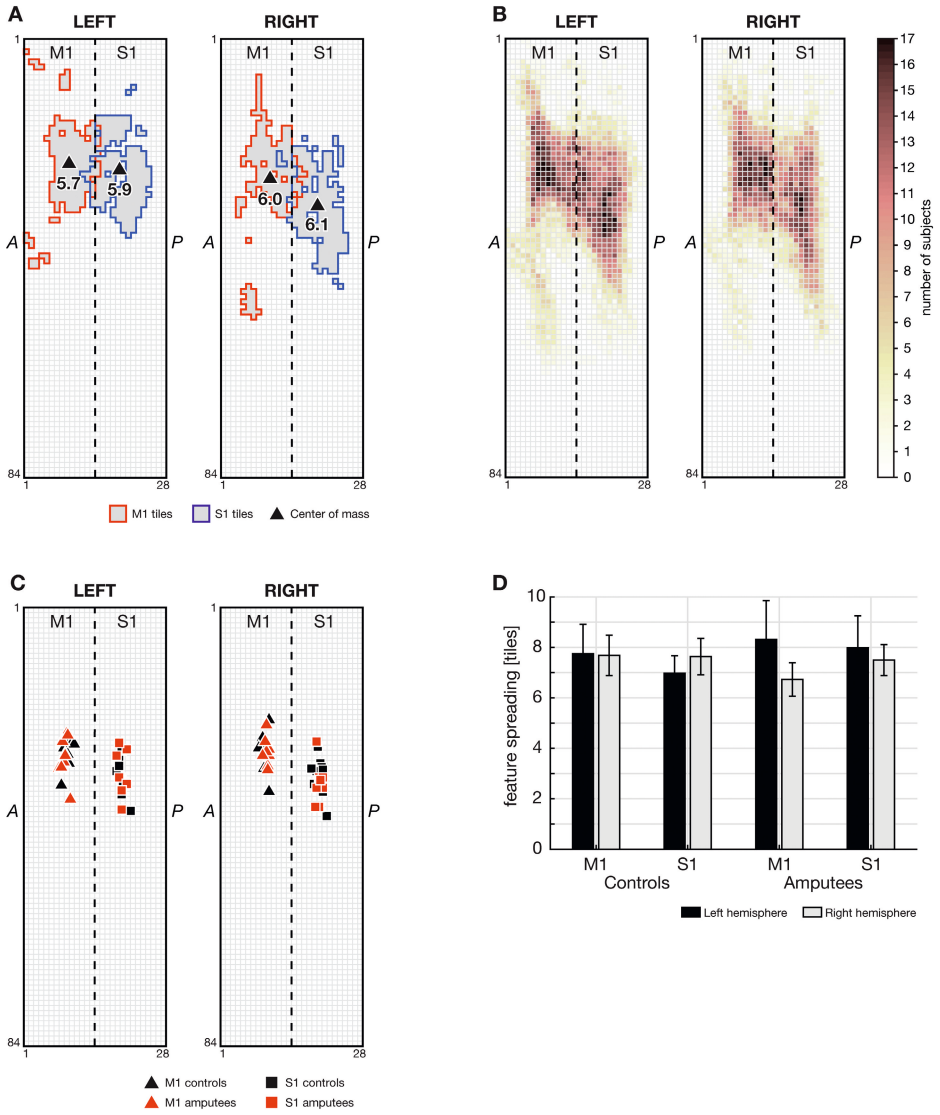

Figure 3. *Spatial extent of selected features inside M1 and S1. A: Mapping of features (250 most activated voxels) for one representative subject (subject A5), for M1 and S1 on left and right hemisphere grids. The dashed line indicates the central sulcus. Around the central sulcus, M1 and S1 ROIs may overlap due to the transformation into tile space and partial volume effects. Triangles indicate the center of mass of M1 and S1, and the number represents the ROI's 'spatial extent', measured in mesh tiles. B: ROIs of all subjects. The color per tile indicates the number of subjects having that tile selected as a feature for classification. C:centers of mass for all subjects for both M1 and S1 on the left and right hemispheres. D: Spatial extent of features per hemisphere in M1 and S1 for controls and amputees (mean with 95% confidence interval). There was no significant difference in spatial extent between left and right hemispheres, or between controls and amputees.*

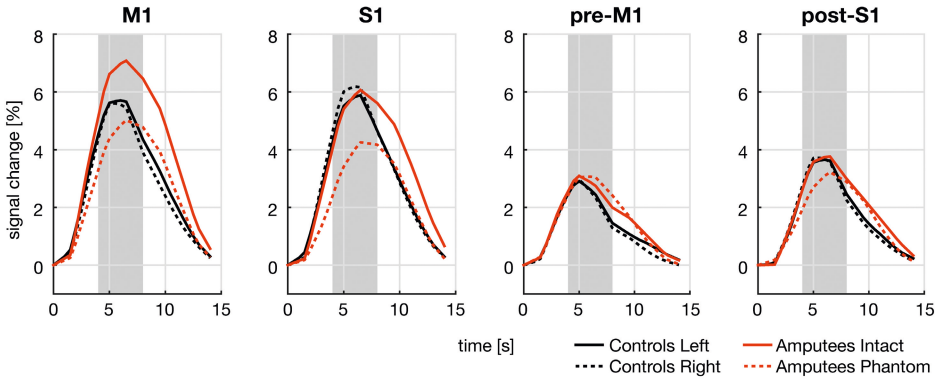

Figure 4. *BOLD responses for each of the four ROIs and each hand for controls and amputees. BOLD responses are expressed in percent signal change, averaged over all trials. Time point 0 indicates the start of the trial. Only S1, there was a significant difference in the BOLD response between the phantom hand of amputees and the intact hand of controls within the interval of 4–8 seconds (indicated by the grey shading).*

Independent t-tests to compare the BOLD responses between controls and amputees for each ROI only in the right/phantom hand revealed that only S1 demonstrated a significant difference [$t(15) = -2.24$, $P = 0.040$], whereas the other ROIs did not [M1: $t(15) = -0.60$, n.s.; pre-M1: $t(15) = 0.81$, n.s.; post-S1: $t(15) = -0.69$, n.s.].

Correlation with phantom pain, age, and years since amputation

We did not find significant correlations in any ROI between the 'phantom movement ability score' or the 'phantom pain score' and the classification score of the phantom hand (Pearson correlation, Figure 5). There was no significant correlation between age and classification score in any of the groups, hands, or ROIs. Although all ROIs showed a negative trend, with higher classification scores found for people with the most recently acquired amputation, no ROI showed a significant correlation of classification score with years since amputation, using a significance level of $P = 0.05$, Bonferroni corrected for five tests.

Gesture execution performance and data glove amplitude

Gesture execution performance was assessed by classification of the data glove recordings of the intact hand in amputees, and of both hands in control subjects. The classification scores were significantly above chance level (94% ± 6%, $P < 0.001$) with a minimum score of 79%.

Analysis of the data glove flexion sensor amplitude demonstrated minimal motion in the hand that should be kept still during the task compared to the hand that should be moving, with subject A2 as the only exception (Figure 6). In both amputees and controls, there was no significant correlation between still hand amplitude and classification score from ROI 'GRAND'.

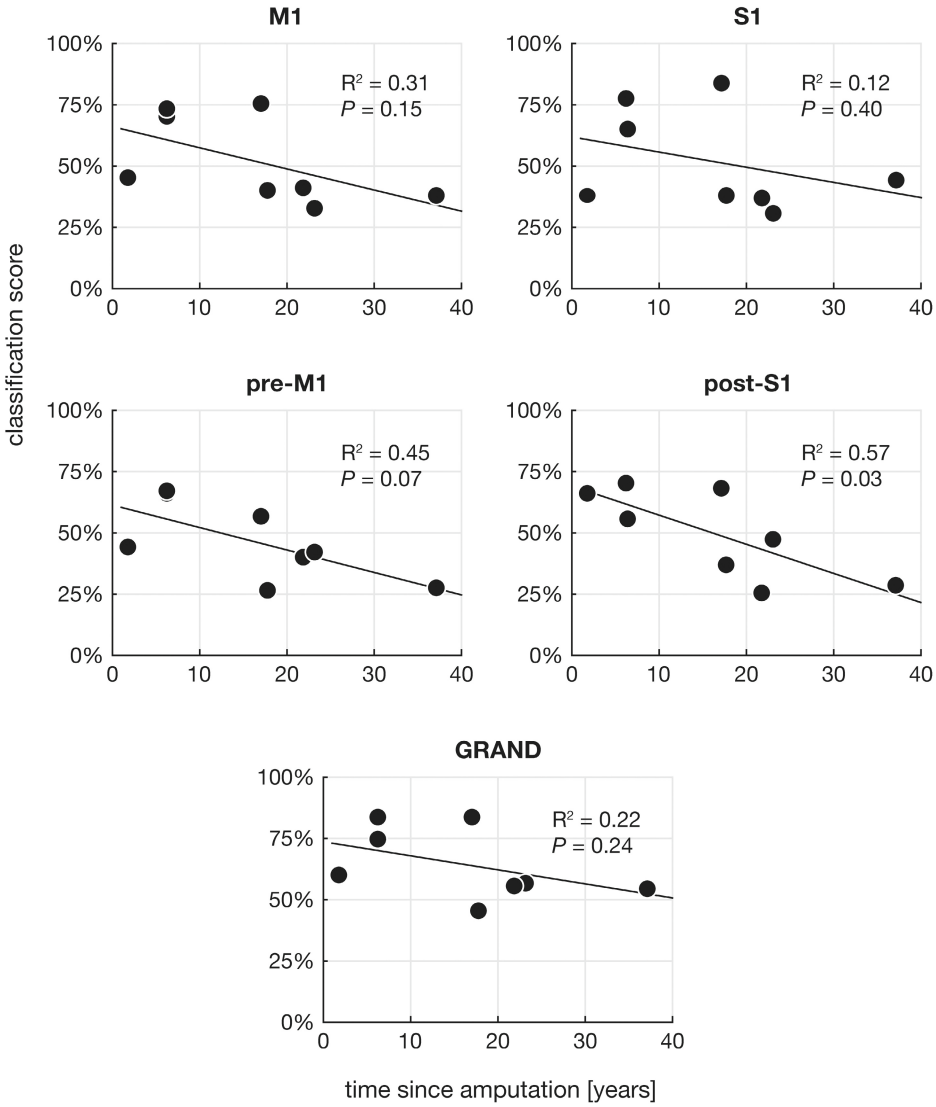

Figure 5. *Classifications scores for the different ROIs as a function of time since amputation. Altough a negative trend can be observed in all ROIs, no ROI showed a significant correlation when Bonferroni corrected for multiple (five) comparisons.*

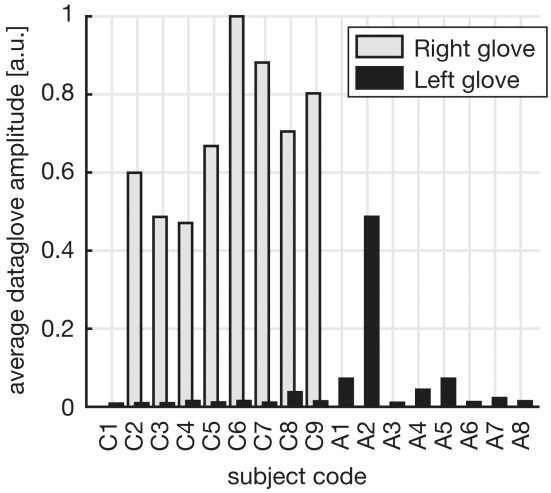

Figure 6. *Data glove amplitudes for the left and right hand glove during a right (phantom) hand task. There was no right glove recording for amputees. Amplitudes of the left (intact) hand, which should remain still during the task, are small compared to amplitudes of the moving hand, with amputee subject A2 being an exception.*

Conservative definition of M1

To verify that M1 activity was not due to S1 activity, classification scores were calculated from a conservative definition of M1, $M1_{no\text{-}fundus}$. The resulting classification scores (controls left: 46% ± 12%, controls right: 43% ± 15%, amputees intact: 55% ± 12%, amputees phantom: 48% ± 19%) all remained well above chance level, as with the 'full' M1.

Discussion

We investigated whether the detailed topographic representation of the hand is preserved in people with above-elbow arm amputation. As a measure of (preserved) representation, we used the decodability of attempted complex hand gestures from four different contralateral ROIs of the sensorimotor hand area in amputees (M1, S1, pre-M1, post-S1), and compared this to the decodability of gestures executed with the intact hand. Data of able-bodied controls were used as an extra reference. In controls and amputees, classification scores for both hands were significantly above chance in all ROIs.

M1 hand representation after amputation

For M1, there was no difference between the classification scores for attempted movement of the phantom hand in amputees and executed right hand movement in controls. BOLD responses of amputees were similar to those of the control subjects. Previous fMRI studies have shown that phantom hand movements result in a clear activation of the contralateral M1, similar to executed intact hand movement in amputees and controls (Ersland *et al.*, 1996; Raffin *et al.*, 2012; 2016; Roux *et al.*, 2003), but did not investigate whether also the representation of composite finger movements in M1 remains intact. Although our classification approach does not directly assess topography in the

traditional sense, it does provide an insight in the representation of hand movements, as it inherently relies on spatial patterns. Moreover, we cannot entirely exclude the possibility that the representations of complex hand movements change after denervation, but since we are able to decode composite hand movements from the cortex, the most straightforward conclusion is that the hand representations in M1 contralateral to the phantom hand are unaffected by denervation, also at the high level of detail associated with complex hand movements involving multiple fingers simultaneously.

The exact border between M1 and S1 can vary between subjects and does not necessarily have to be located exactly at the fundus of the central sulcus, leading to a possible contribution of S1 activity on the decodability of M1. However, we tested the classification on ROI $M1_{no\text{-}fundus}$, where the fundus of the central sulcus has been left out, and they remained well above chance level, indicating that decoding is not due to activity in S1 cortex.

Decodability and BOLD response in S1

Interestingly, S1 demonstrated the highest decodability, with classification scores being significantly higher than from other ROIs for both hands of controls, and for the intact hand of amputees. Even for the phantom hand in amputees, S1 decodability was similar to that of the other ROIs, albeit significantly lower than S1 scores of the right hand of controls. As such, our findings confirm and extend previous studies that showed persistent body part representation (at a more coarse level) after amputation or spinal cord injury by 1) activation within S1 during attempted foot (Cramer *et al.*, 2005; Hotz-Boendermaker *et al.*, 2008; 2011) and hand (Gharabaghi *et al.*, 2014; Raffin *et al.*, 2012) movement and 2) preserved finger somatotopy of the phantom hand in S1 by moving the phantom hand (Kikkert *et al.*, 2016) or by microstimulation (Flesher *et al.*, 2016).

We hypothesize that the preservation of decodability is associated with the role of S1, which is thought to reflect not only somatosensory feedback, but also anticipatory information necessary for rapid movement correction (Helmholtz, 1924). Indeed, activity in S1 has been found in subjects whose proprioceptive feedback has been disabled by an ischemic nerve block (Christensen *et al.*, 2007). Moreover, a movement-associated activity increase in S1, preceding M1 activation and the actual movement, has been demonstrated using electrocorticography (Sun *et al.*, 2015). Our results support the notion that the decodability of complex hand movements in S1 can be viewed as a combination of feed-forward and feedback processes. The fact that the attempted gestures in amputees, which only generate feed-forward influences on S1 activity, could be decoded from S1 at the same level as decoding from M1 in phantom and actual movements, further strengthens the notion that primary sensorimotor cortex is hardly (if at all) affected by amputation.

The difference between decodability and BOLD amplitude for the phantom hand compared to actual movements may also be associated with amputation-induced structural changes. Indeed, it has been demonstrated that grey matter volume is reduced in the denervated cortex of amputees (Makin *et al.*, 2013), and that reduced BOLD responses may be associated with grey matter thinning (Taylor *et al.*, 2009). Future studies may elucidate the influence of structural changes on the decodability of complex movements.

Delayed reorganization after amputation

There is evidence for both immediate and delayed reorganizational changes after amputation (Pearson *et al.*, 2003; Wall *et al.*, 2002). Animal studies have indicated that within minutes to hours after amputation, the receptive fields of an amputated digit become responsive to stimulation of neighbouring parts of the hand (Calford and Tweedale, 1988). The few human studies on this topic suggest that reorganization occurs rapidly as well (Weiss *et al.*, 2000). Delayed effects of amputation have been demonstrated in the case of a new shoulder representation in denervated forelimb cortex of rats over a period of weeks (Pearson *et al.*, 2003). In addition, for human lower-limb amputees, a negative correlation between cortical thickness in V5/MT+, as well as white matter integrity in areas involved in visuospatial processing, and years since amputation have been described (Jiang *et al.*, 2015; 2016), suggesting that slow reorganizational processes continue to occur long after amputation. Although the ROIs showed a negative trend in the correlation between post-S1 decodability and years since amputation, this correlation was never significant when corrected for multiple comparisons. Therefore, the data suggest that the effect of time (if any) on the phantom hand representation in M1 and S1 is small, keeping in mind that the number of subjects limits the power of the analysis.

Maximizing classification scores

The data of our control subjects agree with, and extend, a previous fMRI study from our group that showed that it is possible to classify multiple executed hand gestures from the sensorimotor areas in able-bodied people with high accuracy (Bleichner *et al.*, 2016). The above-chance classification we observed for all ROIs is suggestive for the presence of a detailed hand representation in each of the four studied regions of the sensorimotor system in controls and amputees. Whether or not a discrete somatotopy for individual fingers exists in M1 is subject to debate [see for example (Graziano and Aflalo, 2007) for an overview of possible organization principles of M1]. In cases where within-limb somatotopy was found in M1 and compared to that of S1, the latter demonstrated a more discrete and segregated organization (Cunningham *et al.*, 2013; Hluštík *et al.*, 2001). This difference in organization has been attributed to the more integrative role M1 plays in motor control (Cunningham *et al.*, 2013) and could explain why, in the present study, classification scores were highest in S1, as the method used here is inherently based on spatial activity patterns. Unfortunately, straightforward inference of the different organisational principles in M1 and S1 is not possible in our study due to the nature of machine learning.

We are aware of several potential confounds that can contribute to the classification accuracy and their comparisons between controls and amputees. First, it is known that stump muscles even in above-elbow amputees can be activated when attempting to move the phantom hand, and that these activations are reproducible and different from activation patterns of the stump itself (Reilly *et al.*, 2006). However, it is unknown whether the same effect of this peripheral reorganisation is present for the fine-grained finger movements like the ones that were used here. Therefore, we cannot completely rule out the possible influence of this confound. Second, the control group is overall younger than the amputee group. However, since we were still able to decode successfully in amputees, we believe that our conclusions would remain valid in spite of this age difference. Third, we compared the phantom hand of amputees with the dominant (right) hand of controls. Although it can be argued

that the dominant hand of amputees is now their intact hand by definition, we did not want to make any assumptions about the effects of change of hand dominance on decoding from both hemispheres, especially since all amputees (except for one) acquired their amputation in adulthood.

Compared to our previous gesture decoding study in able-bodied volunteers, we observed better classification scores. When combining all ROIs, the mean score for 4 gestures was 63% (chance level 25%) (Bleichner *et al.*, 2013), whereas we now obtained 64 – 79 % (depending on hand and group) for a chance level of 16.7%. An interesting aspect is whether the subjects' movements or activation patterns would become better decodable after a period of training. For this report, subjects practised the task daily in the week before scanning, to gain fluency in making the gestures. A longer training session might reveal a learning curve in decoding accuracy. Also, training can be offered using fMRI neurofeedback, a technique in which information about brain activity patterns is provided to the subject in real-time. Neurofeedback has proven to be an effective method to shape brain activity in certain areas (Weiskopf, 2012), and may improve discriminative power of activity patterns.

The high classification scores we obtained for attempted gestures in amputees, especially from the combined ROI, indicate that the sensorimotor hand region of these patients may be, and remain, a suitable source of signals for BCI applications, such as multidimensional arm prosthesis control, also years after denervation. For such a BCI application, signal acquisition methods need to be wearable and accommodate high spatial detail, both of which can be accomplished with high density electrocorticography (ECoG) (Bleichner *et al.*, 2016; Branco *et al.*, 2017). We have shown previously that fMRI BOLD activation demonstrates good spatial correspondence with ECoG (Hermes *et al.*, 2012; Siero *et al.*, 2014). For an ECoG-based BCI application, decoding from either M1 or S1 separately may be of interest, since limiting the size of an implant is beneficial in terms of limiting the surgical risk. Since the classification scores from both areas is high, it means that they both serve as promising targets for ECoG-based BCI.

In conclusion, our results demonstrate that complex attempted hand movements can be decoded well from primary motor cortex in people with arm amputation, suggesting that even years after denervation, this area has not lost its detailed spatial representation integrity associated with combined finger movements, and still contain a sufficient level of information for decoding. The same holds for adjacent sensory and premotor regions. Given the similar classification results for amputees and able-bodied subjects, it may be speculated that when having to resort to able-bodied people for BCI research (when inclusion of the target population is difficult because of low numbers or vulnerability), the use of executed movements provides useful insight in the organization and behaviour of the cortical hand region in patients.

Acknowledgements

Thanks to all participants for their contribution, and to dr. M.A.H. Brouwers and prof. dr. C.K. van der Sluis for their assistance in subject recruitment.

Funding

This work was made possible by the ERC Advanced Grant 320708 (iCONNECT) granted to NFR.

References

Aflalo T, Kellis S, Klaes C, Lee B, Shi Y, Pejsa K, et al. Decoding motor imagery from the posterior parietal cortex of a tetraplegic human. Science 2015; 348: 906.

Andersson P, Pluim JPW, Siero JCW, Klein S, Viergever MA, Ramsey NF. Real-Time Decoding of Brain Responses to Visuospatial Attention Using 7T fMRI. PLoS ONE 2011; 6: e27638.

Bleichner MG, Freudenburg ZV, Jansma JM, Aarnoutse EJ, Vansteensel MJ, Ramsey NF. Give me a sign: decoding four complex hand gestures based on high-density ECoG. Brain Structure and Function 2016; 221: 203.

Bleichner MG, Jansma JM, Sellmeijer J, Raemaekers M, Ramsey NF. Give Me a Sign: Decoding Complex Coordinated Hand Movements Using High-Field fMRI. Brain Topography 2013; 27: 248.

Branco MP, Freudenburg ZV, Aarnoutse EJ, Bleichner MG, Vansteensel MJ, Ramsey NF. Decoding hand gestures from primary somatosensory cortex using high-density ECoG. NeuroImage 2017; 147: 130.

Calford MB, Tweedale R. Immediate and chronic changes in responses of somatosensory cortex in adult flying-fox after digit amputation. Nature 1988; 332: 446.

Christensen MS, Lundbye-Jensen J, Geertsen SS, Petersen TH, Paulson OB, Nielsen JB. Premotor cortex modulates somatosensory cortex during voluntary movements without proprioceptive feedback. Nature Neuroscience 2007; 10: 417–419.

Cohen LG, Bandinelli S, Findley TW, Hallett M. Motor reorganization after upper limb amputation in man. Brain 1991; 114: 615.

Cramer SC, Lastra L, Lacourse MG, Cohen MJ. Brain motor system function after chronic, complete spinal cord injury. Brain 2005; 128: 2941.

Cunningham DA, Machado A, Yue GH, Carey JR, Plow EB. Functional somatotopy revealed across multiple cortical regions using a model of complex motor task. Brain Research 2013; 1531: 25.

Dechent P, Frahm J. Functional somatotopy of finger representations in human primary motor cortex. Human Brain Mapping 2003; 18: 272.

Desikan RS, Ségonne F, Fischl B, Quinn BT, Dickerson BC, Blacker D, et al. An automated labeling system for subdividing the human cerebral cortex on MRI scans into gyral based regions of interest. NeuroImage 2006; 31: 968.

Destrieux C, Fischl B, Dale A, Halgren E. Automatic parcellation of human cortical gyri and sulci using standard anatomical nomenclature. NeuroImage 2010; 53: 1.

Dettmers C, Adler T, Rzanny R, van Schayck R, Gaser C, Brückner L, et al. Increased excitability in the primary motor cortex and supplementary motor area in patients with phantom limb pain after upper limb amputation. Neuroscience Letters 2001; 307: 109.

Donoghue JP, Sanes JN. Peripheral nerve injury in developing rats reorganizes representation pattern in motor cortex. Proceedings of the National Academy of Sciences 1987; 84: 1123.

Elbert T, Flor H, Birbaumer N, Knecht S, Hampson S, Larbig W. Extensive reorganization of the somatosensory cortex in adult humans after nervous system injury. NeuroReport 1994; 5: 2593.

Ersland L, Rosén G, Lundervold A, Smievoll AI, Tillung T, Sundberg H. Phantom limb imaginary fingertapping causes primary motor cortex activation: an fMRI study. NeuroReport 1996; 8: 207.

Flesher SN, Collinger JL, Foldes ST, Weiss JM, Downey JE, Tyler-Kabara EC, et al. Intracortical microstimulation of human somatosensory cortex. Science Translational Medicine 2016; 8: 361ra141.

Gharabaghi A, Naros G, Walter A, Roth A, Bogdan M, Rosenstiel W, et al. Epidural electrocorticography of phantom hand movement following long-term upper-limb amputation. Frontiers in Human Neuroscience 2014; 8

Graziano MSA, Aflalo TN. Mapping Behavioral Repertoire onto the Cortex. Neuron 2007; 56: 239.

Hadoush H, Sunagawa T, Nakanishi K, Endo K, Ochi M. Motor somatotopy of extensor indicis proprius and extensor pollicis longus. NeuroReport 2011; 22: 559.

Haxby JV, Gobbini MI, Furey ML, Ishai A, Schouten JL, Pietrini P. Distributed and Overlapping Representations of Faces and Objects in Ventral Temporal Cortex. Science 2001; 293: 2425.

Helmholtz von H. Helmholtz's Treatise on Physiological Optics. 1924.

Hermes D, Miller KJ, Vansteensel MJ, Aarnoutse EJ, Leijten FSS, Ramsey NF. Neurophysiologic correlates of fMRI in human motor cortex. Human Brain Mapping 2012; 33: 1689.

Hluštík P, Solodkin A, Gullapalli RP, Noll DC, Small SL. Somatotopy in Human Primary Motor and Somatosensory Hand Representations Revisited. Cerebral Cortex 2001; 11: 312.

Hotz-Boendermaker S, Funk M, Summers P, Brugger P, Curt A, Kollias SS. Preservation of motor programs in paraplegics as demonstrated by attempted and imagined foot movements. NeuroImage 2008; 39: 383.

Hotz-Boendermaker S, Hepp-Reymond M-C, Curt A, Kollias SS. Movement Observation Activates Lower Limb Motor Networks in Chronic Complete Paraplegia. Neurorehabilitation and Neural Repair 2011; 25: 469.

Jiang G, Li C, Wu J, Jiang T, Zhang Y, Zhao L, et al. Progressive Thinning of Visual Motion Area in Lower Limb Amputees. Frontiers in Human Neuroscience 2016; 10

Jiang G, Yin X, Li C, Li L, Zhao L, Evans AC, et al. The Plasticity of Brain Gray Matter and White Matter following Lower Limb Amputation. Neural Plasticity 2015; 2015: 1.

Kikkert S, Kolasinski J, Jbabdi S, Tracey I, Beckmann CF, Johansen-Berg H, et al. Revealing the neural fingerprints of a missing hand. eLife 2016; 2016

Lotze M, Flor H, Grodd W, Larbig W, Birbaumer N. Phantom movements and pain An fMRI study in upper limb amputees. Brain 2001; 124: 2268.

Makin TR, Scholz J, Filippini N, Slater DH, Tracey I, Johansen-Berg H. Phantom pain is associated with preserved structure and function in the former hand area. Nature Communications 2013; 4: 1570.

Martuzzi R, van der Zwaag W, Farthouat J, Gruetter R, Blanke O. Human finger somatotopy in areas 3b, 1, and 2: A 7T fMRI study using a natural stimulus. Human Brain Mapping 2012; 35: 213.

Merzenich MM, Nelson RJ, Stryker MP, Cynader MS, Schoppmann A, Zook JM. Somatosensory cortical map changes following digit amputation in adult monkeys. The Journal of Comparative Neurology 1984; 224: 591.

Mitchell TM, Hutchinson R, Niculescu RS, Pereira F, Wang X, Just M, et al. Learning to Decode Cognitive States from Brain Images. Machine Learning 2004; 57: 145.

Oldfield RC. The assessment and analysis of handedness: The Edinburgh inventory. Neuropsychologia 1971; 9: 97.

Pearson PP, Li CX, Chappell TD, Waters RS. Delayed reorganization of the shoulder representation in forepaw barrel subfield (FBS) in first somatosensory cortex (SI) following forelimb deafferentation in adult rats. Experimental Brain Research 2003; 153: 100.

Raffin E, Mattout J, Reilly KT, Giraux P. Disentangling motor execution from motor imagery with the phantom limb. Brain 2012; 135: 582.

Raffin E, Richard N, Giraux P, Reilly KT. Primary motor cortex changes after amputation correlate with phantom limb pain and the ability to move the phantom limb. NeuroImage 2016; 130: 134.

Reilly KT, Mercier C, Schieber MH, Sirigu A. Persistent hand motor commands in the amputees' brain. Brain 2006; 129: 2211.

Roux F-E, Lotterie J-A, Cassol E, Lazorthes Y, Sol J-C, Berry I. Cortical Areas Involved in Virtual Movement of Phantom Limbs: Comparison with Normal Subjects. Neurosurgery 2003; 53: 1342–1353.

Röricht S, Meyer BU, Niehaus L, Brandt SA. Long-term reorganization of motor cortex outputs after arm amputation. Neurology 1999; 53: 106.

Siero JCW, Hermes D, Hoogduin H, Luijten PR, Ramsey NF, Petridou N. BOLD matches neuronal activity at the mm scale: A combined 7T fMRI and ECoG study in human sensorimotor cortex. NeuroImage 2014; 101: 177.

Sun H, Blakely TM, Darvas F, Wander JD, Johnson LA, Su DK, et al. Sequential activation of premotor, primary somatosensory and primary motor areas in humans during cued finger movements. Clinical Neurophysiology 2015; 126: 2150.

Taylor KS, Anastakis DJ, Davis KD. Cutting your nerve changes your brain. Brain 2009; 132: 3122.

Turner JA, Lee JS, Martinez O, Medlin AL, Schandler SL, Cohen MJ. Somatotopy of the motor cortex after long-term spinal cord injury or amputation. IEEE Transactions on Neural Systems and Rehabilitation Engineering 2001; 9: 154.

Vansteensel MJ, Pels EGM, Bleichner MG, Branco MP, Denison T, Freudenburg ZV, et al. Fully Implanted Brain–Computer Interface in a Locked-In Patient with ALS. New England Journal of Medicine 2016; 375: 2060.

Wall JT, Xu J, Wang X. Human brain plasticity: an emerging view of the multiple substrates and mechanisms that cause cortical changes and related sensory dysfunctions after injuries of sensory inputs from the body. Brain Research Reviews 2002; 39: 181.

Weiskopf N. Real-time fMRI and its application to neurofeedback. NeuroImage 2012; 62: 682.

Weiss T, Miltner WHR, Huonker R, Friedel R, Schmidt I, Taub E. Rapid functional plasticity of the somatosensory cortex after finger amputation. Experimental Brain Research 2000; 134: 199.

Wu CWH, Kaas JH. Reorganization in Primary Motor Cortex of Primates with Long-Standing Therapeutic Amputations. Journal of Neuroscience 1999; 19: 7679–7697.

CHAPTER 3

Distinct representation of ipsilateral hand movements in sensorimotor areas

Bruurmijn, M. L. C. M., Raemaekers, M., Branco, M. P., Ramsey, N. F., & Vansteensel, M. J. (2021). Distinct representation of ipsilateral hand movements in sensorimotor areas. European Journal of Neuroscience, 54(10), 7599– 7608. https://doi.org/10.1111/ejn.15501

CHAPTER 3

Abstract

There is ample evidence that the contralateral sensorimotor areas play an important role in movement generation, with the primary motor cortex and the primary somatosensory cortex showing a detailed spatial organization of the representation of contralateral body parts. Interestingly, there are also indications for a role of the motor cortex in controlling the ipsilateral side of the body. However, the precise function of ipsilateral sensorimotor cortex in unilateral movement control is still unclear. Here we show hand movement representation in the ipsilateral sensorimotor hand area, in which hand gestures can be distinguished from each other and from contralateral hand gestures. High-field fMRI data acquired during the execution of six left and six right hand gestures by healthy volunteers showed ipsilateral activation mainly in the anterior section of precentral gyrus and the posterior section of the postcentral gyrus. Despite the lower activation in ipsilateral areas closer to the central sulcus, activity patterns for the twelve hand gestures could be mutually distinguished in these areas. The existence of a unique representation of ipsilateral hand movements in the human sensorimotor cortex favors the notion of transcallosal integrative processes that support optimal coordination of hand movements.

Introduction

In the last decades, the role of the contralateral hemisphere in the generation of limb movement has been vastly studied (Vulliemoz et al. 2005). It has been shown that the majority of the sensorimotor pathways cross the midline towards the contralateral side of the body, and the strongest sensorimotor cortex activation is associated with contralateral movements (Kim et al. 1993). However, there are strong indications that not all human motor fibers decussate in the brainstem (Alawieh et al. 2017) and that both hemispheres are connected by callosal pathways (Aboitiz et al. 1992), suggesting a role of the ipsilateral sensorimotor cortex in movement control, both in non-human (Donchin et al. 1998; Kermadi et al. 1998, 2000; Soteropoulos et al. 2011) and in humans primates (Debaere et al. 2001; Diedrichsen et al. 2013). Indeed, the corpus callosum and several cortical areas, including the premotor cortex, primary motor cortex (M1) and supplementary motor area (SMA), are thought to be involved in coordinating *bimanual* hand movements (Eliassen et al. 2000; Debaere et al. 2001; Diedrichsen et al. 2013). Additionally, the ipsilateral sensorimotor areas seem to play a role in *unimanual* movement control. Evidence for such function comes, among others, from transcranial magnetic stimulation studies (Kobayashi et al. 2003) and from studies showing task-related modulation of sensorimotor activity during movements of the ipsilateral hand (Seidler et al. 2004; Verstynen 2004; Buetefisch et al. 2014). Another recent study found that in ipsilateral M1, BOLD activity increases when the task required more precise motor movements (Barany et al. 2020). Furthermore, similar to the contralateral homunculus representation, the sensorimotor cortex contains a detailed and organized spatial representation of movements of different *ipsilateral* body parts (Scherer et al. 2009; Hotson et al. 2014; Fujiwara et al. 2017; Downey et al. 2020). However, although ipsilateral representation has been found even for individual fingers (Diedrichsen et al. 2013), it is also known that, in general, activation patterns elicited from complex hand movements, consisting of simultaneous flexion and extension of multiple fingers, are not simple a linear combination of these single-digit patterns (Hamed et al. 2007). We therefore studied ipsilateral activation patterns for complex, multi-digit hand movements, and the role of the sensorimotor areas in ipsilateral hand movement control, by directly investigating whether complex unilateral movements of the left and right hand could be distinguished from each other within one hemisphere.

We investigated the representation of complex hand gestures with high-field (7 tesla) functional magnetic imaging (fMRI). Nine healthy, able-bodied volunteers performed six unimanual hand gestures associated with the characters '8', 'F', 'L', 'S', 'W', and 'Y' of the American Manual Alphabet, with their right and left hand (in separate runs). As in our previous work (Bruurmijn et al. 2017), we divided the sensorimotor cortex into four regions-of-interest (ROIs: M1, S1, pre-M1, post-S1) to study the hand gesture representations in detail, where M1 represented the posterior part of the precentral gyrus (primary motor cortex), pre-M1 the anterior part of the precentral gyrus, S1 the anterior part of the postcentral gyrus (primary somatosensory cortex) and post-S1 the posterior part of the postcentral gyrus.

Methods

Subjects

For the current study, we re-analysed data recorded for an earlier study (Bruurmijn et al. 2017). Nine healthy, able-bodied control subjects (mean age 44 ± 21 years, 4 females, all right handed as confirmed by the Edinburgh Handedness Inventory (Oldfield 1971)) performed a hand gesture task, while functional brain images were acquired using 7 Tesla MRI. All subjects gave written informed consent to participate in this study, which was approved by the Medical Research Ethics committee Utrecht, according to the Declaration of Helsinki (Association 2013).

Gesture Task

In a single 7T fMRI scan session, subjects performed a unimanual hand gesture task. Prior to scanning, subjects were familiarized with the hand gestures, which were associated with the characters '8', 'F', 'L', 'S', 'W', and 'Y' of the American Manual Alphabet. In the week before scanning, subjects practiced at home for 15 minutes per day in making the gestures with each hand.

One task run consisted of 10 trials per gesture. During the task, one of the six characters was presented pseudo-randomly on the screen every 15.6 seconds for subjects C1 and C2, and every 16 seconds for the other subjects. Subjects made the gesture corresponding to the character shown and held the gesture for 6 seconds before relaxing. Each subject performed 4 task runs: 2 runs with the right hand (R1 and R2), and 2 runs with the left hand (L1 and L2). Before each run, the subject was instructed which hand to use. This yielded a total of 20 trials per gesture for each hand.

Data acquisition

MRI data were recorded using a Philips Achieva 7T MRI system with a 32-channel head coil. Anatomical T1- and PD-weighted images were acquired first (TR/TE = 6/1.4 ms, FA = 8°, voxel size = 1 × 1 × 1 mm^3). For scans during the Hand Gesture Task, an EPI sequence was used (TR/TE = 1300/27 ms for subjects C1 and C2, TR/TE = 1600/27 ms for all other subjects, FA = 70°, acquisition matrix size = 104 × 129, 26 slices, no gap, voxel size = 1.6 × 1.6 × 1.6 mm^3).

Task preprocessing

Functional scans from the hand gesture task were preprocessed using SPM12 (http://www.fil.ion.ucl.ac.uk/spm/). Scans were aligned and coregistered with the anatomical T1. For each subject, a beta-map and a t-map were calculated per run (L1, L2, R1, and R2) by fitting a general linear model (GLM), using the contrast "movement versus rest", without making a distinction between the different gestures. All statistical maps were calculated in subject space.

Regions of interest

M1 and S1 are the primary regions of interest, obtained in subject space using the Destrieux Atlas (Destrieux et al. 2010) and Desikan-Killiany Atlases (Desikan et al. 2006). However, to also assess higher level motor cortex as well, the areas anterior to M1 (pre-M1, part of the premotor area) and posterior to S1 (post-S1, roughly corresponding with Brodmann area 2), were also included as ROIs.

These four ROIs are therefore defined as follows, in which we have used the names of the regions in DKA and DA, and where '+' denotes the voxel-wise union, and '^' denotes the intersection of two regions. M1 consists of the primary motor cortex and the posterior part of the precentral gyrus ($PrecentralGyrus_{DA}$ + [$CentralSulcus_{DA}$ ^ $PrecentralGyrus_{DKA}$]). S1 consists of the primary sensory cortex, the anterior part of the postcentral gyrus ($PostcentralGyrus_{DA}$ + [$CentralSulcus_{DA}$ ^ $PostcentralGyrus_{DKA}$]). Pre-M1 covers the anterior part of the precentral gyrus ($PrecentralSulcus_{DA}$) and post-S1 the posterior part of the postcentral gyrus ($PostcentralSulcus_{DA}$).

Decoding twelve gestures from one hemisphere

To assess the discriminability of hand gestures in the sensorimotor cortex of both the contralateral and ipsilateral hemisphere, a decoding approach was used similar to that of previous work from our group (Bleichner et al. 2013; Bruurmijn et al. 2017). This analysis consists of several steps: voxel selection, classifier training, classifier testing, applied on volumetric data in subject space, and on the right and left hemisphere separately.

Data were split in training and test sets. Per subject, two left and two right hand task data sets were acquired in four separate fMRI runs (L1, L2, R1, and R2), whereas the classifier was trained on contralateral and ipsilateral movements simultaneously. This may have an effect on the overall activation patterns for both hands. This effect was minimized by varying the order of the tasks across subjects. Moreover, the training and test sets were strictly separated. This was done by selecting one run per hand as training set, resulting in four training sets consisting of one left and one right hand run (L1&R1, L1&R2, L2&R1 and L2&R2). In each case, the remaining runs constituted the test set for validation. For each choice of the training set, the voxel selection was done separately, to prevent any bias that would be introduced by the test set.

Per training set, a combined t-map was compiled by taking, from the L and R "movement versus rest" t-maps described above, for each voxel the highest t-value from either the left- or right-hand t-map. Subsequently, from each of the four principal ROIs, the 250 voxels with the highest absolute t-values were selected from the training set. The BOLD signal in these voxels was detrended and transformed into z-scores for each separate run. For each trial, the BOLD amplitude was averaged around its peak, which occurs roughly between 6 to 8 seconds, by taking the mean of scans 5, 6, and 7 for subjects C1 and C2, and scans 4, 5, and 6 for other subjects (due to their difference in fMRI repetition time). This resulted in a 'feature vector' of 250 features per trial.

For the classifier, a support vector machine (SVM) was used, using a linear kernel and parameter C set to a fixed value of 1. Since an SVM is a binary classifier, multiple SVMs needed to be combined. For each pair of gestures, a separate SVM was trained to distinguish between those two gestures (for example, to distinguish a 'right hand 8' from a 'left hand F'). This results in 66 binary classifiers. For classifying a single trial, each of the binary SVMs then casts a vote for the 'winning' gesture. The gesture with the most votes from all binary classifiers was chosen as the classifier result ('prediction'). All 66 binary SVMs had an equal weight in the voting process.

Training a classifier on the training set and applying it on the test set results in a 'predicted' gesture for each trial in the test set. The classification accuracy was calculated as the percentage of correctly classified gestures. Since four training sets were created per subject (together with four associated test sets), the classification procedure was repeated for each training/test set combination, resulting in four independent classification scores. These four classification scores were averaged resulting in one classification score per ROI per subject.

To obtain the chance level (and associated confidence interval) for the classification, the classifier was also trained on data with random permutations (Combrisson and Jerbi 2015) of the gesture label for each subject, hemisphere and ROI. This procedure was repeated 500 times to obtain a distribution of the chance level. Averaging over these iterations yielded a chance level of 8.3% ± 0.06% (which is in agreement with the theoretical chance level for 12 classes). If the confidence interval of the classification scores does not contain the chance level of 8.3%, the classification is considered to be better than chance.

As a post-hoc test, the effects of hemisphere and ROI were evaluated using a two-way repeated measures ANOVA with ROI and hemisphere as within-subject factors, at a significance level of 0.05.

Confusion matrices give insight not only in the accuracy of classification, but also in the nature of errors. The confusion matrices were constructed as a cross-table, in which each cell indicates in percentages how many trials from a particular gesture ('actual gesture') were classified as another gesture ('predicted as …'). Separate confusion matrices were assembled per subject, hemisphere and ROI. Per hemisphere and ROI, one confusion matrix was calculated by averaging across subjects.

Each confusion matrix can be viewed as composed of four quadrants (sub-matrices). The upper left and bottom right quadrant reflect the 'within-hand' confusion: values on the diagonal denote correct classifications, and off-diagonal values reflect confusions with a different gesture from the same hand (e.g. between W_L and F_L). The top right and bottom left quadrant reflect the 'between-hands' confusion: the values on the diagonal of these sub-matrices indicate trials that were classified as the correct gesture type, but with the wrong hand (e.g. between W_L and W_R).

For each subject, confusion matrices for all ROIs were averaged. A mean within-hand confusion score was calculated by averaging all the off-diagonal values in the top left and bottom right quadrant. A mean between-hands confusion score was calculated by averaging all the diagonal values of the top right and bottom left quadrant. A paired-samples t-test was then conducted to compare the mean scores between within-hand and between-hand errors.

Results

For both the left and the right hemisphere, activation maps associated with contralateral hand gestures showed a hotspot in both the pre- and the post-central areas, mainly inside the central sulcus (Figure 1). During ipsilateral hand movements, however, activation was generally lower in regions around the central sulcus (right M1 and left and right S1), but not in regions further away from the central sulcus, both in anterior and posterior direction. This difference in mean activation was tested by paired-samples t-tests on average beta value per ROI for ipsilateral minus contralateral activity with Bonferroni-corrected alpha of 0.05/8 = 0.006, as there were 4 ROIs in each hemisphere: left pre-M1: $t_8 = -2.40$, $P = 0.04$; left M1: $t_8 = -3.38$, $P = 0.01$; left S1: $t_8 = -6.15$, $P < 0.001$; left post-S1: $t_8 = -2.11$, $P = 0.07$; right pre-M1: $t_8 = -2.41$, $P = 0.04$; right M1: $t_8 = -4.02$, $P = 0.004$; right S1: $t_8 = -4.77$, $P = 0.001$; right post-S1: $t_8 = -4.24$, $P = 0.003$.

For ROIs M1, S1, and post-S1 of both the left and the right hemisphere, the classification scores for decoding twelve gestures were significantly higher than chance level (Figure 2A, group-mean scores ranging from 14.0% to 35.4%, chance level 8.33%), indicating that it is possible to discriminate between the representation of hand gestures for the left and right hand from the *same* subareas of the sensorimotor cortex. Two-way repeated measures ANOVA revealed that there was a significant main effect of ROI ($F_{3,6} = 10.8$, $P = 0.008$), with M1 and S1 demonstrating the highest classification scores. There was no significant main effect of hemisphere ($F_{3,6} = 1.06$, $P = 0.43$) and no significant interaction effect of ROI and hemisphere on the classification score ($F_{3,6} = 3.77$, $P = 0.08$). This indicates that, although sample sizes are small, there is currently no evidence that there is a difference between hemispheres.

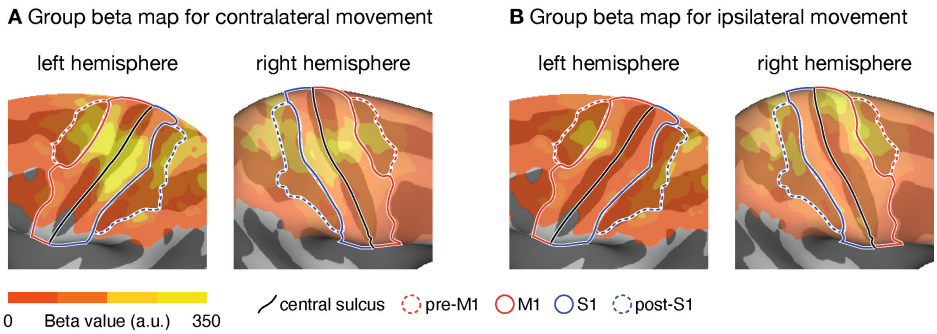

Figure 1. *Group activation patterns for contralateral and ipsilateral hand gestures. Colors indicate beta values averaged over subjects and are displayed on the average FreeSurfer brain, in which light and dark gray reflect gyri and sulci, respectively. The central sulcus and ROIs for classification are delineated. A: Beta maps for contralateral movement (right hand activity plotted on the left hemisphere and left hand activity plotted on the right hemisphere). B: Beta maps for movement of the ipsilateral hand. Ipsilateral activity is mostly located anterior and posterior to the central sulcus, whereas activity inside the sulcus is low.*

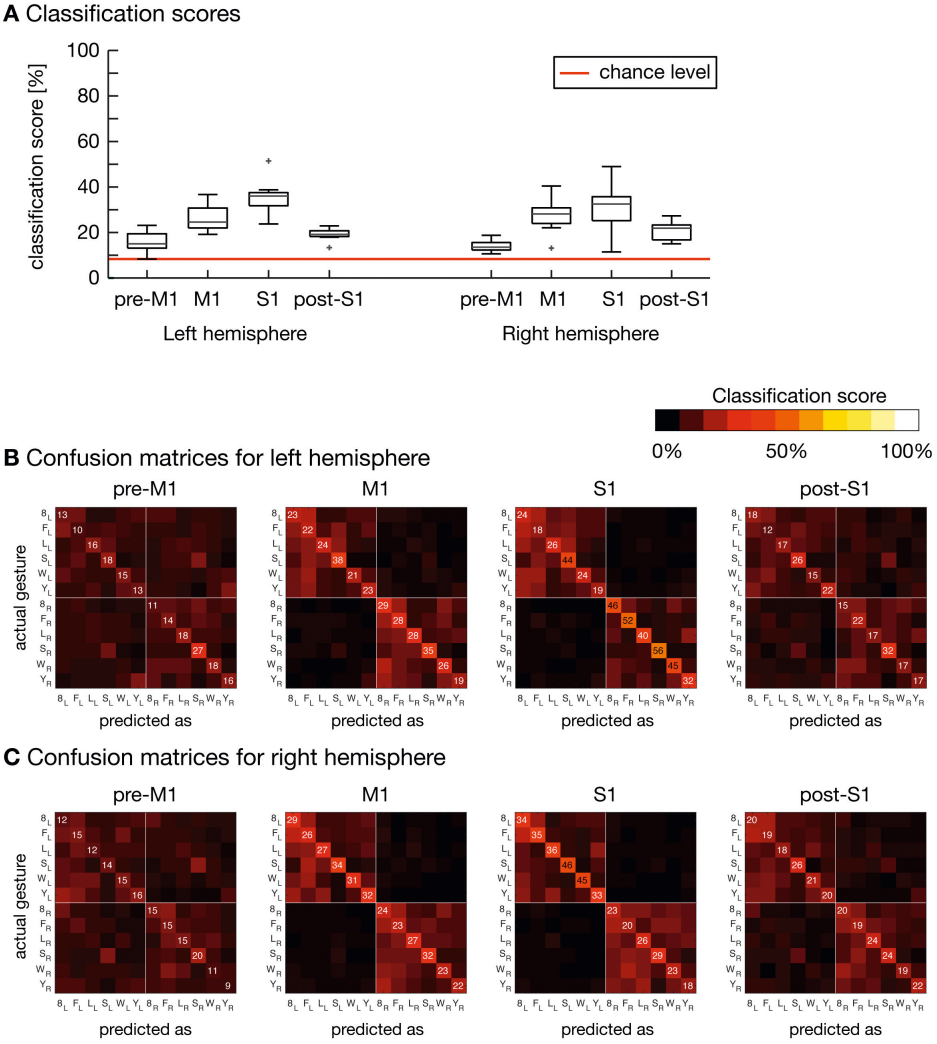

Figure 2. *A: Classification scores for all 12 classes (contralateral and ipsilateral hand movements), per ROI. The red line indicates chance level for 12 classes (8.3%, as simulated by the random permutation test). B and C: Confusion matrices for decoding ipsilateral and contralateral gestures from four ROIs in the left (B) and right (C) hemisphere, averaged across subjects. The rows of the matrix reflect how the trials for each gesture were classified (in percentage). The diagonal thus shows the percentage of correctly classified trials for each gesture. Subscripts indicate gestures of the left ('L') and the right ('R') hand.*

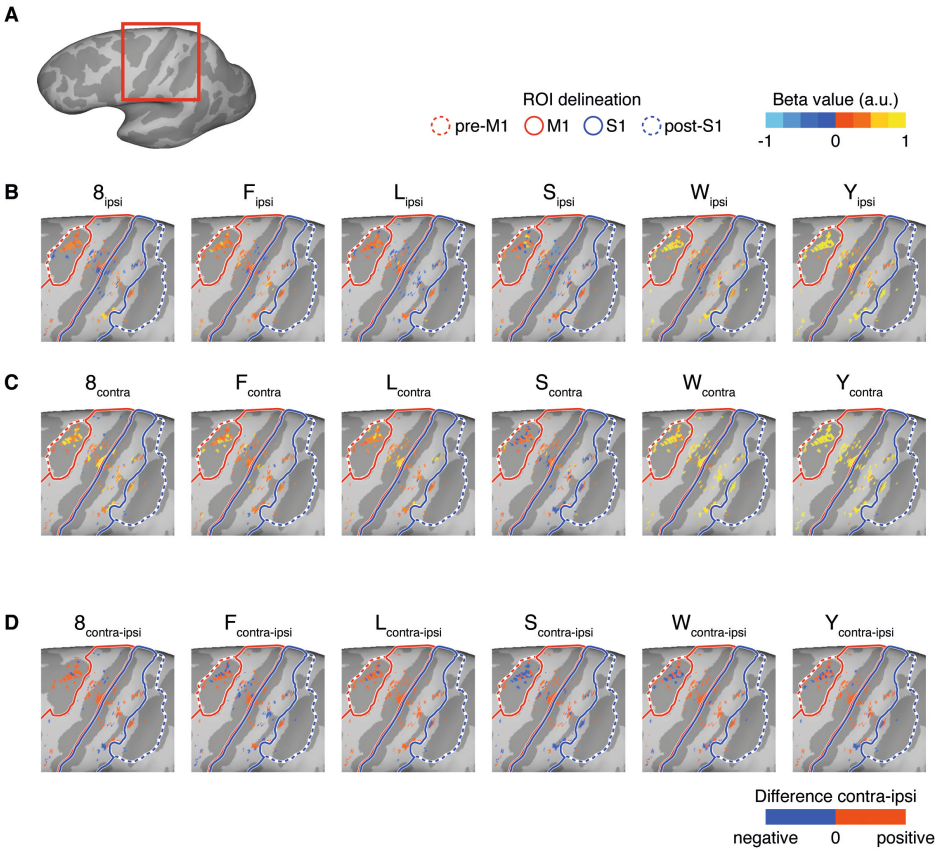

Figure 3. *Activity in voxels selected for classification, for ipsilateral and contralateral gestures on the left hemisphere for one subject (C4). A: inflated brain surface from FreeSurfer, where light gray indicates gyri, and dark indicates sulci. The red box indicates the zoom window in the lower panels. B: Beta pattern for each ipsilateral gesture (left hand movement). The ROIs used for classification are delineated. C: Beta values for each contralateral gesture (right hand movement). D: differential beta pattern per gesture (contra - ipsi).*

Confusion matrices (Figure 2B and C) reveal that gestures from the contralateral hand generally demonstrated higher classification scores than gestures from the ipsilateral hand. A paired-samples t-test showed a significant difference between within-hand and between-hands confusion scores ($t_8 = 2.63$, $P = 0.03$), indicating that confusion is more likely to happen between different gestures of the same hand (for example, W_L with F_L) than between the same gestures of the left and right hand (for example, W_L with W_R). This result may be explained by the difference in amplitude between ipsilateral and contralateral activations mentioned above. Since the tasks involved only moving one hand at a time, it is possible that the activity that was found for the ipsilateral hand is just a 'mirrored' version of the representation on the contralateral hemisphere, with only a lower amplitude, which in itself would drive classification (Scherer et al. 2009). However, if this were true, the BOLD patterns for a gesture made with the ipsilateral and contralateral hand would be highly similar. To investigate this, we plotted the average beta patterns per gesture (see Figure 3 for the left hemisphere of one representative subject C4).

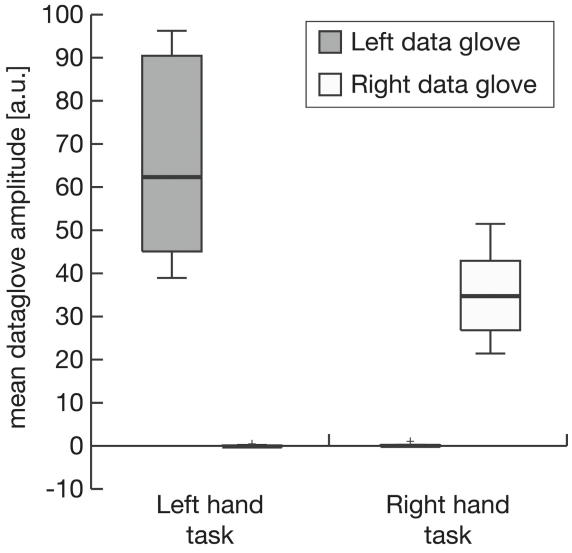

Figure 4. *Data glove amplitudes (averaged over all trials and subjects in arbitrary units) for both hands during the left hand task and the right hand task. The amplitudes of the hand that needs to be kept still are small with respect to the amplitudes of the hands with which the tasks were executed.*

These patterns show that the same gesture generates different spatial patterns for the contralateral and ipsilateral hand, supporting the notion of a distinct and independent representation of the ipsilateral hand gestures within the sensorimotor cortex. A potential bias for the presence of ipsilateral activity could be uninstructed movement of the contralateral hand during ipsilateral trials. However, finger flexion measurements using a data glove worn during the tasks confirmed that gestures were executed unimanually (Figure 4).

Discussion

Our present results reveal the existence of a detailed representation of ipsilateral hand gestures in the human sensorimotor cortex that can be distinguished from the representation of contralateral hand movements in this area, indicating that (subpopulations of) neurons within the human sensorimotor cortex are distinctly associated with ipsilateral hand movement. Importantly, the difference in representation is not merely the result of different levels of activation between ipsilateral and contralateral hand gestures, but is associated with spatially distinct activation patterns, especially in primary somatosensory and motor cortex.

Observations about the activity of ipsilateral hand movement activity are in line with earlier reports (Verstynen 2004; Hanakawa et al. 2005; Diedrichsen et al. 2013; Buetefisch et al. 2014), as well as with single-cell studies in non-human primates that demonstrated that the sensorimotor cortex contains subsets of neurons that activate specifically during ipsilateral movement (Tanji et al. 1988; Donchin et al. 1998; Kermadi et al. 1998). The current study extends these findings to humans and shows ipsilateral hand movement representation at the level of mm-sized neuronal ensembles,

which may indicate higher concentrations of ipsilateral neurons responding in specific foci. The ROIs M1 and S1 demonstrated the highest classification scores, despite relatively low activity levels. This finding shows that to the ability to decode detailed movements from the cortex does not require high activity in the target regions and agrees with previous findings from Diedrichsen et al. (Diedrichsen et al. 2013).

We propose that the observation that both hands activate differentiable patterns in the same hemisphere reflects the presence of at least a subset of cross-callosal projections that conveys information about movements of one hand from the contralateral to the ipsilateral sensorimotor area and that exhibits a convergence on specific foci within the ipsilateral hand area that are distinct from foci in the same region activated during contralateral hand movements. These findings indicate that at least part of the cross-callosal projections are concentrated in foci that are at a spatial scale that is detectable with fMRI (1.5-2 mm). If ipsi- and contra-lateral hand movement representations are in reality more detailed than this range (smaller ensemble sizes than 1.5-2 mm), the current resolution may have led to averaging across adjacent ensembles, and classification may improve with increasing fMRI resolution.

Transcallosal projections have been attributed both inhibitory and excitatory roles (Knaap and Ham 2011). The specificity of ipsilateral patterns for different gestures shown in the current study, only visible with a classification algorithm, cannot be explained by the concept of cross-callosal inhibition of the hand region. Given the reports on inhibitory function (Beaulé et al. 2012), however, we argue that both excitatory and inhibitory projections exist, but that the former bears functional relevance in terms of informing one hemisphere of the movements of the ipsilateral hand, thereby integrating information from both hemispheres, and contributing to optimal coordination of hand movements with respect to the rest of the body. This mechanism may also explain why unilateral stroke often affects contralateral and ipsilateral movements (Colebatch and Gandevia 1989; Sainburg and Duff 2006).

According to recent work, examining active finger presses and passive finger stimulation of one hand in both hemispheres, ipsilateral representations are mostly associated with planning and initiation of motor acts and less with feedback control, since ipsilateral finger-specific representation was most clear in premotor and parietal regions (Berlot et al. 2019). However, despite the lower activity in the M1 and S1 ROIs, we found the highest decoding accuracy in these areas, indicating that ipsilateral and contralateral representations are especially distinct in these primary sensorimotor areas, which would be in line with a role for ipsilateral areas during the actual execution phase of the hand gestures. Different levels of complexity of the movements performed in this study and the work of Berlot et al. (Berlot et al. 2019) may be associated with this discrepancy. Indeed, increasing movement complexity is known to be associated with increased activation of ipsilateral M1 (Seidler et al. 2004; Verstynen 2004; Buetefisch et al. 2014) and transcallosal integration and ipsilateral movement control have been suggested to be especially relevant or pronounced for more complex movements (Knaap and Ham 2011).

However, there are several shortcomings to the current study. First, performance of the support vector machine could have been made worse by requesting subjects to only move a single hand during each task run. For recording all hands, the task run was repeated to obtain two runs for the right hand and two runs for the left hand. When decoding both hands from the same hemisphere, runs for different hands needed to be combined. The recalibration at the start of each run of fMRI scans may have made the BOLD estimates within runs slightly more similar, which could bias the classifier toward correct identification of at least the hand. Therefore, the training set did not include trials from within the same run as the test set. if all data were acquired in a single run, which would have allowed a leave one out training scheme, increasing the size of the training set. A single run is however impractical due to excessive challenging of the subject and scanner hardware.

A second limitation lies in the possibility of ipsilateral decoding to be driven by variations in difficulty between the movements. Whereas the gestures 8 and F, and W and Y are similar in terms of complexity of movement execution (8 and F are each other's mirrored version in terms of flexion and extension of the fingers, and so are W and Y), the gesture S amounts to making a fist and can be regarded as less demanding. However, the confusion matrices of the classification scores for each gesture, demonstrated that the classification results were not exclusively driven by this difference in complexity, since the diagonal pattern (indicating correct classification) was also present for the other gestures.

Lastly, the choice of parameters for training the support vector machine may have been suboptimal. In this study, classifiers were trained and tested on each subject individually. This was done because activity distributions vary between subjects, and it is crucial to capture minute variations for discriminating between complex gestures. The training of the classifier is affected by a priori choices of hyperparameters or a training kernels and ideally, these choices are optimized for every subject. This however requires substantial amounts of data for independently tuning and testing the classifier, which were not available due to the limitations of an fMRI design. This process would become more accessible with using other recording techniques, such as intracranial recordings, which have a superior temporal resolution.

Taken together, we here provide support for the existence of patches of sensorimotor cortex that are uniquely associated with the execution of complex ipsilateral hand gestures, and propose transcallosal interhemispheric information transfer as a mechanism for the generation of such activity. Our findings shed light on the importance of ipsilateral activity beyond the coordination of bimanual movements.

References

Aboitiz F, Scheibel AB, Fisher RS, Zaidel E. 1992. Fiber composition of the human corpus callosum. Brain Res. **598**:143–153.

Alawieh A, Tomlinson S, Adkins D, Kautz S, Feng W. 2017. Preclinical and Clinical Evidence on Ipsilateral Corticospinal Projections: Implication for Motor Recovery. Transl Stroke Res. **8**:529–540.

Association WM. 2013. World Medical Association Declaration of Helsinki: Ethical Principles for Medical Research Involving Human Subjects. JAMA. **310**:2191–2194.

Barany DA, Revill KP, Caliban A, Vernon I, Shukla A, Sathian K, Buetefisch CM. 2020. Primary motor cortical activity during unimanual movements with increasing demand on precision. J Neurophysiol. **124**:728–739.

Beaulé V, Tremblay S, Théoret H. 2012. Interhemispheric control of unilateral movement. Neural Plast. **2012**:627816.

Berlot E, Prichard G, O'Reilly J, Ejaz N, Diedrichsen J. 2019. Ipsilateral finger representations in the sensorimotor cortex are driven by active movement processes, not passive sensory input. Journal of Neurophysiology. **121**:418.

Bleichner MG, Jansma JM, Sellmeijer J, Raemaekers M, Ramsey NF. 2013. Give Me a Sign: Decoding Complex Coordinated Hand Movements Using High-Field fMRI. Brain Topography. **27**:248.

Bruurmijn MLCM, Pereboom IPL, Vansteensel MJ, Raemaekers MAH, Ramsey NF. 2017. Preservation of hand movement representation in the sensorimotor areas of amputees. Brain. **140**:3166.

Buetefisch CM, Revill KP, Shuster L, Hines B, Parsons M. 2014. Motor demand-dependent activation of ipsilateral motor cortex. Journal of Neurophysiology. **112**:999.

Colebatch JG, Gandevia SC. 1989. The distribution of muscular weakness in upper motor neuron lesions affecting the arm. Brain J Neurology. **112** (Pt 3):749–763.

Combrisson E, Jerbi K. 2015. Exceeding chance level by chance: The caveat of theoretical chance levels in brain signal classification and statistical assessment of decoding accuracy. Journal of Neuroscience Methods. **250**:126.

Debaere F, Swinnen SP, Béatse E, Sunaert S, Hecke PV, Duysens J. 2001. Brain Areas Involved in Interlimb Coordination: A Distributed Network. Neuroimage. **14**:947–958.

Desikan RS, Ségonne F, Fischl B, Quinn BT, Dickerson BC, Blacker D, Buckner RL, Dale AM, Maguire RP, Hyman BT, Albert MS, Killiany RJ. 2006. An automated labeling system for subdividing the human cerebral cortex on MRI scans into gyral based regions of interest. NeuroImage. **31**:968.

Destrieux C, Fischl B, Dale A, Halgren E. 2010. Automatic parcellation of human cortical gyri and sulci using standard anatomical nomenclature. NeuroImage. **53**:1.

Diedrichsen J, Wiestler T, Krakauer JW. 2013. Two Distinct Ipsilateral Cortical Representations for Individuated Finger Movements. Cerebral Cortex. **23**:1362.

Donchin O, Gribova A, Steinberg O, Bergman H, Vaadia E. 1998. Primary motor cortex is involved in bimanual coordination. Nature. **395**:274–278.

Downey JE, Quick KM, Schwed N, Weiss JM, Wittenberg GF, Boninger ML, Collinger JL. 2020. The Motor Cortex Has Independent Representations for Ipsilateral and Contralateral Arm Movements But Correlated Representations for Grasping. Cereb Cortex.

Eliassen JC, Baynes K, Gazzaniga MS. 2000. Anterior and posterior callosal contributions to simultaneous bimanual movements of the hands and fingers. Brain. **123**:2501–2511.

Fujiwara Y, Matsumoto R, Nakae T, Usami K, Matsuhashi M, Kikuchi T, Yoshida K, Kunieda T, Miyamoto S, Mima T, Ikeda A, Osu R. 2017. Neural pattern similarity between contra- and ipsilateral movements in high-frequency band of human electrocorticograms. NeuroImage. **147**:302.

Hamed SB, Schieber MH, Pouget A. 2007. Decoding M1 Neurons During Multiple Finger Movements. Journal of Neurophysiology. **98**:327.

Hanakawa T, Parikh S, Bruno MK, Hallett M. 2005. Finger and Face Representations in the Ipsilateral Precentral Motor Areas in Humans. J Neurophysiol. **93**:2950–2958.

Hotson G, Fifer MS, Acharya S, Benz HL, Anderson WS, Thakor NV, Crone NE. 2014. Coarse electrocorticographic decoding of ipsilateral reach in patients with brain lesions. Plos One. **9**:e115236.

Kermadi I, Liu Y, Rouiller EM. 2000. Do bimanual motor actions involve the dorsal premotor (PMd), cingulate (CMA) and posterior parietal (PPC) cortices? Comparison with primary and supplementary motor cortical areas. Somatosens Mot Res. **17**:255–271.

Kermadi I, Liu Y, Tempini A, Calciati E, Rouiller EM. 1998. Neuronal activity in the primate supplementary motor area and the primary motor cortex in relation to spatio-temporal bimanual coordination. Somatosens Mot Res. **15**:287–308.

Kim S, Ashe J, Hendrich K, Ellermann J, Merkle H, Ugurbil K, Georgopoulos A. 1993. Functional magnetic resonance imaging of motor cortex: hemispheric asymmetry and handedness. Science. **261**:615–617.

Knaap LJ van der, Ham IJM van der. 2011. How does the corpus callosum mediate interhemispheric transfer? A review. Behav Brain Res. **223**:211–221.

Kobayashi M, Hutchinson S, Schlaug G, Pascual-Leone A. 2003. Ipsilateral motor cortex activation on functional magnetic resonance imaging during unilateral hand movements is related to interhemispheric interactions. NeuroImage. **20**:2259.

Oldfield RC. 1971. The assessment and analysis of handedness: The Edinburgh inventory. Neuropsychologia. **9:**97.

Sainburg RL, Duff SV. 2006. Does motor lateralization have implications for stroke rehabilitation? J Rehabilitation Res Dev. **43**:311.

Scherer R, Zanos SP, Miller KJ, Rao RPN, Ojemann JG. 2009. Classification of contralateral and ipsilateral finger movements for electrocorticographic brain-computer interfaces. Neurosurgical Focus. **27**:E12.

Seidler RD, Noll DC, Thiers G. 2004. Feedforward and feedback processes in motor control. NeuroImage. **22**:1775.

Soteropoulos DS, Edgley SA, Baker SN. 2011. Lack of Evidence for Direct Corticospinal Contributions to Control of the Ipsilateral Forelimb in Monkey. Journal of Neuroscience. **31**:11208.

Tanji J, Okano K, Sato KC. 1988. Neuronal activity in cortical motor areas related to ipsilateral, contralateral, and bilateral digit movements of the monkey. J Neurophysiol. **60**:325–343.

Verstynen T. 2004. Ipsilateral Motor Cortex Activity During Unimanual Hand Movements Relates to Task Complexity. Journal of Neurophysiology. **93**:1209.

Vulliemoz S, Raineteau O, Jabaudon D. 2005. Reaching beyond the midline: why are human brains cross wired? Lancet Neurology. **4**:87–99.

CHAPTER 4

Decoding Attempted phantom hand movements from ipsilateral sensorimotor areas after amputation

—

Bruurmijn LCM, Raemaekers M, Branco MP, Vansteensel MJ, Ramsey NF. Decoding attempted phantom hand movements from ipsilateral sensorimotor areas after amputation. J Neural Eng. 2021 Sep 23;18(5). doi: 10.1088/1741-2552/ac20e4. PMID: 34433158.

CHAPTER 4

Abstract

Objective

The sensorimotor cortex is often selected as target in the development of a Brain-Computer Interface, as activation patterns from this region can be robustly decoded to discriminate between different movements the user executes. Up until recently, such BCIs were primarily based on activity in the contralateral hemisphere, where decoding movements still works even years after denervation. However, there is increasing evidence for a role of the sensorimotor cortex in controlling the ipsilateral body. The aim of this study is to investigate the effects of denervation on the movement representation on the ipsilateral sensorimotor cortex.

Approach

Eight subjects with acquired above-elbow arm amputation and nine controls performed a task in which they made (or attempted to make with their phantom hand) six different gestures from the American Manual Alphabet. Brain activity was measured using 7T functional MRI, and a classifier was trained to discriminate between activation patterns on four different regions of interest (ROIs) on the ipsilateral sensorimotor cortex.

Main results

Classification scores showed that decoding was possible and significantly better than chance level for both the phantom and intact hands from all ROIs. Decoding both the left (intact) and right (phantom) hand from the same hemisphere was also possible with above-chance level classification score.

Significance

The possibility to decode both hands from the same hemisphere, even years after denervation, indicates that implantation of motor-electrodes for BCI control possibly need only cover a single hemisphere, making surgery less invasive, and increasing options for people with lateralized damage to motor cortex like after stroke.

Introduction

When investigating brain activity associated with movements in the context of brain-computer interfaces (BCIs), it is intuitive to consider sensorimotor activity contralateral to the side of movement, since the vast majority of axons of the corticospinal tract cross the midline in the brainstem (Kim *et al.*, 1993). However, the ipsilateral hemisphere may also contain detailed information on motor movements. In the context of implantable BCIs, being able to decode movement information also from the ipsilateral hemisphere opens the possibility of electrode implantation on a single hemisphere. However, it is required that the ipsilateral movement representation is still intact after denervation. This is the topic we address in this study.

The primary sensorimotor cortex (primary motor cortex M1 and primary sensory cortex S1) reveals a somatotopic organisation, in which the different body parts are orderly layed out along the cortex (Penfield & Boldrey, 1937). For different movements, this organisation yields different (spatial) activation patterns (Grodd *et al.*, 2001), even on the level of within-limb movements, such as individual finger movements (Dechent & Frahm, 2003; Hadoush *et al.*, 2011; Diedrichsen *et al.*, 2013; Siero *et al.*, 2014). The existence of these spatially distinguishable patterns and the fact that the activity is under voluntary control makes the sensorimotor cortices an ideal target area for implanted BCIs (Leuthardt *et al.*, 2004; Wolpaw, 2007; Vansteensel *et al.*, 2016). Machine learning algorithms can then be trained using activation patterns in the sensorimotor cortex for particular movements, with the aim of identifying the movement that was made by the participant, which can then be used to drive an actuator or communicative device (Hochberg *et al.*, 2006; Collinger *et al.*, 2013).

In addition to movement representations on the contralateral hemisphere, the ipsilateral hemisphere may also contain detailed information on motor movements, as not all axons pathways cross the midline (Alawieh *et al.*, 2017), and because the two hemispheres are connected via the corpus callosum (Aboitiz *et al.*, 1992). Indeed, the ipsilateral sensorimotorcortex is shown to activate during movements, albeit less strongly than the contralateral hemisphere (Seidler *et al.*, 2004; Verstynen, 2004). By a virtual lesion using transcranial magnetic stimulation, the ipsilateral M1 has been found to play a role in the timing of muscle recruitment (Davare *et al.*, 2006). Also, the amount of ipsilateral activity correlates with task difficulty and skill (Seidler *et al.*, 2004; Buetefisch *et al.*, 2014).

The presence of activity ipsilateral to the side of movement has the potential for doubling the degrees of freedom obtainable from a single hemisphere, and thus from a unilateral BCI implant. This would be relevant for people who lost hand function following contralateral stroke. Indeed, decoding movements from the ipsilateral cortex, both coarse arm movements as well as fine-grained individual finger articulations, has been successfully applied using different modalities, such as electrocorticography (Scherer *et al.*, 2009; Bundy & Leuthardt, 2019), functional MRI (Diedrichsen *et al.*, 2013; Gallivan *et al.*, 2013; Berlot *et al.*, 2019) and microelectrode arrays (Downey *et al.*, 2020). However, the context of these studies does not match the conditions under which BCIs would be applied in practise, which would typically involve people who are paralysed or who have lost limbs. These clinical conditions could challenge the well-ordered somatotopic

mapping through brain plasticity causing shifts in movement- or sensory-based brain activation patterns. Studies in individuals with upper-limb amputation have reported an 'invasion' of lip, chin and shoulder activity patterns into the former hand area (Elbert *et al.*, 1994; Dettmers *et al.*, 2001; Lotze *et al.*, 2001). However, by applying decoding techniques to attempted gestures with the phantom (missing) hand in people with amputation, it has been found that functional representations in the hand area contralateral to the amputation are still intact (Kikkert *et al.*, 2016; Bruurmijn *et al.*, 2017).

It is yet unknown wether ipsilateral activity is still usable for decoding motor movements in people who have been unable to move their limbs for an extended period of time. Similar to the contralateral cortex, the ipsilateral activity seems subject to change after denervation: structural and functional differences have for example been observed in people with amputation compared to controls (Hamzei *et al.*, 2001) and expanded ipsilateral activation has been found in an athlete long jumper with lower-limb amputation (Mizuguchi *et al.*, 2019). In addition, ipsilateral activity in people with arm amputation who moved their intact hand is higher than that of non-amputated control subjects (Bogdanov *et al.*, 2012; Philip & Frey, 2014). Also on a network level, the functional inter-hemispheric connectivity has been found to be reduced after denervation (Bramati *et al.*, 2019).

To investigate if denervation is consequential for the use of *ipsilateral* movement representations for BCI control, we expand our previous work on decoding six (attempted) hand gestures from the sensorimotor cortex (Bleichner *et al.*, 2013; Bruurmijn *et al.*, 2017). Subjects with acquired above-elbow arm amputation were instructed to attempt making detailed gestures with their phantom hand while in a 7T MRI scanner. A control group performed a similar task with only executed hand gestures. A classifier was trained for predicting which gesture was made based on the fMRI activity patterns from the sensory and motor areas ipsilaterally to the moving hand. Parts of the dataset presented here have been published elsewhere, but are included here for reference purposes. This concerns the classification scores from the contralateral hemisphere for both the amputation and control groups (Bruurmijn *et al.*, 2017), and the classification from the ipsilateral hemisphere in the amputation group (Bruurmijn *et al.*, 2020). The results from this study could contribute to improving the speed and efficiency of BCIs that require only an unilateral implantation procedure.

Methods

Subjects

Eight subjects with an amputated arm were recruited (age 52 ± 12 years [M ± SD], 1 female), with transhumeral amputation of their right (N=7) or left hand (N=1). Amputations were acquired between 1.7 and 31.1 years ago (mean and standard deviation 16.4 ± 11.5 years). Nine control subjects were also recruited (no arm amputation, age 44 ± 21 years [M ± SD], 4 females). There was no significant difference in age between the amputation and control group (Mann-Whitney U test, U=28.5, p=0.50). All subjects were right-handed or were right-handed before amputation according to the Edinburgh Handedness Inventory (Oldfield, 1971). The study was approved by the medical-ethical committee of the University Medical Center Utrecht and all subjects gave

their written informed consent in agreement with the declaration of Helsinki (2013) (Association, 2013). We have previously published on part of this data set with a different research question (Bruurmijn *et al.*, 2017).

Gesture task

One week prior to the scanning session, all subjects were familiarized with six hand gestures selected from the American Manual Alphabet: '8', 'F', 'L', 'S', 'W', and 'Y'. Subjects were supplied with an online training video and were instructed to practice daily with both their intact hand and their phantom hand (independently).

During the fMRI scanning session, one character was presented on the screen every 16 seconds, and subjects were instructed to make the corresponding gesture with either their intact hand, or to attempt making the gesture with their phantom hand. The task (60 trials, 10 trials per gesture) was run two times for each hand. On their intact hands, subjects wore data gloves to record finger flexion and extension (5DT Inc., Irvine, USA).

Functional MRI

Data was acquired using a 7T functional MRI (fMRI). Anatomical T1- and proton density-weighted images were acquired first (repetition time [TR]/echo time [TE] = 7.0/1.4 ms, flip angle = 8°, voxel size = 1 × 1 × 1 mm^3 for T1-weighted image; repetition time/echo time = 5.0/1.4 ms, flip angle = 1°, voxel size = 1 × 1 × 1 mm^3 for proton density-weighted image). Prior to the Gesture Task, subjects performed a localiser task in which they opened and closed their intact hand during a 'move cue', and kept their hand still during a 'rest cue' (blocks of 30 seconds each; 4 blocks in total). During this task 120 echo-planar imaging (EPI) images were acquired (TR/TE = 2000/27 ms, flip angle = 70°, acquisition matrix size = 104 × 129, 33 slices, voxel size = 1.6 × 1.6 × 1.6 mm). The results were analyzed in real time using Philips IVIEWBOLD analysis software, and were then used to optimally position the fMRI field of view for the Gesture task.

For the Gesture Task, an EPI sequence was used with TR/TE = 1600/27 ms, FA = 70°, acquisition matrix size = 104 × 129, 26 slices, no gap, and voxel size = 1.6 × 1.6 × 1.6 mm^3. All EPI scans were acquired in transversal orientation, such that both the left and right hand region were in the field of view. A total of 2400 images were acquired in 4 runs of 600 images.

FMRI statistical maps and regions of interest

Preprocessing and first level analysis were performed with SPM12 (Statistical Parametric Mapping, http://www.fil.ion.ucl.ac.uk/spm/). Functional images were slice-time corrected, realigned to the mean functional image, and coregistered with the T1-weighted anatomical scan. A general linear model (GLM) was fitted using six regressors per run (one for each gesture: '8', 'F', 'L', 'S', 'W', and 'Y'). For each gesture, a t-map was calculated based on the contrast 'gesture versus rest', yielding six different t-maps for each hand: '8 versus rest', 'F versus rest', et cetera.

The T1-weighted image was corrected for field inhomogeneities by dividing the T1-weighted image by the proton density weighted image (Moortele *et al.*, 2009). A surface reconstruction was made of the resulting image using Freesurfer (Fischl *et al.*, 1999). The sensorimotor cortex of each hemisphere was divided into four regions of interest (ROIs) (Bruurmijn *et al.*, 2017), based on the FreeSurfer parcellation according to the Desikan-Killiany atlas (DKA) and Destrieux atlas (DA) (Desikan *et al.*, 2006; Destrieux *et al.*, 2010). The four ROIs are defined as follows, in which we have used the names of the regions in DKA and DA, and where '+' denotes the voxel-wise union, and '^' denotes the intersection of two regions. M1 consists of the primary motor cortex and the posterior part of the precentral gyrus ($PrecentralGyrus_{DA}$ + [$CentralSulcus_{DA}$ ^ $PrecentralGyrus_{DKA}$]). S1 consists of the primary sensory cortex, the anterior part of the postcentral gyrus ($PostcentralGyrus_{DA}$ + [$CentralSulcus_{DA}$ ^ $PostcentralGyrus_{DKA}$]). Pre-M1 covers the anterior part of the precentral gyrus ($PrecentralSulcus_{DA}$) and post-S1 the posterior part of the postcentral gyrus ($PostcentralSulcus_{DA}$).

Decoding gestures from the ipsilateral hemisphere

First, we wanted to assess if activity from the ipsilateral hemisphere of people with arm amputation who attempted to move their phantom hand still contained sufficient information to decode the different gestures. The results of decoding from the ipsilateral hemisphere were compared to the results of decoding from the contralateral hemisphere. This was done for the phantom and intact hand in subjects with arm amputation, and for both hands in controls. For this purpose, a support vector machine (SVM) classifier was trained and tested using the activation-levels of voxels of the ipsilateral and contralateral hand as features, for each hemisphere and each ROI.

In each ROI, the 250 voxels that showed the highest t-value in any of the six t-maps for gestures of the ipsilateral hand were selected. The blood-oxygen-level dependent signal (BOLD signal) in these voxels were linearly detrended and converted into z-scores. The BOLD signal is indicative of neuronal activity, but it is delayed and dispersed in time. As the peak of the BOLD response is most likely to contain the most discriminative information (Andersson *et al.*, 2011; Siero *et al.*, 2011), the mean BOLD signal around the peak of the BOLD response (corresponding to scans 4, 5, and 6 of each trial) was used as feature in training the classifier (Bleichner *et al.*, 2013; Bruurmijn *et al.*, 2017).

For each hand, the two runs were concatenated into a single set of 120 trials (right hand runs R1 and R2, and left hand runs L1 and L2). The classifier was trained on a data set created by leaving out 6 trials from the task (one gesture of each type). These left-out trials were then used as the validation set. This process was repeated 20 times for each hand, so that each set of 6 gestures served as the validation set once, yielding a leave-6-out cross validation scheme. The accuracy of the classifier is represented by the percentage of correctly predicted gestures.

For distinguishing between six classes, six binary SVMs are required in a 'one-versus-all' approach: Each SVM is trained to classify between one gesture and all other gestures. When using the classifier on the validation set, the class with the largest distance to the decision boundary is selected as the prediction.

The classification scores for ipsilateral gestures were assessed using a repeated-measures ANOVA using Group (amputation or control) as between subject factor, the four ROIs (pre-M1, M1, S1, post-S1) as separate within-subject measures, and Hand (left or right hand, or intact and phantom hand in amputation group) and Side (contralateral or ipsilateral hemisphere) as repeated within-subject factors. Results were deemed significant when $\alpha < 0.05$.

We conducted a separate analysis to assess to what extent ipsilateral movement activity can be used to classify movements from both hands from a single hemsiphere. For that purpose, we repeated the decoding analysis on both hemispheres of both the amputation and control group, but now with using 12 instead of 6 classes. As training sets we used any combination of the left and right hand (L1 & R1, L1 & R2, L2 & R1, and L2 & R2), which was used to classify the data of the remaining run of each hand. In contrast to the one-versus-all approach for the 6-classes case (for which drawing the borders can be challenging as the number of classes grows), here we used a 'one-versus-one' approach, in which each SVM was trained to choose between two classes. For 12 classes, this results in a combination of 66 SVMs ("12 choose 2"). Results were tested using a GLM with four dependent variables (classification scores in M1, S1, preM1, and postM1) and group (amputation and control subjects) as between subjects factor.

Testing against chance level

For each subject and each hemisphere, the chance level of classification was calculated using 500 iterations of randomly assigned class labels. This chance level was then subtracted from the classification scores before conducting the ANOVA. This way, the significance of the intercept reflects whether classification scores were significantly above chance for each ROI.

Data glove amplitudes

All subjects wore data gloves on their (intact) hands, measuring finger flexion and extension. Data acquired with the data glove was used to assess any confounding effects of hand movement of the hand that should be kept still during the task. For this purpose, the mean data glove amplitude for each hand was correlated with the mean 12-class classification scores (averaged over ROIs and hemispheres).

Results

Classification of the ipsilateral hand (6 classes)

Classification scores (Figure 1) for decoding from the contralateral hemisphere ranged from 20.8% to 95.8% (mean and standard deviation for all subjects, ROIs and hemispheres: 50.9%±17.8%). For decoding from the ipsilateral hemisphere, the classification scores ranged from 20.0% to 83.3% (mean and standard deviation for all subjects, ROIs and hemispheres: 41.1±12.6%). The random permutation test yielded a chance level of 16.7% (overall, averaged over subjects), which is in accordance of the theoretical chance level using six classes. When subtracting the chance level from the classification scores, the intercept of the multivariate test was significantly higher than 0% ($F(4,12)=44.8$, $p<0.001$), meaning that classification in general was higher than chance level. Post-hoc tests revealed that classification scores were significantly higher than chance level in all

ROIs (pre-M1: F(1,15)=165, p<0.001; M1: F(1,15)=177, p<0.001; S1: F(1,15)=202, p<0.001; post-S1: F(1,15)=183, p<0.001). Interestingly, classifaction was in general higher in the ampution than in the control group (main effect of 'Group'; (F(4,12)=4.0, p=0.027).

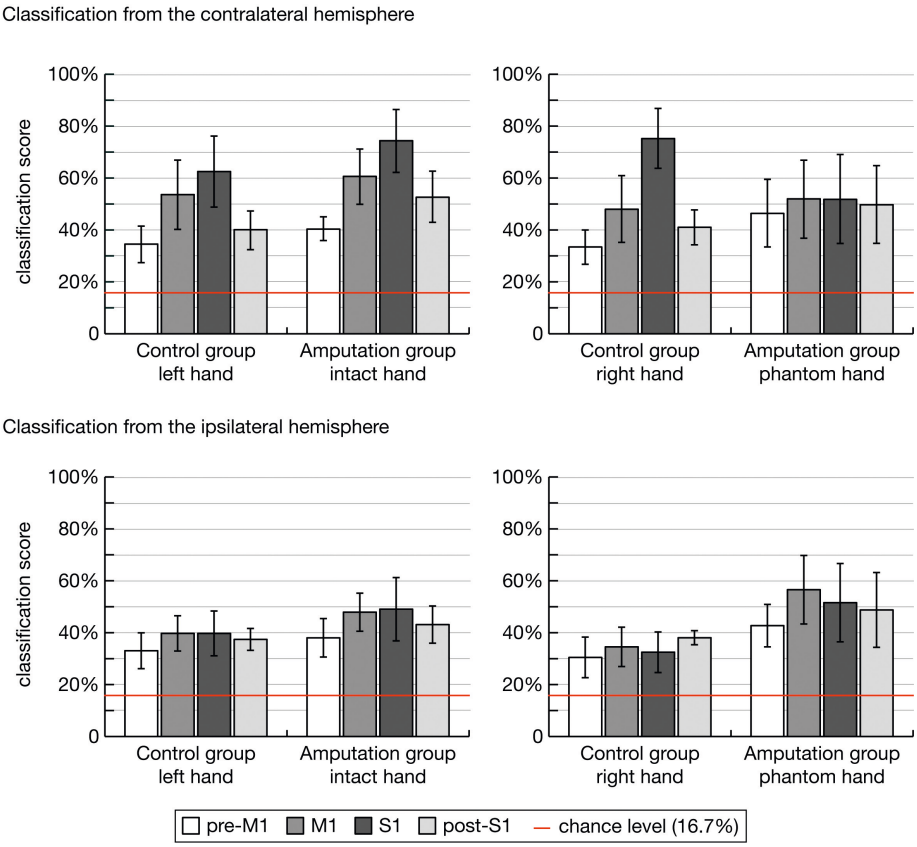

Figure 1. *Classification scores for the left and right hands (or intact and phantom hands in subjects with arm amputation) when decoded from the contralateral hemisphere (A) and from the ipsilateral hemisphere (B). The bars show the average score per group and per ROI, and the whiskers indicate the standard deviation. Data from decoding the contralateral hemisphere (presented before in (Bruurmijn et al., 2017)) and data for the controls (presented in (Bruurmijn et al., 2020)) are shown in this figure for comparison.*

Classification scores also depended on whether gestures were decoded from the ipsilateral or contralateral hemisphere (main effect of 'Side'; F(4,12)=20, p<0.001). Post-hoc tests showed that classification was better from the contra than the ipsi-lateral hemisphere in M1 (F(1,15)=15.5, p=0.001), S1 (F(1,15)=76.7, p<0.001), and post-S1 (F(1,15)=5.46, p=0.034), but not pre-M1 (F(1,15)=3.09, p=0.099). The difference in classification scores between the ipsi and contralateral hemispere varied between amputation and control subjects ('Side*Group' interaction; F(4,12)=4.75, p=0.016), with larger differences in the control group in S1 (S1: F(1,15)=14.7, p=0.002), but not in the other ROIs (M1: F(1,15)=4.5, p=0.05; p=0.002; pre-M1: F(1,15)=0.063, p=0.81; post-S1:

F(1,15)=0.48, p=0.50). For subjects with amputation the classification scores for S1 in the ipsi- and contralateral hemisphere were thus more similar for both hands.

There was also a significant three-way interaction between Side, Group, and Hand (F(4,12)=9.66, p=0.001), which was caused by M1 (F(1,15)=32.28, p<0.001) and S1 (F(1,15)=8.59, p=0.010), but not preM1 (F(1,15)=0.00, p=0.979) and post-S1(F(1,15)=1.67, p=0.215). The combination of the Side*Group and the Side*Group*Hand interactions can be most straightforwardly conceptualized by the notion that classification is better from the contralateral than the ipsilateral hand, but that this effect is absent for the phantom hand of people with amputation, where classification is similar for ipsi- and contralateral hand movements. Furthermore, there was a significant interaction effect of 'Hand*Group' (F(4,12)=7.25, p=0.003), which indicates that the difference between the hands varied between amputation and control subjects. While one would expect such differences to arise as a result of differences between the hands that are present in subjects with amputation but absent in control subjects, we could not support this using any of the post-hoc tests for the 4 ROIs (M1: F(1,15)=0.62, p=0.44; S1: F(1,15)=2.8, p=0.11; pre-M1: F(1,15)=1.75, p=0.21; post-S1: F(1,15)=0.012, p=0.91). There was no significant main effect of 'Hand' (F(4,12)=0.66, p=0.63) and no significant interaction effect of 'Hand*Side' (F(4,12)=3.21, p=0.52).

Classification of both hands from one hemisphere (12 classes)

When focussing on one hemisphere and training a classifier to distinguish between 12 gestures (6 for each hand), the classification scores overall ranged from 8.3% to 60.2% (mean and standard deviation for all groups, hemispheres and ROIs together: 26.3±10.0%). Chance level from the random permutation test was 8.3%, which was in accordance with the theoretical chance level for 12 classes.

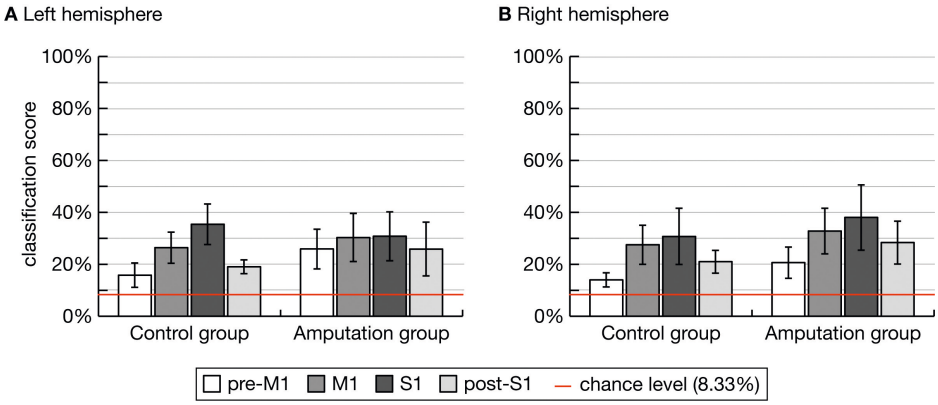

Figure 2. *Classification scores for the decoding of both hands from a single hemisphere, per ROI and per group. The bars show the average score for each ROI. The whiskers indicate the standard deviation. Data for controls are also presented in (Bruurmijn et al., 2020).*

Again, chance level was subtracted from the classification scores, so that the intercept can be used to test the classification scores against chance level. Indeed, there was a multivariate effect for the intercept (F(4,12)=27.34, p<0.001), which conforms above chance-level classification in all ROIs

(M1: F(1,15)=121.4, p<0.001; S1: F(1,15)=113.4, p<0.001; pre-M1: F(1,15)=81.83, p<0.001; post-S1: F(1,15)=121.4, p<0.001).

There was a main effect of 'Group' on the classification scores (F(4,12)=3.74, p=0.034). Post-hoc univariate tests reveal that this effect was mainly caused by the two ROIs pre-M1 (F(1,15)=12.37, p=0.003) and post-S1 (F(1,15)=6.52, p=0.022), where classification was better in subjects with amputation than in control subjects. There was no significant difference between controls and amputated subjects for the other two ROIs (M1: F(1,15)=1.46, p=0.245; S1: F(1,15)=0.081, p=0.780).

There was also a significant main effect of 'Hemisphere' (F(4,12)=4.87, p=0.016). Post-hoc univariate tests show that this effect was mainly located in the ROI pre-M1 (F(1,15)=9.16, p=0.009). The other ROIs do not show a significant difference between hemispheres (M1: F(1,15)=2.60, p=0.128; S1: F(1,15)=0.822, p=0.379; post-S1: F(1,15)=1.42, p=0.253).

Finally, there was a significant interaction effect of 'Hemisphere*Group' (F(4,12)=5.06, p=0.013). This suggests that there is a difference in classification scores between the hemispheres in control subjects compared to subjects with amputation. This interaction effect was only significant in S1 (F(1,15)=18.13, p=0.001), not in the other ROIs (M1: F(1,15)=0.384, p=0.545; pre-M1: F(1,15)=2.19, p=0.160; post-S1: F(1,15)=0.022, p=0.885).

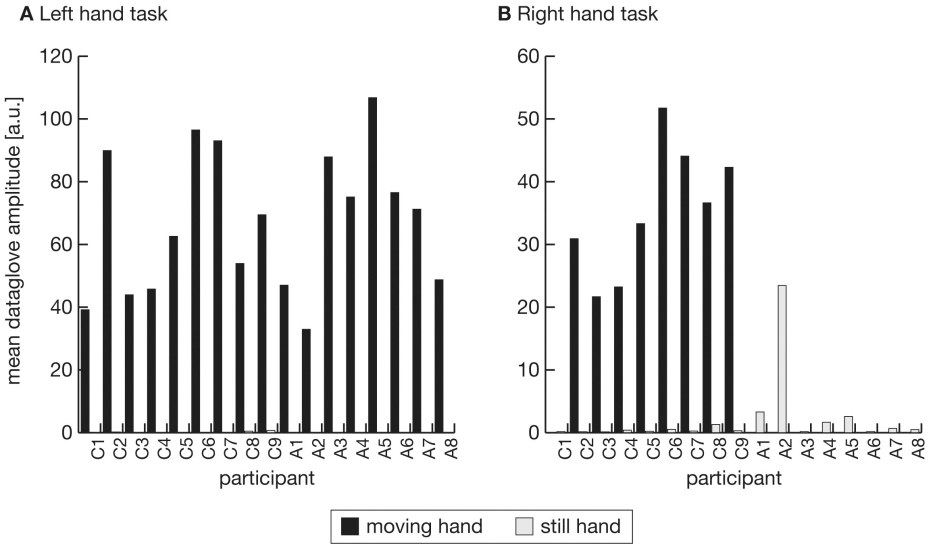

Figure 3. *Mean data glove amplitudes (finger flexion and extension; averaged over all fingers) for the hand that should move making the gestures and for the hand that should be kept still during the 'left hand task' (A) and the 'right hand task' (B). The mean data glove amplitude was calculated over the two runs for each hand combined. Data in B have been presented before in (Bruurmijn et al., 2017).*

Data glove amplitudes and correlation with classification scores

Hand movements were measured using a data glove to assess the presence of confounding motion of the still hand. Data glove mean flexion and extension amplitudes for both the 'moving' and 'still' hands are shown in Figure 3. As expected, data glove amplitudes were lower in the hand that should be kept still during the task (with the exception was subject A2). For neither hand there was a significant correlation with the 12-class classification scores (task 'Left hand', moving hand: $r(15)=0.20$, $p=0.44$; still hand: $r(15)=-0.30$, $p=0.47$; task 'Right hand', moving hand: $r(15)=0.44$, $p=0.28$; still hand: $r(15)=0.36$, $p=0.16$). The between-subject variations in classification accuracy could therefore not be accounted for by unwanted movements of the still hand.

Discussion

In this study, we decoded attempted gestures of a phantom hand in people with arm amputation from the ipsilateral sensorimotor cortex, and compared the results to a control group. Classification scores showed that decoding was significantly better than chance level for both the phantom and intact hands, from both hemispheres in all ROIs of the sensorimotor cortex (M1, S1, pre-M1, and post-S1).

As in our previous work, where we focused on contralateral decoding (Bruurmijn *et al.*, 2017), classification from the ipsilateral hemisphere was possible even years after denervation. Overall, classification was better when decoding gestures from the contralateral hemisphere than from the ipsilateral hemisphere. However, in subjects with arm amputation, the difference in classification scores between the two hemispheres was smaller for the phantom hand than for the intact hand. This finding suggests that in people with amputation, compared to the intact hand, the phantom hands show an ipsilateral representation that is stronger with respect to the contralateral representation. Further research is needed to investigate the nature of this finding.

The two ROIs in the amputation group that were notably succesful (relative to control subjects) in distinguishing between the two hands from one hemisphere were pre-M1 and post-S1. These ROIs were defined to be more anterior and posterior from M1 and S1. Indeed, it has been shown that information about movements can not only be found in the primary sensorimotor cortex, but also in adjacent regions, such as the premotor area (Chouinard & Paus, 2006; Ojakangas *et al.*, 2006). However, also in the amputation group, classification was still best from the primary sensorimotor areas M1 and S1, which implies that these generally carry the most information even for ipsilateral decoding.

As attempted movement of a phantom hand could be challenging for people with hand amputation, especially the detailed articulations that were required for this task, it is possible that subjects unconsciously mirrored the requested movements with their intact hand. To monitor this effect, all subjects wore data gloves that measured flexion and extension of all fingers. During the tasks in which the subjects were instructed to attempt moving their phantom hand, the data glove showed that the intact hand (which should be kept still during this task) was also slightly moved: generally, these amplitudes were higher than those of the still hand in controls. However, there were no

significant correlations between data glove amplitudes and classification accuracy in either group. It is therefore unlikely that these minor hand movements can account for the high classification accuracy when decoding activity of the phantom hand using the ipsilateral hemisphere.

Application to Brain-Computer Interfaces

Our results build upon the increasing evicence that the sensorimotor cortex holds information about the ipsilateral movements (Hotson *et al.*, 2014; Downey *et al.*, 2020) and extends these findings by also showing ipsilateral decoding of fine-grained hand gestures in subjects with arm amputation. Especially the ability to also discriminate between the hands, is an important finding for the development of implantable BCIs, specifically those using subdurally implanted electrode grids (Vansteensel *et al.*, 2016). This suggest the possibility of a unilaterally implanted grid to decode bilateral hand movements, thereby effectively doubling the number of states that can be decoded from a single hemisphere by performing hand movements.

The development of invasive BCIs is most relevant for people with so-called locked-in syndrome (LIS), unable to execute motor commands at all. In this study, we included individuals with arm amputation. For the rehabilitation of this group, multiple solutions have been developed, including prosthetic devices controlled by recording signals from the peripheral nervous system, even providing sensory feedback using afferent signals (for reviews on this topic, see (Navarro *et al.*, 2005; Ghafoor *et al.*, 2017)). However, the results of the present study, and the choice for individuals with arm amputation as subjects, should be understood in the context of implantable BCIs for LIS. While there are differences between people with amputation and people suffering from LIS (as the former were still able to execute hand gestures with their intact hand), we included people with arm amputation because of their ability to perform *attempted* movements rather than executed movements and therefore display the expected similarities in the effects caused by denervation. This study therefore represents a necessary step to establish a solid proof of principle for the possibility to decode motor activity in cortex that is potentially reorganized. How ipsilateral activation patterns develop after denervation of both hemispheres is a topic for future research.

In addition to LIS patients, the current results may also be relevant for people who have hemiparesis following a unilateral stroke affecting the sensorimotor cortex. Grasping of the ipsilateral hand has already successfully been decoded using electrocorticography (ECoG) in patients with tetraplegia and spinal cord injury (Downey *et al.*, 2020) and from patients with a lesion in the motor areas (Hotson *et al.*, 2014). As current results indicate the the ipsilateral hemisphere contains a detailed representation of ipsilateral movements, the non-affected hemisphere could in theory be a target for a BCI that helps a patient to perform movements normally initiated by the damaged hemisphere. However, a currently unknown factor is the nature of the ipsilateral representation, which might also originate from interhemispheric projections from the contralateral motor cortex through the corpus callosum. In that case, the ipsilateral representation could be affected by the stroke. Further research is thus needed on the exact nature and origin of the ipsilateral movement representations and the potential effect of stroke on these representations.

For classification of both hands from the same hemisphere, scores were significantly above chance level. Although this is an indication that meaningful information is present, it should be noted that the chance level threshold is a low bar for a BCI to be effective. In practice, for the users of a BCI, decoding accuracy should be much higher to be of practical use. However, the results presented here are based upon classification of fMRI patterns. For a practical BCI, fMRI is not suitable as a recording modality, as it is costly and not portable, and has a limited temporal resolution. However, it is known that there is a good correspondence between BOLD activity in fMRI and high-frequency band activity in ECoG (Siero *et al.*, 2014). This renders fMRI an eligible non-invasive research tool. Because of other inherent limitations of BOLD measurements, such as scanner noise or head motion, one might expect some gain in classification accuracy when using subdurally implanted electrodes. Bleichner et al. (Bleichner *et al.*, 2016) and Branco et al. (Branco *et al.*, 2017) have shown that gestures can be decoded from the sensorimotor cortex using ECoG with close to perfect accuracy. This indeed indicates the presence of a performance gap between ECoG and fMRI, suggesting the ultimate practical feasibility of an implantable BCI that relies on decoding bilateral movements from a single hemisphere.

In summary, we showed that information for ipsilateral classification is still present in the sensorimotor cortex after denervation. Moreover, we showed that it is possible to decode gestures made with both hands from the same hemisphere, also after denervation. These results open new possibilities for unilaterally implanted BCI solutions.

References

Aboitiz, F., Scheibel, A.B., Fisher, R.S., & Zaidel, E. (1992) Fiber composition of the human corpus callosum. Brain Res, 598, 143–153.

Alawieh, A., Tomlinson, S., Adkins, D., Kautz, S., & Feng, W. (2017) Preclinical and Clinical Evidence on Ipsilateral Corticospinal Projections: Implication for Motor Recovery. Transl Stroke Res, 8, 529–540.

Andersson, P., Pluim, J.P.W., Siero, J.C.W., Klein, S., Viergever, M.A., & Ramsey, N.F. (2011) Real-Time Decoding of Brain Responses to Visuospatial Attention Using 7T fMRI. PLoS ONE, 6, e27638.

Association, W.M. (2013) World Medical Association Declaration of Helsinki: Ethical Principles for Medical Research Involving Human Subjects. JAMA, 310, 2191–2194.

Berlot, E., Prichard, G., O'Reilly, J., Ejaz, N., & Diedrichsen, J. (2019) Ipsilateral finger representations in the sensorimotor cortex are driven by active movement processes, not passive sensory input. Journal of Neurophysiology, 121, 418.

Bleichner, M.G., Freudenburg, Z.V., Jansma, J.M., Aarnoutse, E.J., Vansteensel, M.J., & Ramsey, N.F. (2016) Give me a sign: decoding four complex hand gestures based on high-density ECoG. Brain Structure and Function, 221, 203.

Bleichner, M.G., Jansma, J.M., Sellmeijer, J., Raemaekers, M., & Ramsey, N.F. (2013) Give Me a Sign: Decoding Complex Coordinated Hand Movements Using High-Field fMRI. Brain Topography, 27, 248.

Bogdanov, S., Smith, J., & Frey, S.H. (2012) Former Hand Territory Activity Increases After Amputation During Intact Hand Movements, but Is Unaffected by Illusory Visual Feedback. Neurorehabilitation and Neural Repair, 26, 604.

Bramati, I.E., Rodrigues, E.C., Simões, E.L., Melo, B., Höfle, S., Moll, J., Lent, R., & Tovar-Moll, F. (2019) Lower limb amputees undergo long-distance plasticity in sensorimotor functional connectivity. Scientific Reports, 9.

Branco, M.P., Freudenburg, Z.V., Aarnoutse, E.J., Bleichner, M.G., Vansteensel, M.J., & Ramsey, N.F. (2017) Decoding hand gestures from primary somatosensory cortex using high-density ECoG. NeuroImage, 147, 130.

Bruurmijn, L.C.M., Raemaekers, M., Branco, M.P., Ramsey, N.F., & Vansteensel, M.J. (2020) Distinct representation of ipsilateral hand movements in sensorimotor areas. Manuscript submitted for publication,.

Bruurmijn, M.L.C.M., Pereboom, I.P.L., Vansteensel, M.J., Raemaekers, M.A.H., & Ramsey, N.F. (2017) Preservation of hand movement representation in the sensorimotor areas of amputees. Brain, 140, 3166.

Buetefisch, C.M., Revill, K.P., Shuster, L., Hines, B., & Parsons, M. (2014) Motor demand-dependent activation of ipsilateral motor cortex. Journal of Neurophysiology, 112, 999.

Bundy, D.T. & Leuthardt, E.C. (2019) The Cortical Physiology of Ipsilateral Limb Movements. Trends Neurosci, 42, 825–839.

Chouinard, P.A. & Paus, T. (2006) The Primary Motor and Premotor Areas of the Human Cerebral Cortex. Neurosci, 12, 143–152.

Collinger, J.L., Wodlinger, B., Downey, J.E., Wang, W., Tyler-Kabara, E.C., Weber, D.J., McMorland, A.J., Velliste, M., Boninger, M.L., & Schwartz, A.B. (2013) High-performance neuroprosthetic control by an individual with tetraplegia. Lancet, 381, 557–564.

Davare, M., Duque, J., Vandermeeren, Y., Thonnard, J.-L., & Olivier, E. (2006) Role of the Ipsilateral Primary Motor Cortex in Controlling the Timing of Hand Muscle Recruitment. Cerebral Cortex, 17, 353.

Dechent, P. & Frahm, J. (2003) Functional somatotopy of finger representations in human primary motor cortex. Human Brain Mapping, 18, 272.

Desikan, R.S., Ségonne, F., Fischl, B., Quinn, B.T., Dickerson, B.C., Blacker, D., Buckner, R.L., Dale, A.M., Maguire, R.P., Hyman, B.T., Albert, M.S., & Killiany, R.J. (2006) An automated labeling system for subdividing the human cerebral cortex on MRI scans into gyral based regions of interest. NeuroImage, 31, 968.

Destrieux, C., Fischl, B., Dale, A., & Halgren, E. (2010) Automatic parcellation of human cortical gyri and sulci using standard anatomical nomenclature. NeuroImage, 53, 1.

Dettmers, C., Adler, T., Rzanny, R., Schayck, R. van, Gaser, C., Weiss, T., Miltner, W.H.R., Brückner, L., & Weiller, C. (2001) Increased excitability in the primary motor cortex and supplementary motor area in patients with phantom limb pain after upper limb amputation. Neuroscience Letters, 307, 109.

Diedrichsen, J., Wiestler, T., & Krakauer, J.W. (2013) Two Distinct Ipsilateral Cortical Representations for Individuated Finger Movements. Cerebral Cortex, 23, 1362.

Downey, J.E., Quick, K.M., Schwed, N., Weiss, J.M., Wittenberg, G.F., Boninger, M.L., & Collinger, J.L. (2020) The Motor Cortex Has Independent Representations for Ipsilateral and Contralateral Arm Movements But Correlated Representations for Grasping. Cereb Cortex,.

Elbert, T., Flor, H., Birbaumer, N., Knecht, S., Hampson, S., Larbig, W., & Taub, E. (1994) Extensive reorganization of the somatosensory cortex in adult humans after nervous system injury. NeuroReport, 5, 2593.

Fischl, B., Dale, A.M., & Sereno, M.I. (1999) Cortical Surface-Based Analysis. NeuroImage, 9, 179.

Gallivan, J.P., McLean, D.A., Flanagan, J.R., & Culham, J.C. (2013) Where One Hand Meets the Other: Limb-Specific and Action-Dependent Movement Plans Decoded from Preparatory Signals in Single Human Frontoparietal Brain Areas. J Neurosci, 33, 1991–2008.

Ghafoor, U., Kim, S., & Hong, K.-S. (2017) Selectivity and Longevity of Peripheral-Nerve and Machine Interfaces: A Review. Front Neurorobotics, 11, 59.

Grodd, W., Hülsmann, E., Lotze, M., Wildgruber, D., & Erb, M. (2001) Sensorimotor mapping of the human cerebellum: fMRI evidence of somatotopic organization. Hum Brain Mapp, 13, 55–73.

Hadoush, H., Sunagawa, T., Nakanishi, K., Endo, K., & Ochi, M. (2011) Motor somatotopy of extensor indicis proprius and extensor pollicis longus. NeuroReport, 22, 559.

wHamzei, F., Liepert, J., Dettmers, C., Adler, T., Kiebel, S., Rijntjes, M., & Weiller, C. (2001) Structural and functional cortical abnormalities after upper limb amputation during childhood. NeuroReport, 12, 957.

Hochberg, L.R., Serruya, M.D., Friehs, G.M., Mukand, J.A., Saleh, M., Caplan, A.H., Branner, A., Chen, D., Penn, R.D., & Donoghue, J.P. (2006) Neuronal ensemble control of prosthetic devices by a human with tetraplegia. Nature, 442, 164–171.

Hotson, G., Fifer, M.S., Acharya, S., Benz, H.L., Anderson, W.S., Thakor, N.V., & Crone, N.E. (2014) Coarse electrocorticographic decoding of ipsilateral reach in patients with brain lesions. Plos One, 9, e115236.

Kikkert, S., Kolasinski, J., Jbabdi, S., Tracey, I., Beckmann, C.F., Johansen-Berg, H., & Makin, T.R. (2016) Revealing the neural fingerprints of a missing hand. eLife, 2016, e15292.

Kim, S., Ashe, J., Hendrich, K., Ellermann, J., Merkle, H., Ugurbil, K., & Georgopoulos, A. (1993) Functional magnetic resonance imaging of motor cortex: hemispheric asymmetry and handedness. Science, 261, 615–617.

Leuthardt, E.C., Schalk, G., Wolpaw, J.R., Ojemann, J.G., & Moran, D.W. (2004) A brain-computer interface using electrocorticographic signals in humans. J Neural Eng, 1, 63.

Lotze, M., Flor, H., Grodd, W., Larbig, W., & Birbaumer, N. (2001) Phantom movements and pain An fMRI study in upper limb amputees. Brain, 124, 2268.

Mizuguchi, N., Nakagawa, K., Tazawa, Y., Kanosue, K., & Nakazawa, K. (2019) Functional plasticity of the ipsilateral primary sensorimotor cortex in an elite long jumper with below-knee amputation. NeuroImage: Clinical, 23, 101847.

Moortele, P.-F.V. de, Auerbach, E.J., Olman, C., Yacoub, E., Uğurbil, K., & Moeller, S. (2009) T1 weighted brain images at 7 Tesla unbiased for Proton Density, T2* contrast and RF coil receive B1 sensitivity with simultaneous vessel visualization. Neuroimage, 46, 432–446.

Navarro, X., Krueger, T.B., Lago, N., Micera, S., Stieglitz, T., & Dario, P. (2005) A critical review of interfaces with the peripheral nervous system for the control of neuroprostheses and hybrid bionic systems. J Peripher Nerv Syst, 10, 229–258.

Ojakangas, C.L., Shaikhouni, A., Friehs, G.M., Caplan, A.H., Serruya, M.D., Saleh, M., Morris, D.S., & Donoghue, J.P. (2006) Decoding Movement Intent From Human Premotor Cortex Neurons for Neural Prosthetic Applications. J Clin Neurophysiol, 23, 577–584.

Oldfield, R.C. (1971) The assessment and analysis of handedness: The Edinburgh inventory. Neuropsychologia, 9, 97.

Penfield, W. & Boldrey, E. (1937) Somatic motor and sensory representation in the cerebral cortex of man as studied by electrical stimulation. Brain, 60, 389–443.

Philip, B.A. & Frey, S.H. (2014) Compensatory Changes Accompanying Chronic Forced Use of the Nondominant Hand by Unilateral Amputees. Journal of Neuroscience, 34, 3622.

Scherer, R., Zanos, S.P., Miller, K.J., Rao, R.P.N., & Ojemann, J.G. (2009) Classification of contralateral and ipsilateral finger movements for electrocorticographic brain-computer interfaces. Neurosurgical Focus, 27, E12.

Seidler, R.D., Noll, D.C., & Thiers, G. (2004) Feedforward and feedback processes in motor control. NeuroImage, 22, 1775.

Siero, J.C., Petridou, N., Hoogduin, H., Luijten, P.R., & Ramsey, N.F. (2011) Cortical Depth-Dependent Temporal Dynamics of the BOLD Response in the Human Brain. J Cereb Blood Flow Metabolism, 31, 1999–2008.

Siero, J.C.W., Hermes, D., Hoogduin, H., Luijten, P.R., Ramsey, N.F., & Petridou, N. (2014) BOLD matches neuronal activity at the mm scale: A combined 7T fMRI and ECoG study in human sensorimotor cortex. NeuroImage, 101, 177.

Vansteensel, M.J., Pels, E.G.M., Bleichner, M.G., Branco, M.P., Denison, T., Freudenburg, Z.V., Gosselaar, P., Leinders, S., Ottens, T.H., Boom, M.A.V.D., Rijen, P.C.V., Aarnoutse, E.J., & Ramsey, N.F. (2016) Fully Implanted Brain–Computer Interface in a Locked-In Patient with ALS. New England Journal of Medicine, 375, 2060.

Verstynen, T. (2004) Ipsilateral Motor Cortex Activity During Unimanual Hand Movements Relates to Task Complexity. Journal of Neurophysiology, 93, 1209.

Wolpaw, J.R. (2007) Brain-computer interfaces as new brain output pathways. J Physiology, 579, 613–619.

DISCUSSION

Summary and Discussion

A Brain-Computer Interface (BCI) offers the opportunity to restore lost functions for people with severe paralysis, as in the case of 'locked-in syndrome' (LIS), in which case no motor output is possible at all. A BCI records brain signals and translates those into a useful control signal. For example, brain signals from the sensorimotor areas of the brain can be used to drive a robotic arm or a communicative device.

Searching for useful and reliable brain signals is one of the challenges in BCI research. The primary motor cortex (M1) and neighbouring primary sensory cortex (S1) are known to comprise detailed information about movements. These areas are thefore excellent targets for a BCI. For a variety of modalities, such as electroencephalography (EEG), intracranial recordings (electrocorticography, ECoG) and functional magnetic resonance imaging (fMRI), it has been shown that brain activity in these areas can be *decoded* to infer the detailed movements a person makes, or tries to make. However, BCIs are developed for people without motor output. An important question for BCI research is therefore whether the *detailed* movement representations in M1 and S1 are still intact in case activity in these areas no longer generates actual movements. In this thesis, I investigated this topic with the help of people with arm amputation.

Cgrid: visualizing brain activity from the sensorimotor cortex

Decoding movements from the brain relies on the movement-related activity patterns, which are both temporal and spatial. A trained classifier is able to distinguish between these patterns. With functional MRI as the recoding modality for this project, the spatial aspect is prominent. As classifiers can seem a black box for the human viewer, it is useful to develop a way to visualize these spatial patterns. This allows for simple comparison even by visual inspection of activation patterns over subjects.

Therefore, in Chapter 1, we developed an intuitive representation of the sensorimotor cortex, 'Cartesian geometric representation with isometric dimensions of the sensorimotor cortex' (Cgrid-SMX). This novel method allowed for straightforward visualization and assessment of activity patterns in the sensorimotor cortex. We used the observation that the shape of the sensorimotor cortex can be roughly sketched as a trapezoid. The algorithm we described used the anterior border of the motor cortex, the central sulcus, and the posterior border from the flattened sensory cortex as starting points. Polynomials were fitted though these borders in a flat map, and the fitted curves were interpolated to divide the cortex into 24 'columns' (small areas running from dorsal to ventral). These columns were then divided into 84 'rows'. This constituted a 24 ′ 84 tiled mesh. This mesh can be populated by taking the average beta (activity) map of a given movement task. Activation patterns that are transformed into Cgrid-SMX space can be easily visualized as a 2D colored matrix, and patterns for different tasks and different subjects can therefore be compared in a straightforward manner.

We applied Cgrid-SMX on the data of 20 healthy subjects, and compared sensorimotor activity patterns between hemispheres and across subjects. This yielded similarities that were comparable

to those obtained with MNI normalization. This assessment demonstrated that Cgrid-SMX yields a consistent representation of the sensorimotor cortex, and we have used it in parts of the research on decoding attempted movements from the sensorimotor cortex described in the other chapters.

For the studies described in Chapters 2-4, we recuited eight people with acquired arm amputation, and in addition nine control subjects without amputation. They were instructed to attempt making several gestures from the American Manual Alphabet with their phantom hand, while brain activity from the sensorimotor cortex was recorded using 7T functional MRI. We defined four ROIs on each hemisphere: M1, S1, and the areas anterior to M1 (pre-M1) and posterior to S1 (post-S1). A machine learning algorithm was trained on each ROI (and on the combination of all ROIs) to discriminate between the activation patterns, thereby predicting the gesture that the subjects had attempted to make.

Decoding gestures of the phantom hand from the contralateral hemisphere

In Chapter 2, we found brain activity in the ROIs that controlled the now-missing hand, which is in agreement with what has been reported previously in fMRI studies of movements of amputated lower limb (Hotz-Boendermaker, Hepp-Reymond, Curt, & Kollias, 2011), attempted fingertapping in amputees (Ersland et al., 1996), intracranial recordings of attempted movements of the phantom hand (Gharabaghi et al., 2014). Also, an intact finger topography has been demonstrated in S1 (Kikkert et al., 2016). We showed that it is possible to discriminate between the different activation patterns from the phantom hand. In M1, there was no difference between the classification scores from the phantom hand and from the intact hand. Neither was there a difference between the results obtained for the phantom hand and the dominant hand of the control group without amputatation. Classification was also possible from pre-M1 and post-S1. This is also in agreement with previous work, where it has been demonstrated that regions adjacent to the primary sensorimotor cortices play a role in movement planning and execution (Martuzzi, Zwaag, Farthouat, Gruetter, & Blanke, 2012).

In S1 of participants with amputation, the classification scores for the phantom hand were significantly lower than those for the intact hand, and than those from controls. We postulate that this is due to the dual nature of S1: it has been shown before that this region is involved in feedback loops for sensory processing, but also in feed-forward loops for motor planning and execution. Due to denervation, the feedback contribution of the network alters, but the planning and execution part remains. Therefore, so remains the possibility to decode movements from S1 after denervation, albeit at lower accuracy than in the intact situation. For the intact hand of amputees and both hands in controls, S1 is the region with the highest classification scores (albeit that the difference in score is not significant in all comparisons with other ROIs). After amputation, the classification scores drop to the level of M1.

Decoding gestures from the ipsilateral hemisphere in controls

Studies on movement representation in the brain typically focus on the contralateral sensorimotor cortex, as the strongest movement-related activity is found there. However, there is increasing evidence that the ipsilateral cortex also plays a role in movement planning and execution. Not all

motor fibers cross the midline (Alawieh, Tomlinson, Adkins, Kautz, & Feng, 2017), and there are trans-callosal connections between the two hemispheres (Aboitiz, Scheibel, Fisher, & Zaidel, 1992). Therefore, in Chapter 3, we also tried an ipsilateral decoding approach: a new classifier was trained on the activity patterns of the same ROIs as with the contralateral study, but this time on patterns from the ipsilateral hemisphere.

As with contralateral decoding, decoding six gestures from the ipsilateral hemisphere in controls was possible with a classification score above chance level. In general, the classification scores of the ipsilateral hemisphere were, however, lower than those of the contralateral side. We then pooled all trials for the left and right hand tasks together, and we trained a classifier to discriminate between six gestures from both hands (12 gestures) from the same hemisphere. This also proved to be possible with above-chance classification scores. Visual inspection of the activity patterns for the different gestures suggest that the patterns for the ipsilateral hand were not merely a 'mirrored' version of the contralateral hand. This suggests a distinct representation movements in the ipsilateral motor areas.

Decoding gestures from the ipsilateral hemisphere in amputees

Studying the effects of denervation on the movement representations in the ipsilateral sensorimotor cortex is also important for the development for (implantable) BCI. Indeed, if it would be possible to decode both hands from the same cortical area, implantation is only needed on one hemisphere, thereby minimizing the risks associated with surgery. Therefore, in Chapter 4, we trained the classifier on the data of the attempted gestures in amputees and decoded the attempted movements from the ipsilateral hemisphere. These ipsilateral classification scores were then again compared to the classification scores from the contralateral hand.

Similar to executed movements of people without amputation, decoding from the ipsilateral hemisphere was also possible for attempted movements of the phantom hand of amputees. As with all our decoding results, the classification score was highest in M1 and S1, and contralateral decoding was still better than ipsilateral decoding. However, interestingly, the *difference* between contralateral and ipsilateral classification scores was lower in the phantom hand than in the intact hand of amputees, and lower than in both hands of the control group. This suggests that after amputation, the ipsilateral representation of the phantom hand is stronger than the ipsilateral representation of the intact hand.

Cortical plasticity after denervation

Contralateral representation of (attempted) movements

The ability to decode between six attempted gestures made with the phantom hand demonstrates that there is still a detailed representation of the hand, even years after denervation. This finding contrasts with earlier studies reporting a change in activity after amputation (Calford & Tweedale, 1988; Merzenich et al., 1984). For example, it has been demonstrated that after arm amputation, receptive fields for other limbs such as the shoulder or face areas 'invade' the region that was formerly associated with the hand area. However, a growing body of evidence shows that the process of adaptability is more complicated than only a takeover by other limbs. The engagement of the

sensorimotor areas in attempted movement of phantom limbs has been shown already at the start of this millenium (Lotze, Flor, Grodd, Larbig, & Birbaumer, 2001; Roux et al., 2003; Turner et al., 2001). These results have been extended, for example with the recent discovery—using a different approach—of representations of the individual fingers after arm amputation (Diedrichsen, Wiestler, & Krakauer, 2013; Kikkert et al., 2016). We instead have chosen for an approach in which we classify complex, multi-finger hand configurations, as these gestures are directly usable in a practical BCI. Despite this different approach, our results contribute to and strenghten the notion of a meaningful representation of the phantom limb: if the denervated areas were taken over fully or partially by encroaching neighbouring activation, or if the representation of phantom movements would become weaker after denervation, decoding with high classification scores would be impossible.

Some studies on cortical change after denervation reported rapid changes: within ten days after amputation of the middle and ring finger, the dipoles (as measured with magnetoencephalography) had moved closer together, which indicates a reorganisation (Weiss et al., 2000). Also delayed changes have been reported, such as a reduced gray matter volume of the denervated cortex (Makin et al., 2013), and thinning of cortical layers in the premotor and visual cortices, correlating with time since amputation (in the order of years) (Jiang et al., 2016, 2015). This correlation is important in the context of a BCI, as it is undesirable that performance and usability decrease over time. However, although we observed a negative trend between classification scores and time since amputation in post-S1, this correlation was not significant.

Ipsilateral representation of (attempted) movements

The significant classification scores from the ipsilateral hemisphere, especially in the case of S1 of the phantom hand, is remarkable. We expected that the higher ipsilateral classification would be found in the intact hand instead: after all, the ipsilateral hemisphere of the intact hand is the contralateral hemisphere of the phantom hand, and since there are no actual hand movements anymore for this area, our initial intuition was that it would take more part in controlling the intact hand. However, our results point in the opposite direction. Several factors could explain this result. First, it is possible that when trying to move the phantom hand, amputees unconsciously also mirrored the movements with their intact hand and thereby generated meaningful activity in the hemisphere contralateral to this moving hand (and thus ipsilateral to the phantom hand). This was monitored by measuring finger flexion and extension during the task using a data glove on the intact hand of amputees and both hands of controls. In the task where amputees were instructed to attempt moving their phantom hand, we observed small finger motion from the intact hand compared to the task in which the subjects were instructed to move the intact hand. We therefore believe it is unlikely that subconscious movements of the intact hand have contributed to the ipsilateral classification scores of the phantom hand. Second, it has been demonstrated that ipsilateral activation increases with increasing task difficulty (Buetefisch, Revill, Shuster, Hines, & Parsons, 2014). Since moving the phantom hand was not equally easy for all recruited amputees (based on a self-reported ability score), the relatively high activity and classification scores obtained for the ipsilateral hemisphere of amputees could be a reflection of this increased effort.

The use of decoding approaches to investigate brain function

Our decoding approach is a useful technique to assess whether the denervated cortex still contains information about attempted movements. As the selected hand gestures are combinations of finger articulations, the activation patterns reflect the muscle constellations needed to make the gestures. The differences in patterns between gestures are therefore likely to be small, and distinguishing them requires a sensitive classifier. In contrast to a general linear model (GLM), as used commonly in fMRI analysis, a support vector machine is able to distinguish between these small differences. However, there are some limitations of this approach. First, our classifier acts a black box: it discriminates between classes based on the activity pattern as a whole, and is therefore not able to decompose it into separate patterns for different movement parameters that are known to be encoded in the sensorimotor cortex, such as limb position and speed of movement (Ebner, Hendrix, & Pasalar, 2009). In our approach, we are unable to investigate the decodability of these movement parameters separately. Second, whereas the classifier is appropriate to distinguish between spatial patterns, it is less suitable for studying the exact topology. This also implies that we could not fully study the *differences* in the representations after denervation. Although we propose that there is still a detailed representation after denervation, it is difficult to assess whether (and how) these spatial patterns have changed after denervation. Finally, spatial patterns are highly individual, and there was no measurement before the amputation. It is therefore impossible to assess the longitudinal developments of the movement patterns of the phantom hand. However, despite this limitation, by visual inspection of the activation patterns, we did not observe any drastic shifts of activation in amputees compared to controls.

Application to Brain-Computer Interface research

In BCI research, there is a desire for increasing the degrees of freedom by recording increasingly complex brain signals. More degrees of freedom allow for a larger reportoire of responses, which will benefit for example the speed of BCI-based communication. Increasing the degrees of freedom asks for implanted devices that can record with higher density from a smaller area of the cortex, but it also requires these brain activity patterns to be meaningful and reliable. The existence of a detailed representation of a phantom hand years after denervation is important in this development. Also, we have demonstrated that it is possible to decode both ipsilateral and contralateral hands from the same hemisphere. In the context of an implantable BCI, this feature can be beneficial, as it in theory allows for implantation on a single hemisphere. This reduces the risks associated with surgery.

For the studies presented in this thesis, we recruited participants with acquired arm amputation. Although BCI technology can be used to drive an advanced arm prosthetic, the BCI research at the UMC Utrecht focuses on people with the locked-in syndrome (LIS). An important difference between the people with amputation in our study and the LIS target population is that the latter can have brain damage as a consequence of amyotrophic lateral sclerosis (ALS) or stroke. Changes in brain structure can affect the representation of detailed movement, or the ability to distinguish between these altered patterns from the cortex.

Another difference between the two groups is that people with LIS have lost (nearly) all motor output, whereas in amputees only the sensorimotor cortex is denervated. This implies that, although amputees had to attempt moving their hand, they still were able to move other body parts. However, we did not find excessive motion of the intact hand during attempted movements of the phantom hand. Also unconscious or unintentional movements of the stump may have affected the classification results. Indeed, a surgical precedure called 'targeted muscle reinnervation' (TMR) is sometimes applied, in which muscles on or near the stump are reinnervated with residual nerves from the amputated limb, allowing for better control of prosthetic devices (Cheesborough, Smith, Kuiken, & Dumanian, 2015). Unfortunately, we did not assess whether our participants had undergone TMS, and we did not use stump muscle activity measurements.

There are some considerations when translating the present results into a practical BCI. First, we have used functional MRI recordings only as a proof of principle, as this method is relatively accessible and easy to conduct in volunteers, non-invasive, and still offers unparalleled high resolution brain recordings. However, the recoding modality needs to be exchanged for one that is wearable and suitable for everyday use. Implantable electrocorticography (ECoG) grids, for example, are much more suitable for a BCI, as they can offer a solution that is available 24 hours a day with minimum set-up time. Complex hand gestures have been decoded using ECoG recordings before in able-bodied participants (Bleichner et al., 2016; Branco et al., 2017). It has also been shown that BOLD activity from functional MRI has an excellent correspondence with gamma signals from ECoG (Hermes et al., 2012; Siero et al., 2014). Therefore, we believe that our decoding results after denervation will translate well to this modality.

Second, the number of classes must be increased. Because our main focus is restoring communication, we have in this work (and in our previous work (Bleichner et al., 2016; Bleichner, Jansma, Sellmeijer, Raemaekers, & Ramsey, 2013; Branco et al., 2017)) chosen for gestures from the sign language alphabet. This way, the user could just hand-spell words, which can then be typed. However, we have only selected six signs. These signs have also been chosen in such a way that they maximally differ in finger flexion and extension (for example, 'W' and 'Y' are each others inverse). A future end-user will need all letters, and possibly numbers, to be able to communicate, although it should be noted that the correspondence of gestures and letters is not a necessity: it is also possible to attach other commands to gestures, such as moving a cursor around on a virtual keyboard.

Third, it is crucial to take into account the demands that are put forward by the (potential) user group, for example on the topic of speed and accuracy. The trials in our experiment had a fixed length of 15 seconds. This equals 4 characters per minute, whereas a typing speed of 15-19 letters per minute would be acceptable to 72% of potential BCI users (Huggins, Wren, & Gruis, 2011). Therefore, an increase in speed compared to out study is essential. Also, since an implanted BCI will be available to the user 24 hours per day, it is important to pay attention to false positives, such as typing letters when the user did not mean to do so. From potential BCI users, 84% were satisfied if unintentional exits from standby mode would occur no more than once per 2-4 hours (Huggins et al., 2011). However, in the present research, rest trials were not included in the task, and

the classifier was not trained on the condition of 'no gesture'. Our classifier training and learning paradigm can therefore not directly be transferred into a practical BCI.

Accuracy is considered one of the most important characteristics of a BCI, according to potential users in the aforementioned survey (Huggins et al., 2011). Classification scores of between 40% and 80% are well above chance level and suggest that there is a meaningful representation. We believe that these classification scores obtained by functional MRI translate well to decodability in intracranial recordings, as we have already observed in previous research by our group (Bleichner et al., 2016, 2013; Branco et al., 2017). But although we like to view this as successful, a big leap still has to be made until this approach offers a usable solution in terms of high accuracy decoding. One needs to find a trade-off between the degrees of freedom and the error rate. This will also be directed by the practical situation, which can vary hugely over subjects, and is dependent on factors like implantation site and the quality of the recorded brain signals.

In conclusion, translating our results to a practical BCI requires additional research. Nevertheless, our finding that there is an intact representation of the phantom hand, both ipsilateral and contralateral, is promising in the development of BCIs that offer many degrees of freedom for restoring communication.

References

Aboitiz, F., Scheibel, A. B., Fisher, R. S., & Zaidel, E. (1992). Fiber composition of the human corpus callosum. *Brain Research*, *598*(1–2), 143–153. doi:10.1016/0006-8993(92)90178-c

Alawieh, A., Tomlinson, S., Adkins, D., Kautz, S., & Feng, W. (2017). Preclinical and Clinical Evidence on Ipsilateral Corticospinal Projections: Implication for Motor Recovery. *Translational Stroke Research*, *8*(6), 529–540. doi:10.1007/s12975-017-0551-5

Bleichner, M. G., Freudenburg, Z. V., Jansma, J. M., Aarnoutse, E. J., Vansteensel, M. J., & Ramsey, N. F. (2016). Give me a sign: decoding four complex hand gestures based on high-density ECoG. *Brain Structure and Function*, *221*(1), 203. doi:10.1007/s00429-014-0902-x

Bleichner, M. G., Jansma, J. M., Sellmeijer, J., Raemaekers, M., & Ramsey, N. F. (2013). Give Me a Sign: Decoding Complex Coordinated Hand Movements Using High-Field fMRI. *Brain Topography*, *27*(2), 248. doi:10.1007/s10548-013-0322-x

Branco, M. P., Freudenburg, Z. V., Aarnoutse, E. J., Bleichner, M. G., Vansteensel, M. J., & Ramsey, N. F. (2017). Decoding hand gestures from primary somatosensory cortex using high-density ECoG. *NeuroImage*, *147*, 130. doi:10.1016/j.neuroimage.2016.12.004

Buetefisch, C. M., Revill, K. P., Shuster, L., Hines, B., & Parsons, M. (2014). Motor demand-dependent activation of ipsilateral motor cortex. *Journal of Neurophysiology*, *112*(4), 999. doi:10.1152/jn.00110.2014

Calford, M. B., & Tweedale, R. (1988). Immediate and chronic changes in responses of somatosensory cortex in adult flying-fox after digit amputation. *Nature*, *332*(6163), 446. doi:10.1038/332446a0

Cheesborough, J., Smith, L., Kuiken, T., & Dumanian, G. (2015). Targeted Muscle Reinnervation and Advanced Prosthetic Arms. *Seminars in Plastic Surgery*, *29*(01), 062–072. doi:10.1055/s-0035-1544166

Diedrichsen, J., Wiestler, T., & Krakauer, J. W. (2013). Two Distinct Ipsilateral Cortical Representations for Individuated Finger Movements. *Cerebral Cortex*, *23*(6), 1362. doi:10.1093/cercor/bhs120

Ebner, T. J., Hendrix, C. M., & Pasalar, S. (2009). Progress in Motor Control. *Advances in Experimental Medicine and Biology*, *629*, 127–137. doi:10.1007/978-0-387-77064-2_7

Ersland, L., Rosén, G., Lundervold, A., Smievoll, A. I., Tillung, T., Sundberg, H., & Hugdahl, K. (1996). Phantom limb imaginary fingertapping causes primary motor cortex activation: an fMRI study. *NeuroReport*, *8*(1), 207. doi:10.1097/00001756-199612200-00042

Gharabaghi, A., Naros, G., Walter, A., Roth, A., Bogdan, M., Rosenstiel, W., ... Birbaumer, N. (2014). Epidural electrocorticography of phantom hand movement following long-term upper-limb amputation. *Frontiers in Human Neuroscience*, *8*. doi:10.3389/fnhum.2014.00285

Hermes, D., Miller, K. J., Vansteensel, M. J., Aarnoutse, E. J., Leijten, F. S. S., & Ramsey, N. F. (2012). Neurophysiologic correlates of fMRI in human motor cortex. *Human Brain Mapping*, *33*(7), 1689. doi:10.1002/hbm.21314

Hotz-Boendermaker, S., Hepp-Reymond, M.-C., Curt, A., & Kollias, S. S. (2011). Movement Observation Activates Lower Limb Motor Networks in Chronic Complete Paraplegia. *Neurorehabilitation and Neural Repair*, *25*(5), 469. doi:10.1177/1545968310389184

Huggins, J. E., Wren, P. A., & Gruis, K. L. (2011). What would brain-computer interface users want? Opinions and priorities of potential users with amyotrophic lateral sclerosis. *Amyotrophic Lateral Sclerosis*, *12*(5), 318–324. doi:10.3109/17482968.2011.572978

Jiang, G., Li, C., Wu, J., Jiang, T., Zhang, Y., Zhao, L., ... Wang, J. (2016). Progressive Thinning of Visual Motion Area in Lower Limb Amputees. *Frontiers in Human Neuroscience*, *10*. doi:10.3389/fnhum.2016.00079

Jiang, G., Yin, X., Li, C., Li, L., Zhao, L., Evans, A. C., ... Wang, J. (2015). The Plasticity of Brain Gray Matter and White Matter following Lower Limb Amputation. *Neural Plasticity*, *2015*, 1. doi:10.1155/2015/823185

Kikkert, S., Kolasinski, J., Jbabdi, S., Tracey, I., Beckmann, C. F., Johansen-Berg, H., & Makin, T. R. (2016). Revealing the neural fingerprints of a missing hand. *ELife*, *2016*(5), e15292. doi:10.7554/elife.15292.001

Lotze, M., Flor, H., Grodd, W., Larbig, W., & Birbaumer, N. (2001). Phantom movements and pain An fMRI study in upper limb amputees. *Brain*, *124*(11), 2268. doi:10.1093/brain/124.11.2268

Makin, T. R., Scholz, J., Filippini, N., Slater, D. H., Tracey, I., & Johansen-Berg, H. (2013). Phantom pain is associated with preserved structure and function in the former hand area. *Nature Communications*, *4*, 1570. doi:10.1038/ncomms2571

Martuzzi, R., Zwaag, W. van der, Farthouat, J., Gruetter, R., & Blanke, O. (2012). Human finger somatotopy in areas 3b, 1, and 2: A 7T fMRI study using a natural stimulus. *Human Brain Mapping*, *35*(1), 213. doi:10.1002/hbm.22172

Merzenich, M. M., Nelson, R. J., Stryker, M. P., Cynader, M. S., Schoppmann, A., & Zook, J. M. (1984). Somatosensory cortical map changes following digit amputation in adult monkeys. *The Journal of Comparative Neurology*, *224*(4), 591. doi:10.1002/cne.902240408

Roux, F.-E., Lotterie, J.-A., Cassol, E., Lazorthes, Y., Sol, J.-C., & Berry, I. (2003). Cortical Areas Involved in Virtual Movement of Phantom Limbs: Comparison with Normal Subjects. *Neurosurgery*, *53*(6), 1342–1353. doi:10.1227/01.neu.0000093424.71086.8f

Siero, J. C. W., Hermes, D., Hoogduin, H., Luijten, P. R., Ramsey, N. F., & Petridou, N. (2014). BOLD matches neuronal activity at the mm scale: A combined 7T fMRI and ECoG study in human sensorimotor cortex. *NeuroImage*, *101*, 177. doi:10.1016/j.neuroimage.2014.07.002

Turner, J. A., Lee, J. S., Martinez, O., Medlin, A. L., Schandler, S. L., & Cohen, M. J. (2001). Somatotopy of the motor cortex after long-term spinal cord injury or amputation. *IEEE Transactions on Neural Systems and Rehabilitation Engineering*, *9*(2), 154. doi:10.1109/7333.928575

Weiss, T., Miltner, W. H. R., Huonker, R., Friedel, R., Schmidt, I., & Taub, E. (2000). Rapid functional plasticity of the somatosensory cortex after finger amputation. *Experimental Brain Research*, *134*(2), 199. doi:10.1007/s002210000456

NEDERLANDSE SAMENVATTING

Nederlandse samenvatting

Het locked-in-syndroom (LIS) is een toestand waarin iemand (grotendeels) niet meer in staat is om vrijwillige bewegingen te maken (American Congress of Rehabilitation Medicine, 1995). LIS kan verschillende oorzaken hebben, zoals een hersenstamberoerte of een neurodegeneratieve aandoening zoals amyotrofe laterale sclerose (ALS), waarbij motorneuronen in de hersenen en hersenstam worden aangetast (Smith & Delargy, 2005). Als gevolg van LIS is het voor personen soms geheel onmogelijk om te communiceren, terwijl communicatie juist een belangrijke factor is in het welbevinden van personen met LIS (Rousseau et al., 2015).

Voor het herstellen van de communicatie zijn diverse hulpmiddelen ontwikkeld die bestuurd kunnen worden met de (geringe) bewegingen die nog wel mogelijk zijn. In veel gevallen zijn oogbewegingen de enige vrijwillige bewegingen die nog intact zijn. In dat geval kunnen zogenoemde eye-trackers uitkomst bieden. Eye-trackers kunnen de kijkrichting afleiden uit de stand van de pupillen en daarmee valt bijvoorbeeld de gebruikersinterface op een computer te besturen. Toch werkt dat niet voor iedereen: soms zijn zelfs oogbewegingen onmogelijk geworden, maar ook in andere gevallen rapporteren gebruikers van hulpmiddelen moeilijkheden bij het gebruik ervan.

Het besturen van hulpmiddelen kan ook door direct gebruik te maken van de hersensignalen. Dit wordt een Brain-Computer-Interface (BCI) genoemd (Wolpaw, 2007). In het UMC Utrecht wordt de Utrecht Neuroprothese (UNP) ontwikkeld voor mensen met LIS (Vansteensel et al., 2016). Dit is een BCI op basis van electro-corticografie (ECoG), waarbij elektroden tijdens een operatie direct op de cortex worden geplaatst. Voor het UNP zijn er elektroden geplaatst op de prefrontale cortex en op de motorcortex (het bewegingsgebied). Als de patiënt probeert een hand te bewegen leidt dat niet tot daadwerkelijke bewegingen (door de LIS), maar de gemeten hersensignalen kunnen wel succesvol gebruikt om een tablet met communicatiesoftware te besturen.

Het besturingssignaal van het UNP is binair: het is 'aan' of 'uit' (beweging of geen beweging). En dat terwijl het corticale handgebied rijke informatie bevat over gedetailleerde handbewegingen. Uit voorgaand onderzoek is gebleken dat het mogelijk is om de bewegingen van individuele vingers af te lezen (te *decoderen*) (Dechent & Frahm, 2003) en om af te lezen welk handgebaar iemand maakte (Bleichner, Jansma, Sellmeijer, Raemaekers, & Ramsey, 2013; Branco et al., 2017).

Bij personen met LIS is er weliswaar hersenactiviteit, maar leidt dit niet meer tot daadwerkelijke bewegingen. Uit de literatuur is bekend dat het ontbreken van zulke output de hersenactiviteit kan veranderen. Bij mensen die een amputatie ondergingen is bijvoorbeeld waargenomen dat het activatiegebied van het geamputeerde lichaamsdeel kleiner werd en dat dit gebied werd 'overgenomen' door naastgelegen activatiegebieden (Lotze, Flor, Grodd, Larbig, & Birbaumer, 2001; Ramachandran, 1993). Er is echter ook bewijs gevonden dat deze veranderingen niet volledig destructief zijn: zo is er bij mensen met armamputatie nog steeds hersenactivatie waar te nemen in het handgebied (Roux et al., 2003; Turner et al., 2001) en is er zelfs een gedetailleerde representatie van individuele vingers waargenomen in de sensorische cortex (Kikkert et al., 2016).

Het doel van de artikelen in dit proefschift is het onderzoeken of het mogelijk is om hersenactiviteit te decoderen na verlies van bewegingsoutput. Met andere woorden: of het mogelijk is om uit de hersenactiviteit af te lezen welke handgebaren iemand heeft *proberen* te maken, terwijl zij dit niet meer echt konden. Hoewel mensen met LIS uiteindelijk het meeste belang hebben bij de resultaten, is het voorliggende onderzoek uitgevoerd bij mensen met een armamputatie. De reden hiervoor is dat het aantal mensen met LIS slechts klein is en dat zij specialistische zorg vergen. Voor mensen met armampuatie is het eenvoudig om mee te doen aan MRI-onderzoek. Een belangrijke overeenkomst tussen personen met armamputatie en met LIS is dat bij beide groepen de motorgebieden intact blijven, maar dat er er geen daadwerkelijke bewegingen meer zijn.

Allereerst presenteren we in hoofdstuk 1 een nieuwe methode om de hersenactivatie uit functionele MRI-scans in de motorgebieden te visualiseren: *Cartesian geometric representation with isometric dimensions* (Cgrid, hoofdstuk 1). Op basis van anatomische hersenscans wordt een rechthoekig raster op sensorische en motorcortex geprojecteerd. Hierdoor ontstaat een coördinatensysteem dat gelijkvormig is tussen proefpersonen, ondanks de individuele anatomische vormverschillen. Dat maakt het gemakkelijker om activatiepatronen tussen proefpersonen te vergelijken. Om de nauwkeurigheid en reproduceerbaarheid te toetsen, is de methode toegepaste op functionele MRI-data van 20 proefpersonen. De correlatie van de Cgrid-patronen tussen proefpersonen was vergelijkbaar met de correlatie tussen activatiepatronen in MNI-ruimte. Hieruit concludeerden we dat Cgrid een stabiele representatie van hersenactivatie oplevert en bruikbaar is in verder onderzoek.

In de hoofdstukken 2 tot en met 4 onderzochten we de representatie van handbeweging na amputatie. Hiervoor werden proefpersonen met een amputatie van de onderarm geworven. In de 7 tesla MRI-scanner kregen de proefpersonen de opdracht om met hun geamputeerde hand (fantoomhand) zes verschillende gebaren te maken (of in elk geval zo goed mogelijk te proberen). De gebaren correspondeerden met de tekens 8, F, L, S, W en Y uit het Amerikaanse hand-alfabet. Vervolgens werd een *classifier* getraind om de functionele-MRI-activatiepatronen van de verschillende handgebaren uit het hand-spellingsalfabet te onderscheiden. Deze classifier werd getraind op hersenactivatiepatronen van de primaire motorcortex (M1), de primaire sensorische cortex (S1) en anterieure en posterieure gebieden (pre-M1 en post-S1) van de hemisfeer contralateraal aan de bewogen hand. Het resultaat van deze classifier (de *decodeerbaarheid*) diende als maat voor de integriteit van de handrepresentatie in de motor- en sensorische cortex.

In hoofdstuk 2 beschrijven we de decodeerbaarheid van de fantoomhand ten opzichte van de intacte hand en van de niet-geamputeerde controlegroep. In de primaire motorcortex (M1) vonden we geen verschillen in decodeerbaarheid tussen de intacte hand en de fantoomhand, of tussen de fantoomhand en de dominante hand van de (niet-geamputeerde) controlegroep. Ook van pre-M1, post-S1 en de primaire sensorische cortex (S1) konden gebaren worden gedecodeerd met een nauwkeurigheid boven kansniveau, maar de S1-decodeerbaarheid van de fantoomhand was wel significant lager dan de decodeerbaarheid van de intacte hand, en ook lager dan de S1-decodeerbaarheid in de controlegroep. Het gebrek aan sensorische input van de fantoomhand kan een mogelijke verklaring zijn voor dit effect.

In hoofdstuk 3 is de methode van het decoderen van handgebaren nogmaals toegepast, maar ditmaal op hersengebieden van de *ipsilaterale* hemisfeer in de groep van niet-geamputeerde proefpersonen. Want hoewel de meeste motorbanen de middellijn kruisen doet een aanzienlijk deel (10%) dat niet (Alawieh, Tomlinson, Adkins, Kautz, & Feng, 2017). Bovendien bestaan er door het corpus callosum verbindingen tussen de twee hersenhelften (Aboitiz, Scheibel, Fisher, & Zaidel, 1992). Het is daarom voorstelbaar dat er ook beweginsinformatie zit in het motorgebied aan dezelfde zijde als de aangestuurde hand (de ipsilaterale zijde). Daarom werd er ook een classifier getraind op activatiepatronen van deze ipsilaterale sensorische en motorgebieden. Dit leverde ook een classificatiescore op die significant hoger was dan kansniveau, zij het iets lager dan de classificatiescore van de contralaterale gebieden. Omdat er dus waardevolle informatie over handgebaren valt af te lezen uit beide hersenhelften, onderzochten we de decodeerbaarheid van *beide* handen vanaf dezelfde hersenhelft. Ook dit bleek mogelijk met significate classificatiescores.

De decodeerbaarheid van ipsilaterale handgebaren bij personen met armamputatie is beschreven in hoofdstuk 4. Net als bij de contralaterale classificatie en de ipsilaterale classificatie in hoofdstuk 3 bleek ook hier de decodeerbaarheid het hoogst in de gebieden M1 en S1 en was de decodeerbaarheid vanaf de contralaterale hersenhelft hoger dan die van de ipsilaterale hersenhelft. Interessant is wel dat de *verschilscore* (contra-minus-ipsilateraal) voor de fantoomhand kleiner was dan voor de intacte hand, of dan de verschilscores voor beide handen van de controlegroep.

De resultaten van dit onderzoek wijzen op een bruikbare representatie van hersensignalen voor het aflezen van handgebaren, ook in het geval van *gepoogde* handgebaren, als er geen daadwerkelijke beweging meer kan worden gemaakt. Dit opent de weg voor vervolgonderzoek, dat zich kan richten op de vertaling van de resultaten naar een praktische BCI voor de doelgroep (personen met LIS).

Bronnenlijst

American Congress of Rehabilitation Medicine. (1995). Recommendations for use of uniform nomenclature pertinent to patients with severe alterations in consciousness. *Archives of Physical Medicine and Rehabilitation*, *76*(2), 205–209. doi:10.1016/s0003-9993(95)80031-x

Bleichner, M. G., Jansma, J. M., Sellmeijer, J., Raemaekers, M., & Ramsey, N. F. (2013). Give Me a Sign: Decoding Complex Coordinated Hand Movements Using High-Field fMRI. *Brain Topography*, *27*(2), 248. doi:10.1007/s10548-013-0322-x

Branco, M. P., Freudenburg, Z. V., Aarnoutse, E. J., Bleichner, M. G., Vansteensel, M. J., & Ramsey, N. F. (2017). Decoding hand gestures from primary somatosensory cortex using high-density ECoG. *NeuroImage*, *147*, 130. doi:10.1016/j.neuroimage.2016.12.004

Dechent, P., & Frahm, J. (2003). Functional somatotopy of finger representations in human primary motor cortex. *Human Brain Mapping*, *18*(4), 272. doi:10.1002/hbm.10084

Kikkert, S., Kolasinski, J., Jbabdi, S., Tracey, I., Beckmann, C. F., Johansen-Berg, H., & Makin, T. R. (2016). Revealing the neural fingerprints of a missing hand. *ELife*, *2016*(5), e15292. doi:10.7554/elife.15292.001

Lotze, M., Flor, H., Grodd, W., Larbig, W., & Birbaumer, N. (2001). Phantom movements and pain An fMRI study in upper limb amputees. *Brain*, *124*(11), 2268. doi:10.1093/brain/124.11.2268

Ramachandran, V. S. (1993). Behavioral and magnetoencephalographic correlates of plasticity in the adult human brain. *Proceedings of the National Academy of Sciences*, *90*(22), 10413. doi:10.1073/pnas.90.22.10413

Rousseau, M.-C., Baumstarck, K., Alessandrini, M., Blandin, V., Villemeur, T. B. de, & Auquier, P. (2015). Quality of life in patients with locked-in syndrome: Evolution over a 6-year period. *Orphanet Journal of Rare Diseases*, *10*(1), 88. doi:10.1186/s13023-015-0304-z

Roux, F.-E., Lotterie, J.-A., Cassol, E., Lazorthes, Y., Sol, J.-C., & Berry, I. (2003). Cortical Areas Involved in Virtual Movement of Phantom Limbs: Comparison with Normal Subjects. *Neurosurgery*, *53*(6), 1342–1353. doi:10.1227/01.neu.0000093424.71086.8f

Smith, E., & Delargy, M. (2005). Locked-in syndrome. *BMJ*, *330*(7488), 406–409. doi:10.1136/bmj.330.7488.406

Turner, J. A., Lee, J. S., Martinez, O., Medlin, A. L., Schandler, S. L., & Cohen, M. J. (2001). Somatotopy of the motor cortex after long-term spinal cord injury or amputation. *IEEE Transactions on Neural Systems and Rehabilitation Engineering*, *9*(2), 154. doi:10.1109/7333.928575

Vansteensel, M. J., Pels, E. G. M., Bleichner, M. G., Branco, M. P., Denison, T., Freudenburg, Z. V., … Ramsey, N. F. (2016). Fully Implanted Brain–Computer Interface in a Locked-In Patient with ALS. *New England Journal of Medicine*, *375*(21), 2060. doi:10.1056/nejmoa1608085

Wolpaw, J. R. (2007). Brain-computer interfaces as new brain output pathways. *The Journal of Physiology*, *579*(3), 613–619. doi:10.1113/jphysiol.2006.125948

ABOUT THE AUTHOR

About the author

Laurentius Cornelis Maria (Mark) Bruurmijn (Waalwijk, December 14, 1985) studied Biomedical Engineering at Eindhoven University of Technology, both at undergraduate (BSc, 2004-2008) and graduate (MSc, 2008-2011) level. He wrote his master's thesis in the BioMedical Image Analysis group, led by prof. dr. ir. Bart ter Haar Romeny, under direct supervision of dr. ir. Remco Duits. This work investigated the Gabor transform and mathematical operations on the resulting frequency score, with an application in calculating the deformation of the human heart in cardiac MRI. In his graduate program, Mark visited the Technion Israel Institute of Technology in Haifa (Israel) for an internship in the Geometric Image Processing Lab of prof. Ron Kimmel, and Alex and Michael Bronstein.

From 2012 to 2017, Mark did his PhD research in the lab of prof. dr. Nick Ramsey. He investigated the cortical representations of the hand after amputation. Using 7T functional MRI, activation patterns in the motor and sensory cortices, following hand gestures from both the intact and the amputated hand, were successfully decoded, indicating that the representation of the hand after denervation is still intact and meaningful. As the target group for Brain-Computer Interfaces often had lost nearly all motor output, being able to decode attempted movements from the sensorimotor cortex is an important finding.

WOORD VAN DANK

Woord van dank

Jullie hebben er lang op moeten wachten. Maar daar is het dan toch. Ein-de-lijk. (Dit zal niet de eerste en ook niet de laatste verwijzing zijn naar de lange duur van mijn promotie.) Het is niet dat ik mijn promotie vergeten was, hoor. Dat kon ook niet, want op gezette tijden werd er door jullie naar geïnformeerd. Het is dan ook mede daardoor dat dit boekje er nu alsnog ligt. Was het niet voor mijn eigen wetenschappelijke trots, dan toch wel om niet steeds met het schaamrood op de kaken te moeten stamelen dat het wel *bijna* af is. Vanwege jullie tomeloze interesse en onvermoeibare aansporingen ben ik daarom dan ook verplicht om enkele woorden van dank aan jullie te richten.

Allereerst natuurlijk mijn grote dank aan mijn promotor Nick. Er was oorspronkelijk nog geen openstaande vacature toen ik je benaderde, meer dan een X aantal jaren geleden (en die X moet worden gelezen in Romeinse betekenis). Toevallig stond er net een groot nieuw project op het punt van beginnen en bood je me de kans om onderzoek te komen doen. Ik weet niet of je na al die jaren inmiddels spijt hebt van die beslissing, maar dat durf ik niet te vragen.

Tijdens het sollicitatiegesprek vroeg je me waar ik nog niet zo goed in was. Ik weet eerlijk gezegd niet meer wat ik toen antwoordde, maar inmiddels kan ik wel een hele lijst opnoemen. "Jezelf leren kennen" heet dat dan, geloof ik. Maar dat was gelukkig niet het enige. Je hebt me de kans gegeven om mee te draaien in een inspirerende omgeving met een groep betrokken wetenschappers, die vanuit slechts een handjevol kantoren in het Stratenum bijzondere dingen doen.

Mariska, mijn eerste werkdag was bij jou. Ik kon direct aan de slag met real-time feedback van activiteit van de DLPFC. Daardoor kreeg ik snel de kans om ervaring op te doen met het programmeren van een taak en met dataverzameling op de 7T-MRI-scanner. Ik waardeer je kritische blik en directe feedback, vooral ook op de manuscripten van artikelen en bij het begeleiden van studenten. Dat was altijd opbouwend en heeft me veel geholpen.

Mathijs ("O hé, Mathijs!"), jij hebt me er in de laatste periode doorheen gesleept. Dat zal soms zwaar zijn geweest. Een kleuter door de supermarkt sleuren is makkelijker. Als ik weer eens mijn zwartgallige kijk op dingen leverde, zorgde jouw nuchtere houding ervoor dat het iets minder zwart werd (donkergrijs). De onschuldige appjes die je zo nu en dan stuurde ("Hi Mark, gaat alles goed met de voorbereidingen?" of, iets vileiner: "Hi Mark, enige progressie?") bezorgden me weliswaar wat stress, maar hebben er toch voor gezorgd dat er uiteindelijk wel wat beweging in bleef zitten. Bedankt voor discussies met jou en voor je aanhoudende betrokkenheid!

En dan zijn daar natuurlijk mijn illustere kantoorgenoten. Nou ben ik op afspraken graag op tijd (te vroeg) aanwezig en ga ik vaak laat (te laat) weer weg, maar dat ik hier van ons als eerste startte en als een van de laatsten eindig staat daar volledig los van. *Et bene pendentes!*

Elmar, ik heb je in de afgelopen jaren leren kennen als iemand die makkelijk dingen regelt, niet bang is om mensen te bellen (o, gruwel) en met af en toe een goeie duidelijke mening. Tijdens ons

befaamde tripje naar San Francisco heb je een onmisbare rol gespeeld die ik niet snel zal vergeten. Zie dat maar als een soort toelatingsexamen voor het paranimf-schap, want ook daarvoor wil ik je natuurlijk hartelijk bedanken!

Efraïm, ook jij bent als paranimf essentieel in het voltooien van deze periode. Je bent ook nog eens de grote aanjager, tourmanager en leider van de Gamma-band, hoewel ze door die naam bij dB's waarschijnlijk steeds dachten dat we elkaar kenden van de bouwmarkt. Je hebt in gesprekken de gave om zaken rustig te analyseren en volstrekt logisch te laten klinken, iets waar mijn cynisme niet tegenop gewassen is.

Max, zijn wij nou heel verschillend of lijken we juist op elkaar? Dat zouden we kunnen bediscussiëren, want daar houden we allebei van en dat hebben we ook veel gedaan. Om er aan het eind achter te komen dat we allebei advocaat van de duivel speelden. Maar ja, je moet wat als je met z'n tweeën 's nachts in de auto naar Tsjechië rijdt. Bedankt voor je tegendraadse, eigenwijze maar waardevolle samenwerking!

Sacha, bedankt voor je gezelligheid en je altijd behulpzame instelling. En ik heb bewondering voor je eetlust, waarvan zelfs het personeel in Amerikaanse all-you-can-eatrestaurants onder de indruk is.

Mariana, your optimism is catching. You are truly able to motivate people to become as enthusiastic as you are, about anything. You are always ready to help other people. Thanks for the wonderful collaboration!

Natuurlijk zijn er talloze andere groepsgenoten die ik wil bedanken. Erik, voor je brede kennis en kunde. Zac, voor je diepgaande specialistische kennis. Martin, als mijn voorganger in mijn project en een van de eersten (met Zac) die ik sprak voordat ik in de groep kwam. Wouter, voor je werk aan Cgrid. En natuurlijk Annemiek, Julia, Meron, Anouk, Miek, Maria en iedereen op wiens werk ik mocht voortbouwen en iedereen die met het werk doorgaat!

Ik heb ook het geluk gehad om enkele studenten met hun stageproject te mogen begeleiden. Irina, Isabelle, Laura en Philippe, bedankt dat jullie je project bij ons (bij mij) hebben gedaan. Jullie dwongen mij steeds om ook goed na te denken over de doelstelling van mijn eigen project. Ik heb dat als heel waardevol ervaren!

Zonder de deelnemers aan het onderzoek was er geen data geweest. Ik wil daarom ook alle proefpersonen (met en zonder armamputatie) bedanken voor hun deelname, het thuis oefenen van de handgebaren en het doorstaan van de lange sessie in de MRI-scanner. Voor het werven van de deelnemers met armamputatie gaat mijn dank naar de revalidatieartsen Michael Brouwers (De Hoogstraat) en Anne Visser-Meily (UMC Utrecht). Ook bedank ik graag de vereniging KorterMaarKrachtig voor hun hulp bij de zoektocht naar deelnemers voor het onderzoek.

Ook buiten het UMC Utrecht heb ik mensen jarenlang beziggehouden met "die promotie die ik nog moet afronden".

Esther en Marjolein, onze intensieve samenwerking begon op hetzelfde moment als mijn promotieproject. De start van die promotie lijkt voor mij korter geleden, maar voor wat betreft onze samenwerking is het alsof we nooit anders hebben gedaan. We hebben door onze verschillende expertises een taakverdeling die als vanzelf lijkt te zijn ontstaan. Jullie weten ook dat ik meestal niet ver vooruit werk. Het meeste krijg ik gedaan op het laatste moment, het liefst diep in de nacht. Gelukkig blijf ik daar tot nu toe bij jullie mee wegkomen. Bedankt voor jullie vriendschap, steun, professionaliteit, creativiteit en al jullie aansporingen!

Toen mijn aanstelling bij het UMC Utrecht erop zat, kon ik aan de slag bij het YOUth-onderzoek. Zo bleef ik dichtbij en kon ik nog een dag in de week gebruiken voor het publiceren van de artikelen en het afronden van het proefschrift. In theorie. In de praktijk gebeurde dat ook wel, maar met lange tussenpozen. Die treuzelachtigheid kwam niet door mijn YOUth-collega's, want ook jullie bleven mij onafgebroken aansporen. Lilli, bedankt voor je vele gevraagde en ongevraagde adviezen. Femke: koffie en *joie de vivre*! Gwen, voor onder andere het spontane Scandinavische-film-uitje. Juliëtte, bedankt dat je me een tijdje lang aan het einde van de dag naar het UMC hebt gestuurd om een artikel af te maken. Ook bedankt aan alle andere leden van het kippenhok met wie ik het elitekant… ehm, tuinkantoor mocht delen: Marieke, Liset, Ivonne, Laura, Ron, Jolien, Leon, Myrthe plus de vele, vele betrokkenen van het zo gezellige KinderKennisCentrum. Als ik weer eens bleef hangen in een monoloog op maandag, hoefde iemand maar te zeggen "Hoe is het eigenlijk met je promotie?" om me weer tot de orde te roepen. Al is het YOUth-onderzoek nu óók weer ten einde, jullie zijn inmiddels minstens net zo blij als ikzelf dat dit proefschrift nu toch eindelijk klaar is.

Op mijn huidige werkplek in het Langeveldgebouw voel ik me inmiddels ook thuis door mijn fijne collega's. Jim, bedankt voor je humor, adviezen (al dan niet op academisch vlak) en je openheid. Boris, Son, Michael, Dennis, Django, Wouter, Halim, Martin, Martijn, Rens, Chris, Sanne, Elise en Oscar, bedankt voor jullie fijne collegialiteit!

Als laatste is natuurlijk een dankwoord voor mijn familie op z'n plaats. Dank aan mijn ouders, Cees en AnneMarie, en aan mijn broer Coen samen met Hanneke en Maud. Bij rapportgesprekken op de basisschool hoefde ik meestal niet veel te vrezen, behalve steevast voor één aspect: het werktempo. Inmiddels is wel gebleken dat ze gelijk hadden, die juffen. Desondanks is het nu wel ten einde, mede door jullie steun en niet-aflatende interesse. Ik ben jullie dankbaar dat jullie me altijd de mogelijkheden hebben gegeven om mijn interesses te volgen. Ook als dat net even wat langer duurt dan gepland.

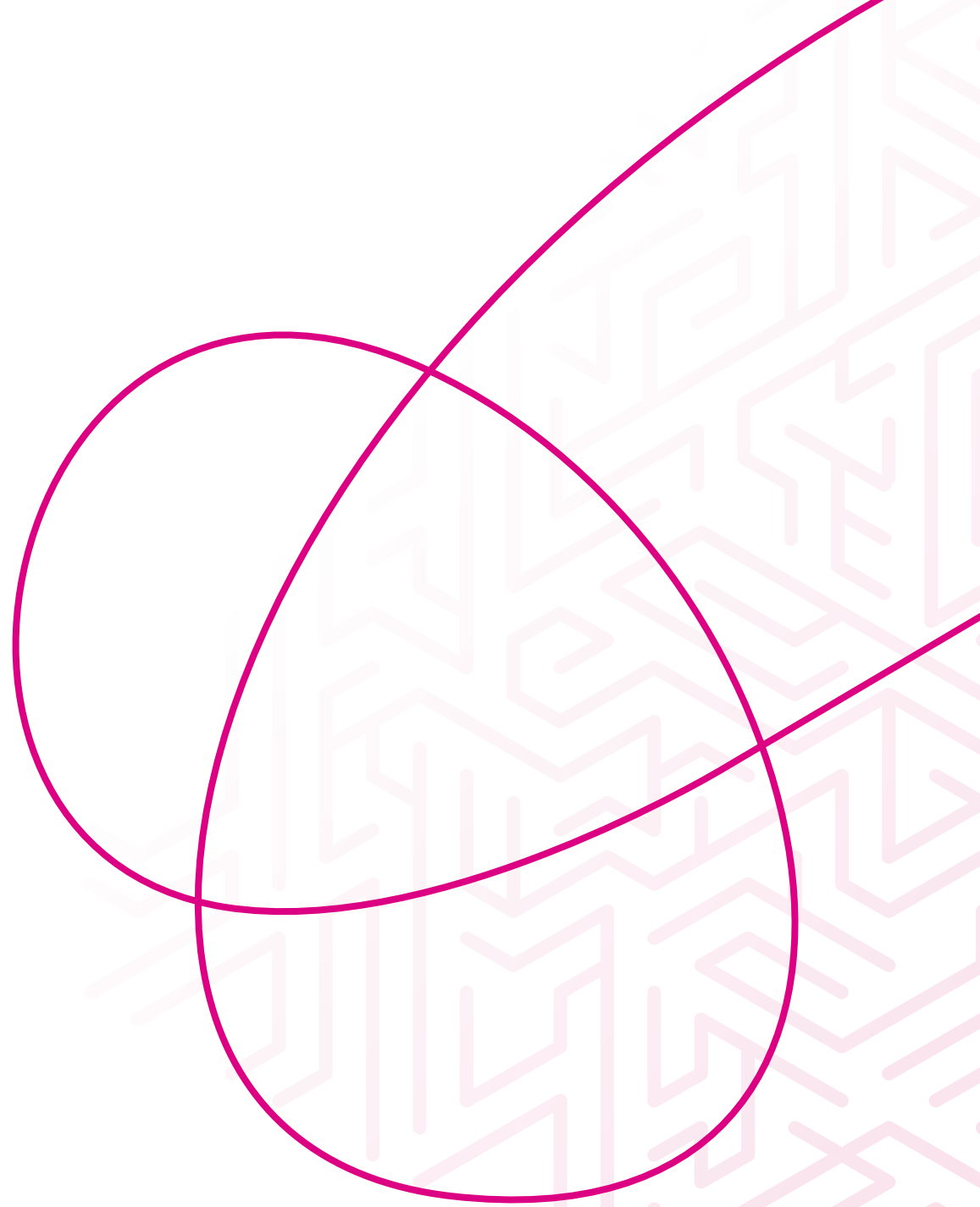

UMC Utrecht Universiteit Utrecht ISBN 978-90-393-7665-2